

PERFORMANCE EVALUATION OF FERROCHROME ASH BASED ALKALI ACTIVATED SLAG MORTARS

Thesis

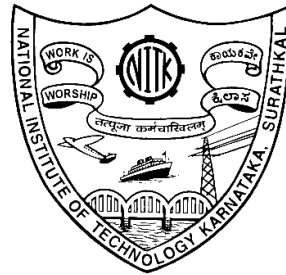
Submitted in partial fulfilment of the requirements for the degree of

DOCTOR OF PHILOSOPHY

by

CHETHAN KUMAR B

158011CV15F14



**DEPARTMENT OF CIVIL ENGINEERING
NATIONAL INSTITUTE OF TECHNOLOGY KARNATAKA
SURATHKAL, MANGALORE – 575 025
JULY, 2022**

PERFORMANCE EVALUATION OF FERROCHROME ASH BASED ALKALI ACTIVATED SLAG MORTARS

Thesis

Submitted in partial fulfilment of the requirements for the degree of

DOCTOR OF PHILOSOPHY

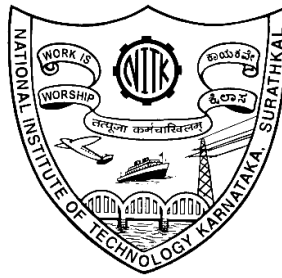
by

**CHETHAN KUMAR B
158011CV15F14**

Under the guidance of

**Dr. Subhash C. Yaragal
Professor**

**Dr. B. B. Das
Associate Professor**



**DEPARTMENT OF CIVIL ENGINEERING
NATIONAL INSTITUTE OF TECHNOLOGY KARNATAKA
SURATHKAL, MANGALORE – 575 025**

JULY, 2022

DECLARATION

By the Ph.D. Research Scholar

I hereby *declare* that the Research Thesis entitled **“PERFORMANCE EVALUATION OF FERROCHROME ASH BASED ALKALI ACTIVATED SLAG MORTARS”**, which is being submitted to the **National Institute of Technology Karnataka, Surathkal** in partial fulfilment of the requirements for the award of the Degree of **Doctor of Philosophy** in the **Department of Civil Engineering** is a *bonafide report of the research work carried out by me*. The material contained in this Research Thesis has not been submitted to any University or Institution for the award of any degree.

158011  CV15F14, CHETHAN KUMAR B

(Register Number, Name & Signature of the Research Scholar)

Department of Civil Engineering

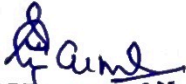
National Institute of Technology Karnataka, Surathkal

Place: NITK-Surathkal

Date: 04-07-2022

C E R T I F I C A T E

This is to *certify* that the Research Thesis/Synopsis entitled **“PERFORMANCE EVALUATION OF FERROCHROME ASH BASED ALKALI ACTIVATED SLAG MORTARS”**, submitted by CHETHAN KUMAR B., (Register Number: 158011CV15F14) as the record of the research work carried out by him/~~her~~, is *accepted as the Research Thesis/Synopsis submission* in partial fulfillment of the requirements for the award of degree of **Doctor of Philosophy**.



(Dr. SUBHASH C. YARAGAL)

Research Guide

(Name and Signature with

Date and Seal)

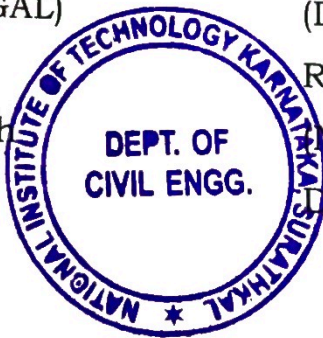


(Dr. B. B. DAS)

Research Guide

(Name and Signature with

Date and Seal)



07/07/2022

Chairman - DRPC

(Signature with Date and Seal)

Chairman (DRPC)

Department of Civil Engineering
National Institute of Technology Karnataka, Surathkal
Mangalore - 575 025, Karnataka, INDIA

ACKNOWLEDGEMENT

With deep sense of gratitude, I express my heartfelt thanks to my research supervisor **Dr. Subhash C. Yaragal**, Professor, BOG and Former Dean (P&D), and **Dr. B. B. Das**, Associate Professor, Department of Civil Engineering, NITK for their invaluable guidance, encouragement and motivation throughout my research work. I am indebted to them for their wholehearted interest and keenness in every phase of research work and thesis preparation their moral support, guidance, interactions, discussions and precious suggestions have greatly helped me to complete this research work. It has been my greatest opportunity and pleasure to work under them. Their crucial comments have guided me to publish my research work in acclaimed International Journals. I would also like to convey my sincere thanks to my Research Progress Assessment Committee members, **Dr. Sunil B. M.**, Department of Civil Engineering, and **Dr. Harsha Vardhan**, Department of Mining Engineering for providing valuable suggestions, comments and encouragement at various stages of this research work.

I would like to thank, **Prof. B.R. Jayalexshmi** Head of the Department of Civil Engineering and the former Heads **Prof. K. Swaminathan**, **Prof. Varghese George** and **Prof. D. V. Reddy**, for all the support throughout my stay at NITK campus. I am also thankful to all faculty and staff of Civil Engineering Department for their help and support.

I am also thankful to **Mr. Nataraja, R.** (Former foreman), **Mr. Geetesh** (Foreman), **Mr. Vishwanatha M. Devadiga**, and **Mr. Ramanath Acharya** (Lab Staff), Structural Engineering Laboratory, Department of Civil Engineering, National Institute of Technology Karnataka, Surathkal for their valuable support and co-operation during the research work.

I am forever grateful to my father **Sri. C. Bommegowda**, mother **Smt. T. Vijaya**, and my sisters **Smt. Mangala, B.** and **Smt. Kusuma, B.** who provided me the best education and encouraged in all my endeavors. I am grateful to my wife **Mrs.**

Bhavana Andani, who has been influential in motivating me in this journey with her moral support and cooperation.

I lovingly acknowledge the moral support and help extended by my research colleagues during this journey. Their informal support and encouragement has been very crucial. I am grateful to everybody who helped and encouraged me during this research work.

Chethan Kumar B

ABSTRACT

The use of ground granulated blast furnace slag (GGBS), fly ash (FA), silica fume (SF), etc. are gaining importance as cementitious materials for researchers, as these reduce carbon footprint, indirectly providing a viable solution to the threat of global warming and waste disposal problems. In particular, industrial byproducts are very promising in their use, due to their mechanical strength and long-term durability performance under aggressive conditions. Hitherto, one of the industrial byproducts not largely researched is ferrochrome ash (FCA). FCA is obtained from the gas cleaning plant of ferrochrome industries during the production of chromium. One of the possible ways of utilizing FCA is as a binder in the alkali activated slag (AAS) binder system. The addition of FCA in the AAS system addresses one of the important issue of the landfill problem and associated cost reduction. The main aim of the present study is to synthesize an AAS system using FCA as a binder material. Three important factors, including alkaline dosage ($\text{Na}_2\text{O} = 4\text{-}6\%$ of the binder), modulus of silica ($M_s = 0.75\text{-}1.75$), and FCA replacement in the AAS binder system (0-50%) were considered for the experimental design. The microstructure and mineralogical studies were performed using scanning electron microscopy - energy dispersive spectroscopy (SEM-EDAX) image analysis and X-ray diffraction (XRD), respectively. Functional group identification was carried out using the Fourier Transform Infrared (FTIR) spectroscopy. Durability studies like, volume of permeable voids (VPV), sulphate attack, acid attack, elevated temperature studies, and ecological studies were also carried out. Optimization of FCA based AAS mortars were done based on grey relational analysis (GRA), technique for order preference by similarity to ideal solution (TOPSIS), and desirability function approach (DFA).

As the replacement of FCA increases in the AAS mortars, N-A-S-H is observed to be predominant with the co-existence of C-S-H, C-A-S-H, and gismondine. The reduction of C-S-H, C-A-S-H, and gismondine is the main reason for the reduction in compressive strength in FCA based AAS mortars compared with 100% GGBS based AAS mortars. As the amount of Na_2O dosage increases, compressive strength of FCA

based AAS mortar mixture also increases. VPV of FCA based mortar mixture decreases with increase in Na_2O dosage. Sulphate and acid resistance of FCA based AAS mortar mixture increases with increase in Na_2O dosage. VPV also increases with increase in FCA content. Sulphate and acid resistance decreases with increase in FCA content in AAS mortar mixtures. Elevated temperature resistance of AAS mortar mixture increases with increase in both FCA content and Na_2O dosage. $\text{ECO}_{2\text{eq}}$ and EE_{eq} increases with increase in Na_2O dosage. However, $\text{ECO}_{2\text{eq}}$ and EE_{eq} decreases with increase in FCA content. Ranking obtained from DFA method is found to be best alternative for optimal mixture identification in terms of VPV, sulphate resistance, and acid resistance of FCA based AAS mortar mixtures. TOPSIS method ranking order can be used for obtaining optimal mixture identification of these mortar mixtures in terms of elevated temperature resistance, $\text{ECO}_{2\text{eq}}$ and EE_{eq} .

TABLE OF CONTENTS

Sl. No	Title	Page No
	DECLARATION	
	CERTIFICATE	
	ACKNOWLEDGEMENT	
	ABSTRACT	
	TABLE OF CONTENTS	i
	LIST OF TABLES	vii
	LIST OF FIGURES	ix
1	INTRODUCTION	1
	1.1 GENERAL	1
	1.2 CEMENT	1
	1.3 ALKALI ACTIVATED BINDERS	2
	1.4 ACTIVATOR MODULES AND ALKALI DOSAGE	3
	1.5 FERROCHROME INDUSTRY AND ITS BYPRODUCTS	4
	1.6 GROUND GRANULATED BLAST FURNACE SLAG	5
	1.7 FINE AGGREGATE	6
	1.8 SCOPE OF WORK	8
	1.9 ORGANIZATION OF THESIS	8
	1.10 CLOSURE	10
2	LITERATURE REVIEW	11
	2.1 GENERAL	11
	2.2 DURABILITY OF ALKALI ACTIVATED MATERIAL	14
	2.2.1 Sulphate resistance	14
	2.2.2 Acid resistance	15
	2.2.3 Volume of permeable voids	16
	2.2.4 Elevated temperature studies	17
	2.2.5 Ecological studies	20
	2.3 OPTIMIZATION METHODS	20
	2.3.1 Grey relational analysis	21

2.3.2	Technique for order preference by similarity to ideal solution	22
2.3.3	Desirability function approach	24
2.4	RESEARCH GAP	25
2.5	OBJECTIVES OF THE RESEARCH WORK	26
2.6	CLOSURE	26
3	MATERIALS AND METHODOLOGY	27
3.1	GENERAL	27
3.2	MATERIALS	27
3.2.1	Cement	27
3.2.2	Ferrochrome ash	28
3.2.3	Lime	29
3.2.4	Ground granulated blast furnace slag	30
3.2.5	Alkaline solution	32
3.2.6	Natural fine aggregate	33
3.3	PREPARATION OF FERROCHROME ASH BASED ORDINARY PORTLAND CEMENT MORTAR MIXTURE AND TESTING	34
3.4	PREPARATION OF FERROCHROME ASH BASED ALKALI ACTIVATED SLAG MORTAR MIXTURE AND TESTING	36
3.5	SCANNING ELECTRON MICROSCOPY, X-RAY DIFFRACTION, AND FOURIER-TRANSFORM INFRARED SPECTROSCOPY	37
3.6	VOLUME OF PERMEABLE VOIDS ON ALKALI ACTIVATED SLAG BASED MORTAR MIXTURES	37
3.7	ACID RESISTANT TESTS ON ALKALI ACTIVATED SLAG BASED MORTAR MIXTURES	37
3.8	SULPHATE RESISTANT TESTS ON ALKALI ACTIVATED SLAG BASED MORTAR MIXTURES	38
3.9	ELEVATED TEMPERATURE STUDIES ON FERROCHROME ASH BASED MORTARS	39
3.10	ECOLOGICAL STUDIES OF FERROCHROME ASH BASED MORTAR MIXTURES	40
3.11	OPTIMIZATION METHODS USED FOR FERROCHROME ASH	42

	BASED ALKALI ACTIVATED SLAG MORTAR MIXTURES	
	3.11.1 Grey relational analysis	43
	3.11.2 Technique for order of preference by similarity to ideal solution	44
	3.11.3 Desirability function approach	46
	3.12 FLOW CHART OF PRESENT RESEARCH WORK	48
	3.13 CLOSURE	48
4	FERROCHROME ASH-ITS USAGE POTENTIAL IN ORDINARY PORTLAND CEMENT AND ALKALI ACTIVATED SLAG MORTARS	49
	4.1 GENERAL	49
	4.2 FERROCHROME ASH AS SUPPLEMENTARY CEMENTITIOUS MATERIAL IN ORDINARY PORTLAND CEMENT BASED MORTAR MIXTURES	49
	4.2.1 Consistency of ferrochrome ash based ordinary Portland cement mortar mixtures	50
	4.2.2 Compressive strength of ferrochrome ash based ordinary Portland cement mortar mixtures	50
	4.2.3 Mineralogical studies on ferrochrome ash based ordinary Portland cement mortar mixtures	51
	4.2.4 Elevated temperature studies on ferrochrome ash based ordinary Portland cement mortar mixtures	52
	4.3 EFFECT OF FERROCHROME ASH IN ALKALI ACTIVATED SLAG MORTAR MIXTURES	55
	4.3.1 Effect of ferrochrome ash replacement on compressive strength of alkali activated slag binder system	55
	4.3.2 X-ray diffraction analysis of ferrochrome ash based alkali activated slag binder system	57
	4.3.3 Scanning electron microscopy-Energy dispersive spectroscopy analysis of ferrochrome ash based alkali activated slag binder system	60
	4.3.4 Fourier-transform infrared spectroscopy of alkali activated slag mortars mixtures	64
	4.3.5 Ecological and cost analysis of ferrochrome ash based mortar	65

	mixtures	
	4.4 CLOSURE	66
5	DURABILITY AND OPTIMIZATION STUDIES OF ALKALI ACTIVATED SLAG/ FERROCHROME ASH BASED MORTARS	67
	5.1 GENERAL	67
	5.2 VOLUME OF PERMEABLE VOIDS OF ALKALI ACTIVATED SLAG MORTAR MIXTURES	67
	5.3 SULPHATE ATTACK ON ALKALI ACTIVATED SLAG MORTAR MIXTURES	70
	5.4 ACID ATTACK ON ALKALI ACTIVATED SLAG MORTAR MIXTURES	74
	5.5 OPTIMIZATION OF FERROCHROME ASH BASED ALKALI ACTIVATED SLAG MIXTURES BY GREY RELATIONAL ANALYSIS	78
	5.6 OPTIMIZATION OF FERROCHROME ASH BASED ALKALI ACTIVATED SLAG MIXTURES BY TECHNIQUE FOR ORDER OF PREFERENCE BY SIMILARITY TO IDEAL SOLUTION	81
	5.7 OPTIMIZATION OF FERROCHROME ASH BASED ALKALI ACTIVATED SLAG MIXTURES BY DESIRABILITY FUNCTION APPROACH	83
	5.8 SPEARMAN'S CORRELATION COEFFICIENT OF GREY RELATIONAL ANALYSIS, TECHNIQUE OF ORDER PREFERENCE SIMILARITY TO THE IDEAL SOLUTION, AND DESIRABILITY FUNCTION APPROACH METHOD RANKING	85
	5.9 CLOSURE	86
6	ELEVATED TEMPERATURE AND ECOLOGICAL STUDIES OF ALKALI ACTIVATED SLAG/FERROCHROME ASH BASED MORTARS	87
	6.1 GENERAL	87
	6.2 ELEVATED TEMPERATURE STUDIES ON FERROCHROME ASH BASED ALKALI ACTIVATED SLAG MORTAR MIXTURES	88
	6.3 COMPARISON BETWEEN OPENLCA AND ECOINVENT BASED	90

	ANALYSIS RESULTS OF EMBODIED CARBON DI-OXIDE EMISSION AND EMBODIED ENERGY	
	6.4 EMBODIED CARBON DI-OXIDE EMISSION STUDIES ON FERROCHROME ASH BASED ALKALI ACTIVATED SLAG MORTAR MIXTURES	92
	6.5 EMBODIED ENERGY STUDIES ON FERROCHROME ASH BASED ALKALI ACTIVATED SLAG MORTAR MIXTURES	96
	6.6 GREY RELATIONAL ANALYSIS ON ELEVATED TEMPERATURE AND ECOLOGICAL PARAMETERS OF FERROCHROME ASH BASED ALKALI ACTIVATED SLAG MORTAR MIXTURES	97
	6.7 TECHNIQUE OF ORDER PREFERENCE SIMILARITY TO THE IDEAL SOLUTION ON ELEVATED TEMPERATURE AND ECOLOGICAL PARAMETERS OF FCA BASED ALKALI ACTIVATED SLAG MORTAR MIXTURES	101
	6.8 DESIRABILITY FUNCTION APPROACH ON ELEVATED TEMPERATURE AND ECOLOGICAL PARAMETERS OF FERROCHROME ASH BASED ALKALI ACTIVATED SLAG MORTAR MIXTURES	104
	6.9 SPEARMAN'S CORRELATION COEFFICIENT OF GREY RELATIONAL ANALYSIS, TECHNIQUE OF ORDER PREFERENCE SIMILARITY TO THE IDEAL SOLUTION, AND DESIRABILITY FUNCTION APPROACH METHOD RANKING	106
	6.10 CLOSURE	106
7	CONCLUSIONS	107
	7.1 GENERAL	107
	7.2 CONCLUSIONS	107
	7.3 SCOPE FOR FUTURE RESEARCH	109
	REFERENCE	111
	LIST OF PUBLICATIONS	125
	BIO-DATA	127

LIST OF TABLES

Table No.	Title	Page No.
3.1	Chemical oxide composition of OPC (by % weight)	28
3.2	Chemical oxide composition of FCA (by % weight)	28
3.3	Chemical oxide composition of GGBS (by % weight)	31
3.4	Calculation of different ingredient quantity used in alkaline solution preparation	33
3.5	Sieve analysis results of NFA	34
3.6:	Mixture composition of FCA based OPC mortar mixtures	35
3.7	Mixture composition of FCA based AAS mortar mixtures	36
3.8	Quantity, Ecoinvent modules and market rates of materials of FCA based mortar mixtures used in ecological analysis.	41
4.1	Compressive strength of FCA based mortar mixtures at various levels of water curing period.	51
4.2	Residual compressive strength of FCA based OPC mortar mixtures	53
4.3	Compressive strength of different AAS binders with different curing period	56
4.4	EDAX analysis of atomic weight percentage of the AAS binder system	63
4.5	ECO _{2eq} , EE _{eq} , and cost of different mortar mixes	66
5.1:	VPV of FCA based AAS mortar mixture with various levels of alkaline solution concentration	69
5.2	Compressive strength of sulphate exposed AAS mortar mixture for a time period of 180 days	71
5.3	Normalized compressive strength values of sulphate exposed AAS mortar mixtures	72
5.4	Compressive strength of acid exposed AAS mortar mixtures for a time period of 90 days	76
5.5	Normalized compressive strength values of acid exposed AAS mortar mixtures.	77
5.6	Grey relational generation and deviation value of FCA based AAS mortar mixtures	79
5.7	GRC, GRG and ranking of FCA based AAS mixtures	80
5.8	Response table for GRG by considering durability aspects.	80

5.9	Normalized decision matrix and weighted normalized decision matrix of FCA based AAS mortar mixtures	81
5.10	Positive, and negative ideal solution, closeness coefficient and ranking of FCA based AAS mortar mixtures	82
5.11	Response table for closeness coefficient by considering durability aspects	83
5.12	Individual desirability, overall desirability values and ranking of FCA based AAS mortar mixtures	84
5.13	Response table for overall desirability by considering durability aspects	85
6.1	Compressive strength and residual compressive strength of FCA based AAS mortar mixture under ambient and elevated temperature condition	90
6.2	Comparison between OpenLCA and Ecoinvent based analysis results of ECO_{2eq}	91
6.3	Comparison between OpenLCA and Ecoinvent based analysis results of EE_{eq}	91
6.4	Calculation of ECO_{2eq} of FCA based AAS mortar mixtures using Ecoinvent database	94
6.5	Calculation of EE_{eq} of FCA based AAS mortar mixtures using Ecoinvent database	95
6.6	Responses used in GRA, TOPSIS, and DFA method	98
6.7	Normalized and deviation value of responses used in GRA method	99
6.8	GRC, GRG value and ranking of different mixtures	99
6.9	Responses of GRG values of FCA based AAS mortar mixtures in GRA method	100
6.10	Normalized decision matrix and weighted decision matrix of different FCA based AAS mortar mixtures used in TOPSIS method	102
6.11	Positive and negative ideal solution, closeness coefficient and ranking order of FCA based AAS mortar mixtures	102
6.12	Response of closeness coefficient values of FCA based AAS mortar mixtures	103
6.13	Individual desirability, overall desirability and ranking order of different FCA based AAS mortar mixtures	105
6.14	Response of overall desirability values of FCA based AAS mortar mixtures	105

LIST OF FIGURES

Figure No.	Title	Page No.
2.1	Typical flow of TOPSIS method in cementitious material optimization (Rashid et al. 2020).	24
3.1(a)	SEM image of spherical FCA particles	28
3.1(b)	Mineralogical phases of FCA particles	29
3.2(a)	SEM image of lime particles	29
3.1(b)	Mineralogical phases of lime particles (CH - calcium hydroxide, CC - calcium carbonate)	30
3.3 (a)	SEM image of GGBS	31
3.3 (b)	Mineralogical phases of GGBS particles	31
3.4	Weights of water, Na ₂ SiO ₃ , and NaOH required preparing alkaline solution of different Ms ratio.	32
3.5	Compressive strength testing setup	35
3.6	FCA based AAS mortar mixtures exposed under acid solution	38
3.7	FCA based AAS mortar mixtures exposed under MgSO ₄ solution	39
3.8	Programmable electric furnace used for elevated temperature studies	40
3.9	Flow chart of present research work	48
4.1	SEM image of FCA particles	50
4.2	Compressive strength of FCA based OPC mortar mixtures at various levels of water curing periods	51
4.3	XRD analysis of control and FCA based OPC mortar mixtures	52
4.4	Residual compressive strength of FCA based OPC mortar mixtures with respect to different temperatures	53
4.5	SEM image of M1, M2, and M3 exposed to 400 ⁰ C (a, b, and c) and 800 ⁰ C (d, e, and f) respectively	54
4.6	Compressive strength variation of different binders with respect to curing period	57
4.7 (a)	XRD pattern of AAS mortar with 0% FCA and 100% GGBS	59
4.7 (b)	XRD pattern of AAS mortar with 25% FCA and 75% GGBS	59

4.7 (c)	XRD pattern of AAS mortar with 50% FCA and 50% GGBS	60
4.8 (a)	SEM image of AAS binder	61
4.8 (b)	SEM image of AAS binder showing micro crack	61
4.8 (c)	SEM image of AAS binder with 25% FCA and 75% GGBS	61
4.8 (d)	SEM image of AAS binder with 50% FCA and 50% GGBS	61
4.9 (a)	EDAX analysis of 100% GGBS in the AAS binder system	63
4.9 (b)	EDAX analysis of 75% GGBS and 25% FCA in the AAS binder system	63
4.9 (c)	EDAX analysis of 50% GGBS and 50% FCA in the AAS binder system	64
4.10	FTIR spectra of raw materials (GGBS, and FCA), and AAS binder with 0, 25, and 50% FCA replacement	65
5.1	VPV of FCA based AAS mortar mixture with various levels of alkaline solution concentration	69
5.2	Compressive strength of sulphate exposed AAS mortar mixtures for a time period of 180 days	71
5.3	Normalized compressive strength values of sulphate exposed AAS mortar mixtures	72
5.4	Compressive strength of acid exposed AAS mortar mixtures for a time period of 90 days	76
5.5	Normalized compressive strength values of acid exposed AAS mortar mixtures	77
6.1	Compressive strength and residual compressive strength of FCA based AAS mortar mixtures under ambient and elevated temperature condition	88
6.2	ECO _{2eq} value of FCA based AAS mortar mixtures for varies levels alkaline solution of concentration (i.e., 4 - 6% Na ₂ O dosage)	93
6.3	EE _{eq} values of FCA based AAS mortar mixtures for varies levels alkaline solution of concentration (i.e., 4 - 6% Na ₂ O dosage)	97

CHAPTER 1

INTRODUCTION

1.1 GENERAL

Ordinary Portland Cement (OPC) is the main binding material for the production of mortars and concretes. OPC with other materials like aggregates and water forms a composite of required size and shape. OPC can set, harden and adhere to other construction materials like bricks, tiles, stone and reinforced steel, etc to bind them together. Despite several advantages of OPC, the manufacture of cement itself consumes huge amounts of natural resources like, limestone, clay, shellsand chalk with other minerals. Due to the heavy utilization of natural resources in OPC production, the associated natural resources are getting depleted fast. And also, production of cement releases enormous amount of carbon di-oxide (CO₂) which eventually are responsible for global warming and climate change. It is for these reasons that, the researchers are interested in finding sustainable solutions for manufacture of cement or finding ways and means to reduce cement utilization by use of value added industrial byproducts as replacement in right proportion to OPC. The present study is an attempt towards this endeavour.

1.2 CEMENT

Cement industry plays a vital role in national economic growth by generating large amount of revenue to the government, employment opportunity in infrastructure development and urban housing. Cement is the most consumed material in construction sectors. Per capita consumption of cement is about 195kg annually (Bureau of energy efficiency, Ministry of Power, Government of India). India stands as second in the world for the production and consumer of cement. Due to the boom in construction sector, large amount of cement is being consumed. Cement production is energy intensive and releases large amount of CO₂ into the atmosphere. Nearly one tonne of cement production releases around 900kg of CO₂ to

environment. In which, 450kg of CO₂ is from raw material decomposition and the remaining part of CO₂ emission is from burning of fuel (Benhelal et al. 2013). Efforts are on to bring down cement consumption by use of secondary cementitious materials (SCM). Worldwide, SCM were utilized successfully as a fractional alternative to cement. Cement composites composed of SCM are considered as a robust sustainable material (Indian Minerals Year Book, 2018).

1.3 ALKALI ACTIVATED BINDERS

Use of alkali materials in slag dates back to 1930 by Kuhl (Shi et al. 2006). . Since the discovery of alkali activated binders (AAB), they have been used for different applications. Few of alkali activated binders based products are concrete, masonry blocks, pavement, pipes, poles, sinks, trenches, autoclaved aerated concrete, oil-well cements and stabilization of radioactive and hazardous wastes (Shi et al. 2006).

AAB are cement or clinker free binder system and is a new generation material, that is produced from aluminosilicate rich materials in the presence of alkali sources. Aluminosilicate materials act as a precursor and are derived from natural pozzolans, industrial slags, etc. Alkali sources can be any material that can readily provide alkali metal cations (AMC). AMC accelerates reaction kinetics by dissolution of solid precursor used, to raise the pH of the mixture (Wang et al. 1995).

Under the umbrella of AAB there are several types of classifications few are alkali activated slag, geopolymers, alkali activated slag fly-ash binders, etc., AAB is usually produced by the industrial by-products like., GGBS, FA, SF, etc., In production of AAB, precursors used are primarily rich in calcium, aluminosilicate materials and silica minerals. Usually three types of AAB binders can be produced. First type of AAB is which rich in calcium and silica composition, this type of AAB are usually produced with the binder like, GGBS. Second type of AAB is rich in silica and alumina which are generally called as geopolymers and the same can be produced with binders like, Class F FA and Metakaolin. Finally, third type of AAB can be produced with calcium, silica and alumina based binders combination. Usually third type of AAB can be obtained with the combination of GGBS + FA.

Krivenko (1994) classified the AAB under the two subheads based on hydration products. The two classifications of AAB are alkali aluminosilicate system (R-A-S-H where R = Na or K) and alkaline- alkaline earth systems (R-C-A-S-H). Alkali aluminosilicate systems are also called as “geocements”, since formation of materials are in the nature of geological process of formation of natural zeolites. If the materials formed are due to poly-condensation rather than hydration process then the formed materials can be called as geopolymers (Davidovits 1994). Whereas, alkaline-alkaline earth systems generally forms calcium silicate hydrate (C-S-H) with low Ca/Si ratio. Production of alkali aluminosilicate system and alkaline- alkaline earth systems are similar in nature but the end products obtained are different in chemical and mechanical properties. Most commonly observed alkaline- alkaline earth systems is alkali activated slag (AAS). GGBS is most suitable material in worldwide for the production of AAS binder systems. Despite of lot of literature on AAS binder system there has been no consensus yet on the chemistry of AAS formation and its end products. Use of AAB as a binding material will reduce environmental impact that is associated with manufacture and use of cement.

1.4 ACTIVATOR MODULES AND ALKALI DOSAGE

Preparation of AAB mixtures compared to OPC based mixtures. One of the essential part in AAS mixture preparation is alkaline solution preparation. Alkaline solution help in the dissolution of binders. Alkaline solution should be prepared prior to the preparation of AAB mixture. Well in advance preparation of alkaline solution will be based strength and durability aspects of AAB mixture required for the intended purpose. In order to have sufficient strength and durability of AAB mixture, prepared alkaline solution need to have required chemical composition. Activator modules and alkali dosage are the two main factors in alkaline solution preparation, which plays a vital role in strength and durability of AAB mixture prepared.

Common alkali materials considered in preparation of alkaline solution preparation are caustic alkalis, non-silicate weak salts, silicates, aluminates, aluminosilicates, non-silicates strong acid salts. Most common alkali materials considered in preparation of alkaline solution is sodium hydroxide (NaOH) and sodium silicates (Na_2SiO_3). NaOH

and Na_2SiO_3 are preferred due to its availability, low cost and low emissions to environment during its production process. Though potassium based alkali material gives higher compressive strength in AAB mixtures but emits higher emissions and high cost for the production compared to sodium based alkaline solution. So, sodium based alkaline solution are commonly used in preparation of AAB mixture preparation.

Activator modules or silicate modules (Ms) is an important factor to be considered while preparing alkaline solution which is used AAB system preparation. If sodium based silicate and hydroxides are used, then Ms can be given as mass ratio of SiO_2 to Na_2O (i.e., $\text{Ms} = \text{SiO}_2/\text{Na}_2\text{O}$). Alkali dosage is the one more factor that influences the strength and durability of AAB mixture. Alkali dosage will be considered from NaOH pellets and Na_2SiO_3 solution in Na_2O . Higher concentration of Na_2O dosage will results in higher compressive strength of in AAB mixture due to the higher dissolution of binders used in preparation of AAB mixtures. Further, higher dissolution of binders will result in denser microstructure of AAB mixtures. This in turn results in reduced porosity and improved durability in AAB mixtures. Beyond the optimal level of Na_2O dosage, further increase in compressive strength gets restricted in AAB mixtures. Lower concentrations of Na_2O dosage will result in reduction of compressive strength in AAB mixtures.

1.5 FERROCHROME INDUSTRY AND ITS BYPRODUCTS

Ferrochrome is a type of ferroalloy and it is produced by electric carbothermic reduction of chromite. Ferrochrome is composed of two elements i.e., chromium and iron. Chromium is produced using chromite ore. In India, Odisha (Sukinda ultramafic belt) and Karnataka (Hassan) are the major sources for chromite ore. Some minor sources of chromite ore are found in the state of Maharashtra. During the year 2018, there were around 25 mines all over India producing 3480 thousand tonnes of chromite ore. In which, 21 mines were in Odisha, 3 mines in Karnataka and one mine in Maharashtra. Percentage of chromium varies from 50-70% by weight in ferrochrome alloy. Ferrochrome is the major alloy in production of stainless steel. Addition of ferrochrome in steel results in stainless character to steel. Almost 80% of

the world's ferrochrome is utilized for the production of stainless steel. Major manufacture of ferrochrome in the world is observed in South Africa, Kazakhstan and India.

For every metric tonne of ferrochrome production, around 1.0-1.2 tonne of solid waste is generated. Ferrochrome ash (FCA) and ferrochrome slag (FCS) are the two major solid wastes produced during ferrochrome production. FCA is obtained in gas cleaning plants. FCS is obtained during the smelting process of stainless steel. These two solid wastes require a lot of space for disposal. In order to address these disposal problems several researchers used FCA and FCS in production of concrete. Since, FCA substances contain alumina and silicate; it can be used as SCM, which reduces the environmental impact associated with production and usage of OPC. Whereas, FCS imparts the quality of binder, natural fine aggregate (NFA) and natural coarse aggregate (NCA) based on the grinding, gradation and cooling process of slag obtained in smelting furnaces. Lind et al. (2001) have carried out experiments on the utilization of FCS in road construction. Nath (2018) used FCS as a binder to study the geopolymerization behaviour of FCS and FA blends. Dash and Patro (2018a, b) studied the effect of FCS as a NFA in concrete. Acharya and Patro (2016) reported the use of FCA as binder. Zelić, (2005) and Gencel et al. (2012) used FCS as NCA and identified that FCS replacement has a significant influence on compressive strength. Utilization of FCA and FCS as construction material reduces land disposal problems, natural resources depletion problems and greenhouse gas emission problem to a substantial extent.

1.6 GROUND GRANULATED BLAST FURNACE SLAG

GGBS is an industrial byproduct obtained from blast furnaces, used to make iron and steel. 300-540kg of slag get generated for every tonne of pig or crude iron production. Specified quantities of iron ore, coke and limestone are fed into a blast furnace and operated at 1500⁰C, and usually two products are generated in a blast furnace i.e., molten iron and slag. Slag settles on top of molten iron, since slag is lighter material compared to molten iron. Manufacture of GGBS involves quenching of blast furnace slag in high pressure water jets or steam. Quenched slag is in the form of glassy

granules, these granules are dried and ground to required size using a vertical roller milling process or rotating ball milling process. GGBS is rich in calcium and highly cementitious. Chemical composition of GGBS varies from plant to plant due to raw materials used in the production of iron (Siddique and Cachim, 2018).

GGBS has wide application in cement industries for the production of Portland slag cement (PSC). PSC is obtained by use of 50-70% of GGBS. Compared to OPC, PSC is more durable (Vedalakshmi, 2008). Conventional blending of GGBS with OPC based mixtures will set more slowly compared to complete OPC based mixtures. According to IS 455-1989, up to 25%-70% GGBS can be used as a replacement to OPC as a binder based on the application.

1.7 FINE AGGREGATE

Besides cement and water, fine aggregate is the one more material which is used in huge quantity in preparation of concrete and mortar. So fine aggregate is an important material used in production of concrete and mortar. Aggregate occupies 60-75% of total volume in concrete. In which, 35% volume is occupied by the fine aggregate in concrete (Mundra et al., 2016). In case of mortar, 55% volume is occupied by the fine aggregate. Fine aggregates are held together in the cementing phases of concrete or mortar. Fine aggregate plays an important role in fresh and hardened state of mortar or concrete prepared. In order to outline the fresh and hardened properties of mortar and concrete, one must need to have a clear insight on property of fine aggregate used to serve for the intended purpose. There are several properties of fine aggregate which influence the fresh and hardened state of mortar. In fresh state, mortar or concrete prepared should able to resist bleeding, segregation and more importantly prepared mortar or concrete mixture must have desired workability to serve for the purpose. In hardened state, prepared mortar or concrete mixture should have sufficient mechanical strength and durability against aggressive chemical environment.

Particles shape, specific gravity, density, voids, percentage of bulking, water absorption and gradation are few properties of fine aggregate which governs the fresh and harden state of mortar and concrete prepared. Fine aggregates fill the gaps

between the coarse aggregate matrixes and reduce the porosity of the cement composites. Reduced porosity will provide strength and durability to the cement composites produced. Required size and gradation of fine aggregates can be obtained by sieving operation. IS 383-2016 specifies fine aggregates must be less than 4.75mm IS sieve. There is no “ideal” grading in case of fine aggregate. However, IS 383-2016 classifies fine aggregate under four zones (i.e., Zone 1, Zone 2, Zone 3 and Zone 4 of fine aggregate) wherein, fine aggregate becomes finer from Zone 1 to Zone 4. Further, fine aggregate size can be identified by the fineness modules, higher the fineness modules implies coarser the fine aggregate. Good grading of fine aggregates will contain all the fractions of sieve size of particles, good grading of fine aggregates will provide minimum voids in mortar and concrete. Reduced void in fine aggregate composition will reduce cement paste content. Reduced paste content will result in less quantity of cement, less quantity water and lower shrinkage. In other term, paste system is more vulnerable to chemical environment compared to many mineral aggregates. So good aggregate grading is essential to reduce the chemical ingress on mortar and concrete produced.

Fine aggregate used as construction materials should be inert and non-reactive in nature. Fine aggregates sourced from streams are usually called as “uncrushed sand” and fine aggregates obtained from crushing of hard stone are usually referred as “crushed sand”. Fine aggregate used should be free from deleterious materials like pyrites, lignite, mica, scale etc. Total percentage of deleterious materials must be less than 5, 2 and 2% for uncrushed sand, crushed sand and manufactures sand respectively. Over exploitation of river sand will leads in depletion of ground water table and results in well failure. On the other hand, there is rapid increase in large quantity of unutilized industrial by-products. Since there is rapid decrease in quality of fine aggregate and restriction of extraction of river sand, IS 383-2016 provides provisions to use the industrial by-products like, copper slag, iron slag and steel slag to certain extent. Use of this industrial by-products will result in reduced environmental problems like, waste disposal problem and compensates the lack of fine aggregate. Before using any of this industrial by-products, engineer in-charge needs to ensure about the quality of by-products against the physical properties,

chemical properties, specification and limits mentioned in standard code of practice judiciously.

1.8 SCOPE OF WORK

Sustainable development is aimed at improving the quality of life for everyone, at present and for generations to come. Due to the exponential growth of urbanization and industrialization, byproducts from industries are becoming an increasing concern. In spite of the good performance of FCA in concrete, it is clear from the literature that limited research works are available on FCA based cementitious materials. So, in order to address this knowledge gap, compressive strength of FCA based mortars is investigated in the present work. X-ray diffraction (XRD) analysis was used to observe mineralogical changes with addition of FCA as replacement to conventional binders. Scanning electron microscope (SEM) has been used to observe micro-structural changes of FCA based mortar mixtures. Further durability aspects of FCA based mortars were also addressed.

1.9 ORGANIZATION OF THESIS

This thesis gives detailed information on use of FCA as binder in AAS mortar. Thesis is structured into seven chapters followed by list of references. Brief descriptions of seven chapters are detailed as follows;

CHAPTER 1

This chapter presents, a brief on importance of sustainable development in the context of cement manufacture, use of SCM, AAB, FCA, GGBS and the scope of work are detailed.

CHAPTER 2

A comprehensive literature review carried out is reported in this chapter. Pertinent literature to provide adequate information related to sustainability in construction

sector, SCM utilization in mortar, FCA based composites, AAB overview, mechanical, durability properties and elevated temperatures performance of OPC, SCM and AAS is presented. Further literatures related to multi criteria decision making (MCDM) and ecological studies were also discussed. Based on comprehensive literature review, the research gaps were identified and considered suitably in formulation of the objectives for the present work.

CHAPTER 3

Chapter 3 gives the details of materials and methods used along with standard codes and literature. The physical and chemical properties of binders, NFA, water and preparation of alkaline solution are reported. Mixture preparation, composition of mixtures, fresh properties, mechanical properties, durability properties, elevated temperature testing, cost analysis, emission calculation, micro-structural characterization and MCDM have been discussed in detail.

CHAPTER 4

Chapter 4 discusses and present results of fresh properties, compressive strengths at different age of curing, effect of modulus silica (M_s), effect of FCA replacement in on OPC, AAS mortar, SEM studies, XRD studies, Fourier-transform infrared spectroscopy (FTIR), emission studies and cost analysis in detail.

CHAPTER 5

The results of durability properties like, volume of permeable voids (VPV), sulphate attack, acid attack, embodied carbon di-oxide (ECO_{2eq}) and embodied energy (EE_{eq}) associated with alkali solution are discussed and presented in this chapter. Further, alkali activated slag/ferrochrome mortar mixtures (AASFC) were optimized using MCDM are also discussed and presented in detail.

CHAPTER 6

Chapter 6 presents the results of elevated temperature studies effect of AASFC mortar mixtures. AASFC mortar mixtures were optimized using MCDM for elevated temperatures exposure.

CHAPTER 7

The major findings drawn based on the present work and scope for the future studies were also discussed in this chapter.

1.8 CLOSURE

In this chapter the importance of using industrial byproducts in the manufacture of cement, to address the importance of sustainable concrete construction is highlighted. A brief on AAB, alkaline activators, ferrochrome industry and its products, GGBS and fine aggregate is presented. Scope of work and the organization of thesis have been presented.

CHAPTER 2

LITERATURE REVIEW

2.1 GENERAL

Demand for construction materials is increasing at a faster rate due to the increase in infrastructure projects. Basic construction materials are cement and steel. Production of cement adversely affects environment by utilizing natural resources and also releases of green house gases. Production of steel also results in depletion of natural resource and produces industrial byproducts in other words value added products. Increase in demand for construction materials on one hand, coupled with increase in large volume of industrial byproducts is a challenging problem. One possible way of reducing production of cement is to find an alternative to OPC binder by utilizing industrial byproducts. Relevant literature review is carried out for the industrial byproducts utilization.

OPC is the most commonly used construction material. To meet the demand of the construction industries, the production of cement has been on the increase at an alarming rate every year. Cement production is associated with the release of 5-7% of total global CO₂ emission into the atmosphere due to burning of limestone (McLellan et al. 2011). Research efforts are ongoing across the world, to reduce the carbon footprint, due to serious environmental emissions. Construction industries need to take decisive measures to reduce CO₂ emissions by utilizing industrial byproducts to the extent possible. In general, majority of the industrial byproducts remain unused and are disposed off in the form of piles and landfills (Yaragal et al. 2016). The use of ground granulated blast furnace slag (GGBS), fly ash (FA), silica fume (SF), etc. are gaining importance as cementitious materials for researchers, as these reduce carbon footprint and indirectly provides a viable solution to the threat of global warming and waste disposal problems. In particular, industrial byproducts are very promising in their use, due to their mechanical strength and long-term durability performance under aggressive conditions (Sahoo et al. 2016; Das and Pandey, 2011).

Studies have advocated the incorporation of industrial byproducts into alkali activated binder (AAB) system (Wang et al. 1995). AAB is a new generation material and is produced from alumino silicate rich materials in the presence of alkali sources. Several studies have been reported, wherein FA has been used in AAS binders. The inclusion of FA in the AAS binders, provides improved workability due to its fine particle size and the morphology of the precursor (Wang et al. 2003). The workability of the AAS system improves due to the spherical shape of the FA used, which tends to provide “ball bearing” effect. Also, the FA introduction provides volumetric stability (Lee et al. 2014). FA, as a sole binder in the alkali activated system, has the problem of long term setting. With the addition of a small amount of slag, the problem of long-term setting time gets mitigated (Lee and Lee 2013). On the other hand, GGBS as sole binder is susceptible to chemical shrinkage, which leads to constant volume change without the application of an external load, thus influencing the long-term performance of the binders (Ye and Radlinska, 2013). As the FA replacement increases, the mechanical strength gets reduced in the AAS binders (Chi and Huang, 2013). Ismail et al. (2013) showed that this reduction in strength can be improved with the reduction in the water-to-binder ratio. Wardhono et al. (2015) have tried a combination of GGBS and FA as a binder. The most effective ratio of the binder being 50% GGBS and 50% FA for the elimination of heat curing in FA activation.

Researchers have tried to improve the properties of an AAS system with several other admixtures and additives. Douglas et al. (1991) studied the effect of lime on AAS and found that the introduction of lime improved the strength of the AAS system. Khater (2013) studied the effect of SF on AAS and stated that the incorporation of SF increased the compressive strength up to 7% due to the consumption of calcium hydroxide, which led to the formation of the calcium silicate hydrate (C-S-H) gel that served as a strength giving compound. Hot et al. (2015) studied the effect of calcium silicon byproduct of the calcium silicon industry, which was activated using potassium hydroxide. Researchers have considered the dosage of molarity five to be optimal in strength achievement. Collins and Sanjayan (1999a) reported the addition of 10% of ultrafine materials like condensed SF, ultrafine FA and ultrafine slag to the AAS. The compressive strength values, with the use of condensed SF in producing

concrete, were higher in the case of all ultrafine materials' blend and lowest in the case of ultrafine FA. However, the compressive strength of ultrafine blended FA showed better results compared with OPC concrete.

Hitherto, one of the industrial byproducts not largely researched is FCA. FCA is obtained from the gas cleaning plant of ferrochrome industries during the production of chromium. Chromium is the major additive used in stainless steel production and is responsible for lustre and non-corrosive properties. The annual global production of ferrochrome is around 6.5-9.5 million tonnes (MT) (Acharya and Patro, 2015). Ferrochrome production requires around 2.5 MT of chromite ore in production of 1 MT of ferrochrome, which results in the release of about 1-1.2 MT of solid waste. The disposal of this huge quantity of solid waste is a challenging problem due to the shortage of landfill areas and environmental issues. Therefore, the potential for utilizing it, in an effective manner without causing environmental and ecological problems needs further studies. FCA develops cementing properties when lime is added as an activator. Studies have reported that with 40% FCA and 7% lime, the mechanical properties of concrete such as compressive strength, split tensile strength and flexural strengths improvement (Acharya and Patro, 2015). Further, durability properties such as resistance to sulphate attack, abrasion, acid resistance and water permeability are also reported to improve considerably (Acharya and Patro, 2016a). Acharya and Patro(2016b) performed toxicity characteristic leaching procedure to ensure potential leaching behaviour of FCA replacement in the OPC based binder system. Acharya and Patro (2016c) further investigated by including FCA as binder and the FCS as NCA. The test results revealed that the contaminant levels were much below the regulatory limits.

Acharya (2014) carried out detailed study on the use of FCA as SCM. Results showed excellent performance under severe environmental conditions, such as sulphate attack, acid attack and abrasion resistance. In recent years, SCM are being utilized and thereby reducing the usage of OPC indirectly addressing issues such as reduced CO₂ emissions and waste disposal problems (Pelisser et al. 2018; Dave et al. 2017; Samad and Shah, 2017; Paris et al. 2016; Rashad, 2015a; Rashad, 2015b). Benefit of SCM and their consequences with alternative materials has been broadly deliberated by many researchers. Further, usage of SCM can be one possible way to reduce the

effect of elevated temperatures. SCM such as, FA, GGBS, etc., consumes Ca(OH)_2 by means of secondary pozzolanic reaction by generation of additional C-S-H gel (Rashad. 2015a; Rashad, 2015b; Rashad and Sadek. 2016; Dave et al. 2017). The generation of additional C-S-H gel increases the mechanical properties.

2.2 DURABILITY OF ALKALI ACTIVATED MATERIAL

Alkali activated materials (AAM) are known for their durable properties and provides sufficient strength. However, durability properties of AAM plays a vital role when AAM is in contact with aggressive environment. AAM are susceptible to chemical attack under various situations and sufficient care need to be taken to endure the chemical attack. Chemical attack on AAM may be caused due to its exposure to acid rain, sulphate rich soils, chemical effluents and aggressive chemical rich waste water. Exposure to chemical environment will affect the durability of AAM and leads to the degradation of AAM. Further chemical exposure will lead to failure of AAM to perform its intended purpose in its long term service with reduced mechanical strength (Provis and Van Deventer, 2013).

2.2.1 Sulphate resistance

Mehta (1983) as reported based on experimental evidence that, ettringite is the main reason for the expansion of concrete in normal Portland cement. This ettringite is formed due to the reaction between hydration products of cement and sulfate rich water. At later stage this expansion leads to cracking and causes loss in strength and stiffness. Sulphate-generated deterioration in normal Portland cement concretes include expansion, cracking, loss of strength and stiffness and sometimes disintegration. Fu et al. (1997) found that, increasing curing temperature, thermal treatment to drying concrete can reduce internal sulfate attack. Expansion in concrete can be delayed, if sand composed of limestone and quartz content of around 34% and 25% respectively when compared to significant amount of limestone and little quartz content. Cao et al. (1997) have shown that composition of cementations materials

plays a vital role in sulfate attack. Portland cement with low tri-calcium aluminate (C_3A) and di-calcium silicate (C_2S) perform in better in sulfate solutions. SCM such as, SF (5%) and FA (40%) replacement shows superior performance. Santhanam et al. (2002) have carried out experiments on cement mortars. The major findings are the steady diffusion of sulfate ions across the brucite surface barrier. The failure is attributed to the formation of magnesium silicate hydrate (M-S-H) by the process of decalcification of CSH under long period of exposure of solution. Ramyar and Inan (2007) reported that replacement of SCM with cement reduces sulfate attack and expansion in composite matrix. Due to reduced amount of C_3A and C_3S/C_2S ratio. Results generalized by providing equation to estimate expansion by knowing admixture replacement and concentration of sulfate solution.

2.2.2 Acid resistance

Sulfuric acid (H_2SO_4) is a very aggressive acid, that reacts with the free lime [$Ca(OH)_2$], in cement paste forming gypsum ($CaSO_4 \cdot 2H_2O$). This reaction is associated with an increase in volume of the concrete by a factor of 2.2. Another destructive action is the reaction between calcium aluminate present in cement paste and gypsum crystals. These two products will form the less soluble reaction product called ettringite ($3CaO \cdot Al_2O_3 \cdot 3CaSO_4 \cdot 32H_2O$). Ettringite is very expansive in nature and causes internal pressure in the concrete, which leads to the formation of cracks. The reacted surface becomes soft and white. Because of these, concrete structure loses its mechanical strength. Aydin et al. (2007) investigated the effect of Class C FA on the H_2SO_4 resistance of concrete. Based on experimental results, it was concluded that, (1) Loss in compressive strength was related to the FA content. The FA replacement seemed to improve the acid resistance of the steam-cured samples as loss percentages dropped to 21% (FA70) from 58% (FA0); (2) Negligible differences in weight-loss were observed for standard cured concrete with increasing FA content.

2.2.3 Volume of permeable voids

Tasnim et al. (2020) have carried out the VPV test on palm oil fuel ash (POFA) based paste samples. POFA used as replacement to OPC with various levels (i.e., 0, 10, 20 and 30%). VPV test is carried out on POFA based specimens size of 50x50x50 mm. Testing is done for the different curing periods of duration 28, 56 and 90 days under ammonium nitrate (NH_4NO_3) solution exposed POFA samples. Degradation of cementitious materials with NH_4NO_3 is commonly observed when cementitious materials are exposed to fertilizers. NH_4NO_3 exposure on OPC based cementitious materials results in decalcification of C-S-H and $\text{Ca}(\text{OH})_2$. Decalcification results in volumetric expansion and results in reduction of mechanical properties. In case of VPV tests, VPV value increases with NH_4NO_3 solution exposure period in case of 100% OPC based paste specimens due to decalcification of calcium hydroxide. Replacement of POFA in OPC paste specimens reduces the VPV value due to the reduction of leaching of $\text{Ca}(\text{OH})_2$ with formation of additional C-S-H gels.

Adesina and Das (2020) carried out a VPV tests on AAM. VPV testing was done based on ASTM C 642 using cylindrical specimens of size 100 mm diameters and 50 mm thickness. 100% GGBS, 50% GGBS + 50% FA and 100% FA based mortar mixtures were considered. All the three mixtures were activated using 8% of lime. 100% FA based mortar mixtures shows higher VPV compared to 100% GGBS based mortar mixture. Higher percentage of VPV is due to the lower reactivity of FA particles in 100% FA based mortar mixtures. Maiti et al. (2020) have studied the effect of titanium oxide (TiO_2) nano-particles on FA based geopolymer (GP) mortars. Three different particle sizes of 100, 50 and 30 nm TiO_2 were used in the FA based GP mortars prepared. VPV tests were conducted on cubic mortar specimens of size of 50X50X50 mm. Addition of 5% of 30 nm TiO_2 particles reduces the VPV values considerably when compared to other FA based GP mortar mixtures. Lower value of VPV indicates, lesser amount of permeable voids. Inclusion of 30 nm TiO_2 particles in FA based GP mortar mixture results in denser microstructure. Presence of adequate amount of TiO_2 in FA based GP mortar mixtures fills the pores or voids present in the mortar matrix. Further, denser microstructure of TiO_2 incorporated FA based GP mortars shows superior performance under chloride environment too. Similar

observations were made with introduction of nano-graphite particles in high performance cementitious nano composites. (Chougan et al. 2020). Saha et al. (2019) studied the effect of ferronickel slag (FNS) as NFA in mortar samples. As the amount of FNS increases, as a replacement to NFA in mortar mixture, percentage increase in VPV also gets increased. Increase in percentage of VPV value is due to the presence of cavities, micro voids, relatively larger particle size and angular shape of FNS particles compared to NFA. Kumar (2019) studied the effect of NFA replacement with recycled fine aggregate (RFA) mortar mixture. Study was carried out on 50 mm cube specimens. As the amount of RFA increases, the VPV also increases, increase in VPV is due to the higher water absorption value of RFA aggregate compared to NFA. Wongkeo et al. (2012) studied the effect of FA, bottom ash (BA) and SF replacement in OPC based mortar mixtures. FA and BA replacement to OPC increases the VPV value at early age (i.e., at 28 days curing). Whereas, SF introduction in OPC based mortar mixtures reduces the VPV value due to filler effect.

Yan et al. (2012) studied the effect of de-inking waste water from waste paper recycling plant on OPC based mortars. Increase in VPV value is observed with increase in the amount of water/binder (W/B) ratio. Water filled space creates the void, higher amount of water content results in higher volume of voids in mortar mixtures. Further, replacement of water with treated water results in an increase in VPV value due to transport properties of final finished mortar mixtures. Atabey et al. (2020) studied the effect of concentration of alkaline solution on FA based GP mortars. VPV testing was carried out using prism specimen of size $40 \times 40 \times 160$ mm by following ASTM C-642 guidelines. As the amount of alkaline solution concentration increases, the VPV value decreases.

2.2.4 Elevated temperature studies

Elevated temperatures due to the accidental event of fire, causes severe strength loss in cementitious materials. Elevated temperature exposure reduces the service life of structure and severely affects its performance. Effect of elevated temperatures on cementitious material, depends on several factors such as cement, aggregate type,

aggregate content, aggregate composition, aggregate size, microstructure and its mineralogical composition.

OPC based cement mortars disintegrates when exposed to 900 °C. Addition of 5% (by weight of OPC) of graphite has showed intact mortar specimens under elevated temperature. Though addition of graphite reduces the compressive strength at ambient condition but resistance to elevated temperature is quite higher compared to OPC based mortars (Cülfik et al. 2002). Mechanical properties of FA and MK based OPC mortars under elevated temperatures have been studied by Nadeem et al. (2013). 20% FA based OPC mortar mixture showed better performance under elevated temperature. Whereas, MK based OPC mortar mixtures were more susceptible to elevated temperatures exposure. MK based OPC mortar mixtures need to be used with due care, when elevated temperature reaches beyond 400 °C. Yazıcı et al. (2012) have studied the effect of FA, SF and pumice as binder in OPC based mortar mixtures under elevated temperatures upto 750 °C. Results also showed that, FA based OPC mortar mixture performance under elevated temperature is quite good compared to other binders. Türkmen and Fındık (2013) investigated the effect of GGBS, natural zeolite and waste glass powder (WGP) as binders with combination of expanded perlite aggregate (EPA) as NFA in OPC based mortar under elevated temperature condition. Increase in compressive strength is observed with elevated temperature exposure of 300 °C. Increase in compressive strength is due to the autoclave effect. 10% GGBS + 25% EPA in OPC based mortar mixture found to be suitable mortar mixture to endure the elevated temperature exposure of 800 °C compared to other mortar mixtures studied. Effect of recurring on elevated temperature was carried by Karahan (2011). Furnace, water and air cooling methods were considered before recurring in water and air for 7 days. Water cooling method showed severe strength loss compared to other methods of cooling. Further, water recurring for 7 days results improvement in residual compressive strength compared to air recurring method.

Karahan and Yakupoğlu (2011) studied the effect of elevated temperatures on AAS mortar mixtures. Alkaline solution concentration is considered as one of the parameter to study the effect of fire on AAS mortar mixtures. Elevated temperature studies were carried out on prismatic specimen of size 40X40X160 mm in electrical

furnace with a heating rate of 12⁰C/min. Before exposing the specimens to elevated temperatures. AAS mortar specimens were preconditioned from curing water and dried to 105 ⁰C in a furnace to avoid explosive spalling and to any damage to the furnace. 1 hour retention period is considered for AAS mortar specimens. After reaching to the desired temperature (1000 ⁰C) and retention period, AAS mortar specimens were cooled to room temperature within the furnace in switched off mode for 24 hours. Compressive strength tests were carried to identify the residual compressive strength of AAS mortar specimens. AAS mortar prepared with sodium silicate (Na₂SiO₃) based alkaline solution showed enhanced mechanical strength compared to AAS mortar prepared with sodium hydroxide (NaOH) and sodium carbonate (Na₂CO₃) based alkaline solution. Further, increase in alkaline solution concentration increases the residual compressive value under elevated temperatures condition.

Rashad et al. (2016) studied the effect of granulated blast furnace slag (GBS) as NFA in AAS mortar mixture. Cube specimens of size 25 mm were cast to conduct elevated temperature studies. Heating rate of 6.67 ⁰C/min, retention period of 2 hour and furnace cooling method is considered for elevated temperature studies on AAS mortar mixtures. GBS based AAS mortar mixtures showed reduced micro-crack under elevated temperature condition. Further, residual compressive strength of GBS based AAS mortar resulted in higher residual compressive strength compared to siliceous based NFA. Zhang et al. (2020a) studied the properties of recycled glass materials in AAS mortar mixture under elevated temperature condition. Slow heating rate of 2.5⁰C/min with 2 hour retention period is considered for the study. Results showed, excellent elevated temperature resistance with incorporation of recycled glass material in AAS mortar mixture.

MK based GP mortar mixtures did not show significant change in residual compressive strength under elevated temperatures condition upto 800 ⁰C (Kuenzel et al. 2013). Qu et al. (2020) studied the effect of preloading damage on FA and GGBS based GP mortar under elevated temperature condition. Presence of higher amount of GGBS in GP mortar mixtures resulted in higher compressive strength at room temperature. Whereas, lower amount of GGBS in GP mortar showed excellent

performance under coupled condition of preloading damage and elevated temperature condition.

2.2.5 Ecological studies

Shah et al. (2021) carried out environmental impact assessment (EIA) of one part AAM using lithium slag as binder. EIA was carried out by means of carbon di-oxide emission (ECO_{2eq}) in terms of strength performance. Result shows that, ECO_{2eq} of lithium slag based AAM is significantly less compared to OPC based mixture.

Na_2SiO_3 is the main source for alkaline solution preparation in production of AAM. Production of Na_2SiO_3 emits large amount of ECO_{2eq} . In order to reduce the impact caused by production, Rajan and Kathirvel (2020) carried out experiment to develop sustainable Na_2SiO_3 . Hydrothermal method is employed to produce Na_2SiO_3 . RHA and NaOH is used as raw material to develop Na_2SiO_3 . Na_2SiO_3 prepared with 2 hour of hydrothermal process found to be optimal solution. Na_2SiO_3 developed were utilized in AAS mixtures preparation. Utilization of synthesized Na_2SiO_3 in AAM mortar mixtures was found to give sufficient compressive strength in hardened state. Further, synthesized Na_2SiO_3 shows 65% lesser ECO_{2eq} compared to conventional commercially available Na_2SiO_3 .

WGP is used as precursor along with FA to prepare AAM. WGP is synthesized to size of 15.4 micron by means of ball milling. WGP utilization in AAM mixture preparation reduces the ECO_{2eq} compared to OPC based mixture. However, increase in ECO_{2eq} is observed with WGP compared to FA, due to the grinding of waste glass for the production of WGP (Xiao et al. 2020). ECO_{2eq} calculation of SF based AASFC mixture were carried out by Zannerni et al. (2020). 62% reduced ECO_{2eq} emissions were observed with introduction of SF in AAS/FA mixture compared to OPC based mixture.

2.3 OPTIMIZATION METHODS

Exhaustive literature survey related to multi-criteria decision method (MCDM) pertaining to cementitious material is carried out. Basically MCDM methods give

“best” and “worst” among the set of “alternatives” which were experimented. In the present case, “alternatives” refers to mixtures experimented.

A brief discussion on MCDM is presented as follows;

- 1) Grey relational analysis (GRA)
- 2) Technique for order preference by similarity to ideal solution (TOPSIS) and
- 3) Desirability function approach (DFA).

Since there is no ideal MCDM and each MCDM method has its own advantage and disadvantage. Optimization methods were organized into three sections, however it is to be noted that other interesting methods do exist as well.

2.3.1 Grey relational analysis

Prusty and Pradhan (2020) carried out experimental study on FA and GGBS based GPC mixture. Taguchi method and GRA method were coupled to reduce and to optimize the FA and GGBS based GPC mixture. GGBS replacement, water to GP solids (GPS) ratio, molarity of NaOH solution, binder content and $\text{Na}_2\text{SiO}_3/\text{NaOH}$ solution ratio were considered as input factors for the preparation of FA and GGBS based GPC mixture. Initial and final setting time, slump value and compressive strength were considered as output responses. GGBS replacement level played vital role and provides major contribution in setting time, compressive strength. Similarly, water to GPS ratio provides major percentage contribution in slump value. GGBS replacement level of 15%, water to GPS ratio of 0.31, molarity of NaOH solution of 14, binder content of 450 kg/m^3 and $\text{Na}_2\text{SiO}_3/\text{NaOH}$ ratio of 2.25 was found to be optimal GPC mixture.

Yaragal et al. (2020) carried out durability studies on the FCS based AASFC mixtures. FCS and FA were considered as input variables in preparation of AASFC mixtures. Full factorial method of design of experiments (DOE) was adopted for durability studies. VPV, residual compressive strength under acid and sulphate environment, $\text{ECO}_{2\text{eq}}$ and EE_{eq} were considered as output responses. 50% FA and 0% FCS based AASFC mixture was found to be optimal mixture. Major contribution to output responses were found to be with FA replacement level compared to FCS content.

Vasanthi and Selvan (2020) carried out investigation on nano-silica (nS) based OPC mortar mixtures. % of nS, W/B ratio and plasticizer content were considered to optimize the OPC based mortar mixtures. Taguchi method of DOE was used to reduce the number of experiments. GRA method was used to optimize the OPC based mixtures under given set of responses (i.e., compressive strength and water absorption). Equal weightage for compressive strength and water absorption was adopted. Based on GRA method 2% nS, 0.5 W/B ratio and 0.25% plasticizer content found to be optimal for the preparation of OPC based mortar mixtures. Further, ranking order indicates 0.5% nS, 0.5 W/B ratio and 0.5% plasticizer was found to be worst mixture compared to other OPC based mixtures studied.

Arıcı and Keleştemur (2019) studied the effect of steel scale as NFA in OPC based mortars. Taguchi method with L_{16} orthogonal array is used to reduce number of experiments. Total four input factors (i.e., OPC binder content, W/B ratio, fine scale steel aggregate (FSSA) and coarse scale steel aggregate (CSSA)) were considered for the experimental investigation. OPC and W/B ratio composed of two levels of variation. Whereas, FSSA and CSSA composed of four levels of variation. Compressive strength, flexural strength and porosity were considered as three output parameters. Compressive strength and flexural strength were maximized to optimize the mixtures. Porosity of the mortar were minimized to optimize the steel scale aggregate content in OPC based mortar. Grey relational grade (GRG) plays vital role in optimization. 500 kg/m^3 OPC, 0.5 W/B ratio, 5% of FSSA and 5% CSSA based OPC mortar mixture was found to be optimal mixture. Whereas, 500 kg/m^3 OPC, 0.6 W/B ratio, 5% of FSSA and 10% CSSA based OPC mortar mixture was found to be worst mixture compared to other mortar mixtures studied. Variation in OPC and W/B ratio input variable predominates the output parameters measured. Percentage contribution of FSSA and CSSA is 15% each on output response studied.

2.3.2 Technique for Order Preference by Similarity to Ideal Solution

TOPSIS is a MCDM method developed by Ching-Lai Hwang and Yoon in 1981. The main idea of TOPSIS is that the chosen alternative should have longest distance from negative ideal solution and shortest distance from positive ideal solution. In case of

cementitious material, TOPSIS method is useful to determine best cementitious mixture in the given set of mixtures. A brief literature related to TOPSIS method application in cementitious materials optimization is discussed below.

Rashid et al. (2020) carried out optimization of RCA based concrete mixtures. Figure 2.1 shows different steps involved, in the TOPSIS method. As stated in before, “alternatives” refers to mixtures to be optimized. “Criteria” refers to maximization or minimization of responses of RCA mixtures studied. Further, other terms in TOPSIS methods are decision matrix, normalization, best and worst ideal solution (or positive and negative ideal solution), separation distance (or Euclidean distance) of each response of alternatives and closeness coefficient of each alternatives (Yaragal et al. 2019).

Yaragal et al. (2019) have carried out the MCDM based optimization of FCS, GGBS and FA content in OPC based concrete. Total numbers of mixtures were reduced by means of Box-Behnkan design of experiments. Total 15 mixtures were considered with various levels of FCS as NCA, FA and GGBS as binder in OPC based mixtures. Principal component analysis was carried out to provide actual weightage for the responses chosen. Responses considered in optimization of FCS based OPC mixture are compressive strength at 28 and 90 days, workability of concrete and density of concrete. 0% FA, 30% GGBS and 50% FCS based OPC mixture attains first rank compared to other mixtures studied.

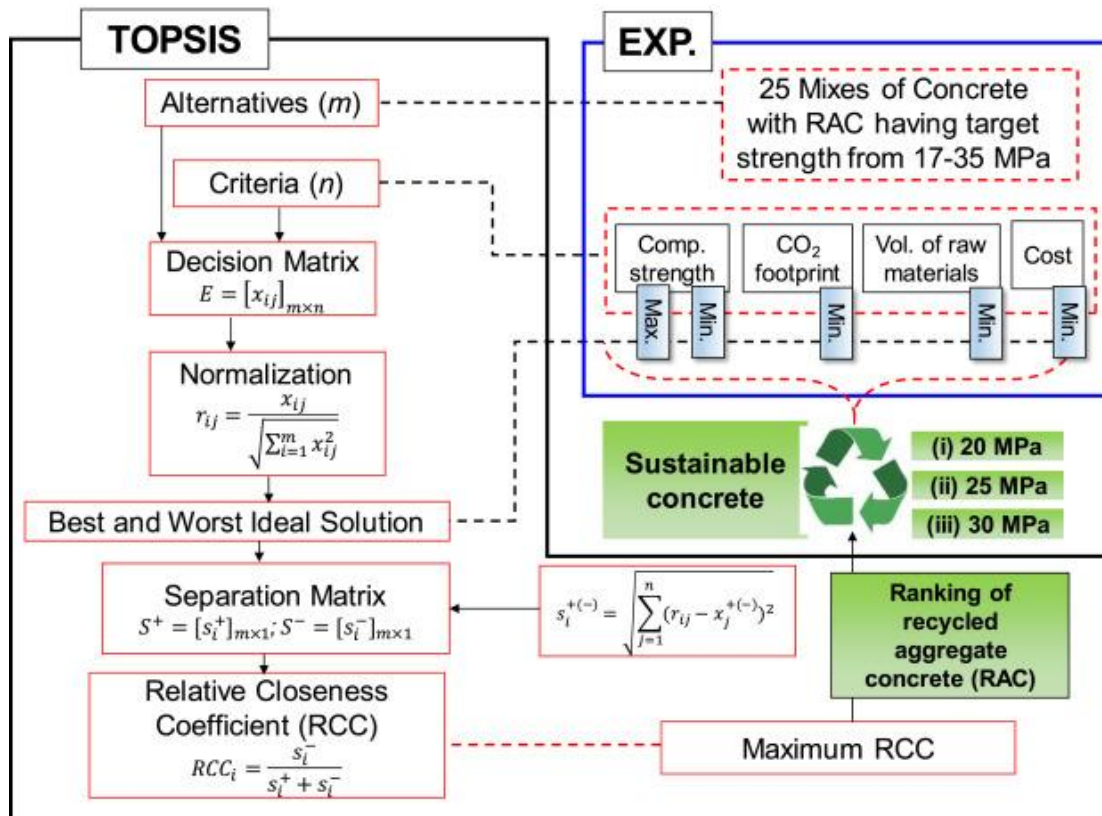


Figure 2.1: Typical flow of TOPSIS method in cementitious material optimization (Rashid et al. 2020).

2.3.3 Desirability function approach

DFA is one of the simplest MCDM in context of computation with reduced number of complex equation. Simplest form of DFA method was proposed by Derringer and Suich (1980). DFA method converts multiple responses into single response. Advantage of scaling of all the responses into single response will reduce the burden of reviewing each response simultaneously to identify optimal mixture. Converted single response values will be in the range of 0 to 1. Individual desirability values are calculated for each response with the aim to converting each response into single response. Several researchers used DFA method in construction material optimization problem and details are described as follows. Sengul and Tasdemir (2009) used DFA method for the optimization of FA and GGBS content in OPC binder with two different W/B ratios. Output responses for the optimization problems were compressive strength, chloride ion permeabilities and cost of concrete mixture. DFA method showed that, 50% GGBS based OPC concrete mixture prepared with

0.38 W/B ratio was found to be optimal mixture based on the responses compressive strength, permeability and cost.

Sonebi (2010) used DFA method to optimize viscosity modifying admixture (VMA) and SF content in cement grout preparation. Central composite fractional experimental design (CCFD) method is used to reduce the number of experiments. W/B ratio, high-range water reducer (HRWR) dosage, VMA dosage and SF content were considered as independent variables. Total sixteen mixtures were experimented to optimize cement grout. Minislump, cohesion plate, marsh cone, washout percentage, compressive strength values were considered as dependent variables to measure the effectiveness of cement grout.

Instead of equal weightage for all the dependent variables, predefined weightages were assigned to dependent variables to obtain overall desirability value of the cement grout mixtures. Cohesion plate test and compressive strength values were assigned higher weightage compared to other dependent variables studied. Overall desirability of cement grout mixture increases with increase in SF content and overall desirability decreases with increase in W/B ratio.

Yaragal et al. (2020) used the DFA method to arrive at optimal AASFC mixture under the elevated temperatures condition. FCS as a replacement to NCA and FA as a replacement to GGBS were considered as independent variable. Compressive strength at ambient condition and residual compressive strength under elevated temperatures were considered as dependent variables. AASFC mixture prepared with 100% FCS and 25% FA content was found to be optimal mixture compared to other mixtures studied.

2.4 RESEARCH GAP

Based on the literature review carried out, following research gaps were identified,

- 1) There is potential for utilization of FCA as a replacement to OPC based mortar preparation.
- 2) Very limited studies on utilization of FCA and there is potential for utilization of FCA as a replacement to GGBS as well in AAS binder system.

- 3) Elevated temperature studies on mortar mixtures with FCA, needs further understanding as there are studies available.
- 4) Performance studies such as sulphate attack, acid attack under aggressive environment with use of FCA in mortar mixtures needs further investigation.

From the exhaustive body of literature it is noticed that, performance of mortar mixtures with FCA needs further understanding. Durability of material is gaining increased importance in recent years. This comes as a result of the inadequate durability performance of several structures built in the previous decades, which places pressing important on construction budgets worldwide.

2.5 OBJECTIVES OF THE RESEARCH WORK

The purpose of this research is to study the performance of mortars with use of FCA as binder and its effect in aggressive environment.

The broad objectives of present research work are categorized under three sub heads;

- 1) Strength characteristics of OPC and AAS mortars with binders replaced by FCA and associated microstructure studies.
- 2) Durability studies on FCA based AAS mortar mixtures and optimization studies.
- 3) Elevated temperature studies and ecological studies on FCA based AAS mortar mixtures.

2.6 CLOSURE

This chapter presents a brief note on FCA as cementitious material and AAS binder system. In addition, VPV, elevated temperature, acid resistance and sulphate resistance studies on AAS binder systems are discussed. Further, literature on optimization methods like, GRA, TOPSIS and DFA have been discussed in detail. Based on the existing literature, research gaps were identified. Objectives were framed to fill the knowledge gap with the identified research gaps.

CHAPTER 3

MATERIALS AND METHODOLOGY

3.1 GENERAL

FCA is used as binder material for production of OPC and AAS based mortar mixtures. In this chapter, materials and methodology used for preparation of FCA based OPC and AAS mortar mixture preparations were described in detail. Procedure to determine and assess the compressive strength, residual compressive strength, durability aspects like acid resistance, sulphate resistance and elevated temperature endurance are described in detail. Further, ecological and economical studies carried out on FCA based OPC and AAS mortar mixtures are discussed. Microstructure analysis and optimization methods are also described in detail.

3.2 MATERIALS

Production of FCA based OPC mortar mixtures includes basic materials like, OPC, FCA, lime, NFA and water. Similarly, FCA based AAS mortar mixtures include several materials like, FCA, GGBS, NFA, water, NaOH and Na₂SiO₃. These basic materials play a vital role in the prepared FCA based OPC and AAS mortar mixtures. Characterization of these materials is essential. Brief details of these materials are as follows.

3.2.1 Cement

53-Grade OPC, conforming to IS 12269-2013 is used in the present study. Chemical oxide composition of OPC is presented in Table 3.1. Physical properties like, specific gravity, Blaine's specific surface area, initial and final setting times were 3.1, 345 m²/kg, 65 minutes and 215 minutes, respectively.

.Table 3.1: Chemical oxide composition of OPC (by % weight).

Constituents	CaO	Al ₂ O ₃	Fe ₂ O ₃	SiO ₂	MgO	Na ₂ O	K ₂ O	SO ₃	Cr ₂ O ₃	LOI
OPC	59.53	9.12	3.52	20.34	2.02	0.19	0.42	2.39	-	1.4

Note: LOI - Loss on Ignition

3.2.2 Ferrochrome ash (FCA)

FCA was supplied from M/s Balasore alloys Ltd., Balasore, Odissa, India. Chemical oxide composition of FCA is presented in Table 3.2. Figure 3.1(a) presents SEM image of spherical FCA particles. XRD pattern of FCA is shown in Figure 3.1(b). FCA is composed of calcium, aluminum, silica, iron, magnesium, sodium and chromium rich minerals like coesite (SiO₂), chromite (FeOCr₂O₃), spinel (MgAl₂O₄), jadeite (NaAlSi₂O₆) and aragonite (CaCO₃).

Table 3.2: Chemical oxide composition of FCA (by % weight).

Constituents	CaO	Al ₂ O ₃	Fe ₂ O ₃	SiO ₂	MgO	Na ₂ O	K ₂ O	SO ₃	Cr ₂ O ₃	LOI
FCA	4.20	11.21	6.15	19.62	15.61	1.34	14.51	-	12.44	4.1

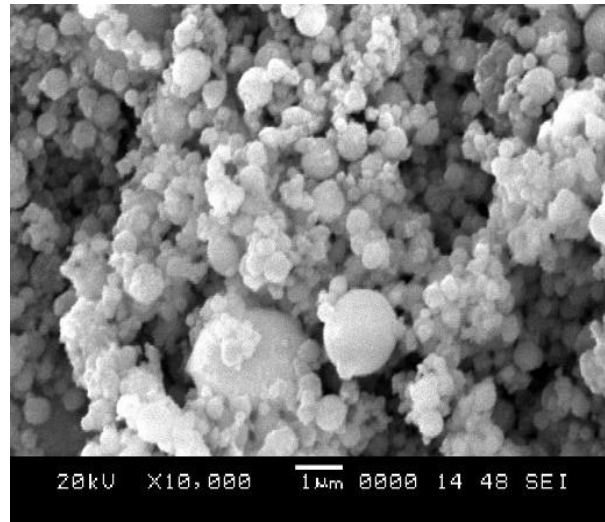


Figure 3.1: (a) SEM image of spherical FCA particles.

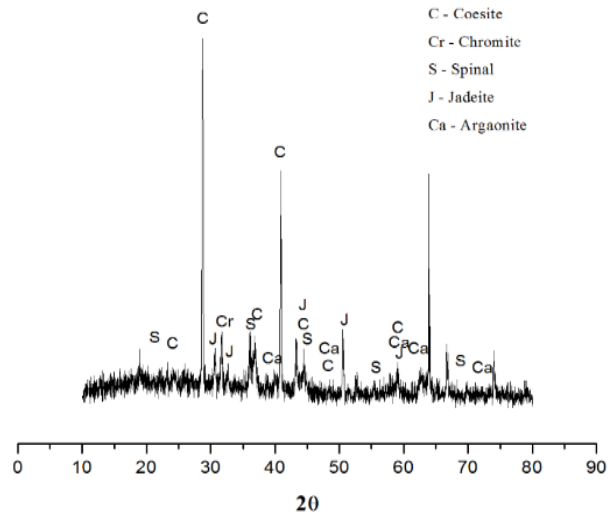


Figure 3.1: (b) Mineralogical phases of FCA particles.

3.2.3 Lime

Lime used in the present study was procured from local market. Figure 3.2 (a) shows SEM image of lime, which is irregular in shape. Figure 3.2 (b) shows mineralogical composition of lime, which mainly consists of calcium hydroxide (CH) and calcium carbonate (CC).

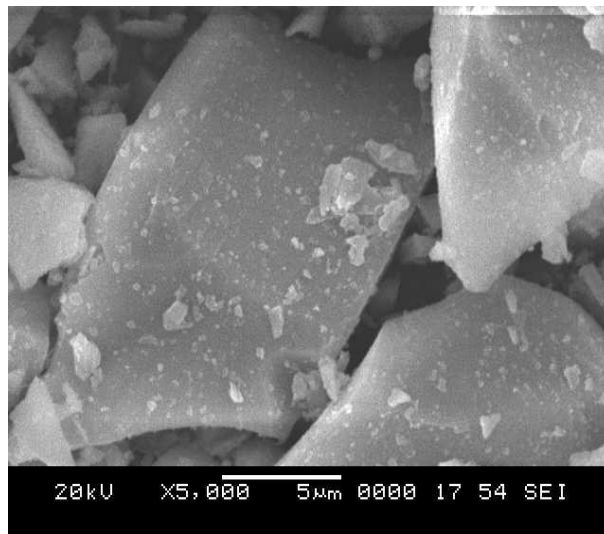


Figure 3.2: (a) SEM image of lime particles.

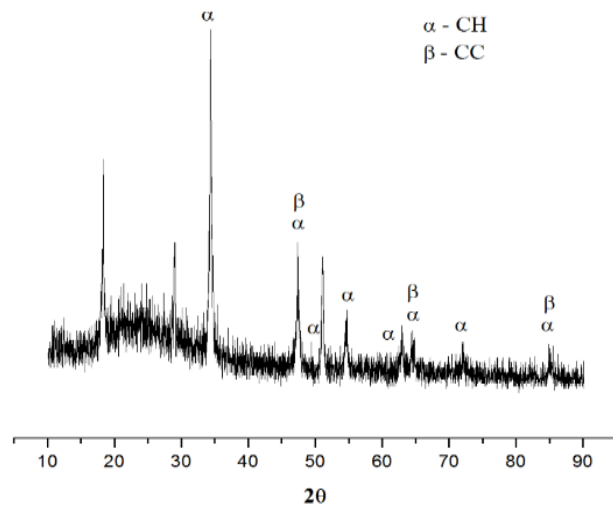


Figure 3.2: (b) Mineralogical phases of lime particles (CH - calcium hydroxide, CC - calcium carbonate).

3.2.4 Ground granulated blast furnace slag

GGBS was supplied by M/s JSW, Bellary, Karnataka, India, GGBS usually found in white colour. The chemical oxide composition of GGBS is shown in Table 3.3. The SEM image of GGBS is shown in Figure 3.2 (a). It is observed that, GGBS is irregular in shape due to the grinding process while producing. Figure 3.2(b), shows XRD pattern of GGBS. GGBS is mainly composed of calcium, aluminium and silica rich minerals like, anorthite ($\text{CaAl}_2\text{Si}_2\text{O}_8$, PDF#-00-041-1486) and gehlenite ($\text{Ca}_2\text{Al}_2\text{SiO}_7$, PDF#-00-035-0755).

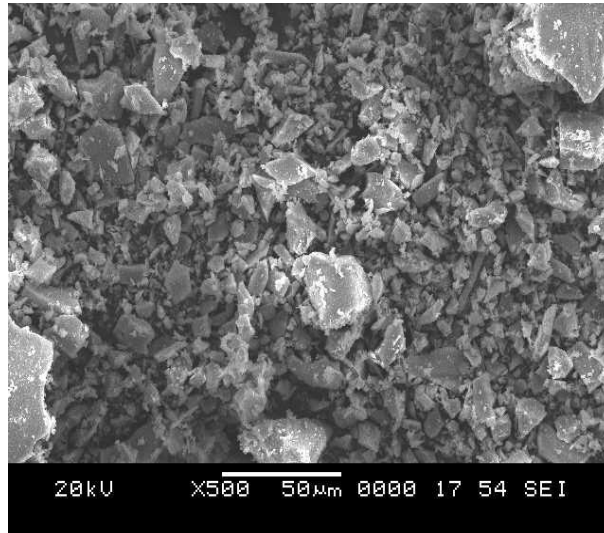


Figure 3.3 (a): SEM image of GGBS particles.

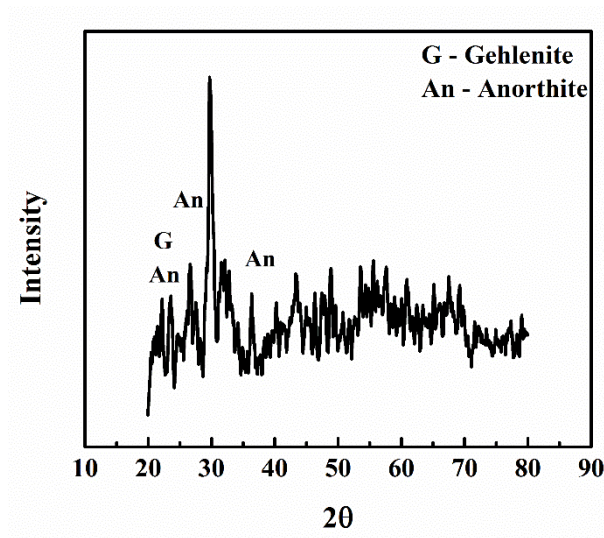


Figure 3.3 (b): Mineralogical phases of GGBS particles.

Table 3.3: Chemical oxide composition of GGBS (by % weight).

Constituents	CaO	Al ₂ O ₃	Fe ₂ O ₃	SiO ₂	MgO	Na ₂ O	K ₂ O	Cr ₂ O ₃
GGBS	35.1	16.9	1.3	32.9	4.5	0.14	0.06	-

3.2.5 Alkaline solution

Alkaline solutions were prepared and used as alkaline activators for the preparation of AAS mortar mixtures. Sodium silicate (Na_2SiO_3) and sodium hydroxide (NaOH) flakes (97% purity) with the required amount of water to maintain W/B ratio of 0.4 with Na_2O dosage and modulus of silica (M_s) were used to cast the specimen in airtight containers. Na_2SiO_3 and NaOH flakes were obtained from the local market. Na_2SiO_3 is mainly composed of 8.5% Na_2O , 28% SiO_2 and 63.5% H_2O . In order to have good workable mixtures, linear relations were developed with R^2 value close to 1. The extra amount of water, Na_2SiO_3 and NaOH flakes required for the preparation of the alkaline solution is graphically presented in Figure 3.4 for different levels of the M_s . It can be noted from Figure 3.4 that as the M_s increases, the amount of extra water to be added decreases due to the presence of the chemically bound water in the Na_2SiO_3 . Table 3.4 shows typical calculation of different materials to be used for the preparation of alkaline solution. Na_2O dosage of 4% and M_s of 1.25 is considered for the calculation of different ingredients used in preparation of alkaline solution.

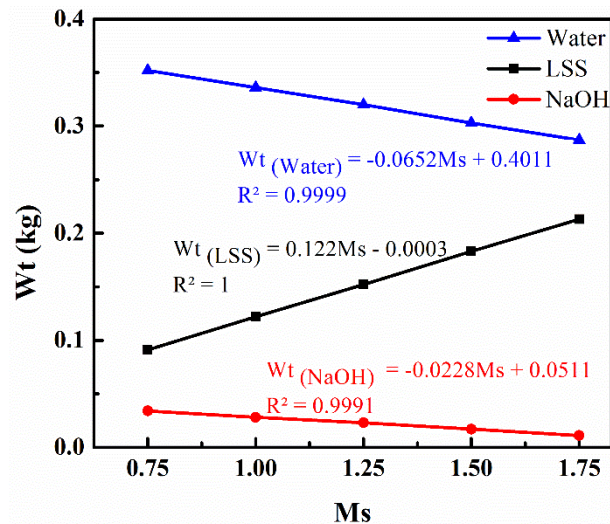


Figure 3.4: Weights of water, Na_2SiO_3 and NaOH required preparing alkaline solution of different M_s ratio.

Table 3.4: Calculation of different ingredient quantity used in alkaline solution preparation.

Sl. No	Flow of Calculation	Quantity	Unit
1	Total quantity of binder	1000	kg
2	W/B ratio	0.4	
3	Na ₂ O dosage	4	%
4	Modulus of silicate (M _s)	1.25	
5	Na ₂ O content present in Na ₂ SiO ₃	0.147	
6	SiO ₂ content present in Na ₂ SiO ₃	0.328	
7	H ₂ O content present in Na ₂ SiO ₃	0.525	
8	Weight of water required to maintain W/B ratio	400	kg
9	Total weight of Na ₂ O content	40	kg
10	Total weight of Na ₂ SiO ₃ content	152.4	kg
11	Na ₂ O content present in Na ₂ SiO ₃ (with reference to Sl. No 10)	22.4	kg
12	NaOH flakes required	22.7	kg
13	Weight of water in Na ₂ SiO ₃	80.0	kg
14	Total weight of water for total mixture	319.97	kg

3.2.6 Natural fine aggregate

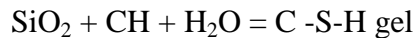
Locally available saturated surface dry and clean natural siliceous sand having 4.75 mm maximum size was used as NFA in the preparation of mortar mixtures. The gradation of sand used conformed to zone II as per IS 383-2016 grading requirement. The specific gravity, fineness modulus, water absorption value and compacted bulk density of sand were 2.54, 2.59, 0.9% and 1681 kg/m³, respectively. Table 3.5 presents the sieve analysis result of NFA.

Table 3.5: Sieve analysis results of NFA.

Sieve Size	10 mm	4.75 mm	2.36 mm	1.18 mm	600 µm	300 µm	150 µm
Cumulative Percentage Passing	100	98	96.2	75.3	53.6	14.8	2.9
Remarks	Zone II (as per IS-383:2016)						

3.3 PREPARATION OF FERROCHROME ASH BASED ORDINARY PORTLAND CEMENT MORTAR MIXTURES AND TESTING PROCEDURE

Due to hydration of tri-calcium silicate and di-calcium silicate, calcium silicate hydrate (CaO, SiO₂, H₂O) & Calcium hydroxide Ca(OH)₂ are formed - CSH and CH gels. Calcium silicate hydrate (C-S-H) gel contributes towards strength, while calcium hydroxide Ca(OH)₂ is an unimportant product & leaches out making the concrete porous. Pozzolanic materials those are added to blend the cement are siliceous or siliceous aluminous materials having little or no cementitious value. But these materials when react with calcium hydroxide Ca(OH)₂ in presence of moisture at ordinary temperature possess cementitious properties.



If additional SiO₂ in shape of pozzolanic material and calcium oxide is made available, there is chance of further creation of C-S-H gel.

Mortar mixtures were prepared by using binder to NFA ratio of 1:3. Along with W/B ratio of 0.4, three mortar mixtures proportion are adopted in the present study. Three mortar mixtures composed of 0%, 10% FCA and 7% lime and 20% FCA and 7% lime as a replacement to OPC. Table 3.6 presents three mixtures composition and its mixture identity.

Table 3.6: Mixture composition of FCA based OPC mortar mixtures.

Sl No.	Mixture ID	Mixture Composition
1	M1	100% OPC + 0% FCA + 0% Lime
2	M2	83% OPC + 10% FCA + 7% Lime
3	M3	73% OPC + 20% FCA + 7% Lime

Mortar cubes were cast using standard moulds as per IS 10086:1982 of size 70.6 mm to measure compressive strength of FCA based OPC mortar mixtures. Cast mortar cubes were allowed to set for one day under room temperature of $24 \pm 5^{\circ}\text{C}$ with relative humidity of $90 \pm 5\%$. The samples were demoulded after 24 hours and then cured under water for 28, 56 and 84 days in water. After 28, 56 and 84 days of water curing, the samples were dried for one hour and then crushed to failure to determine the compressive strength of mortar specimens as per IS 4031(Part 6):1959. Figure 3.5 shows, compressive strength testing setup used to measure compressive strength of mortars. Compressive strength is reported as average of three mortars specimen result.



Figure 3.5: Compressive strength testing setup.

3.4 PREPARATION OF FERROCHROME ASH BASED ALKALI ACTIVATED SLAG MORTAR MIXTURE AND TESTING PROCEDURE

Production of AAS mortar mixtures is quite complex compared to OPC based mortar mixtures. In order to assess the strength parameters, the binder to NFA ratio = 1:3 and W/B ratio = 0.4 of the mortar mixtures was kept constant. Fresh mortars containing 0, 25 and 50% FCA replacing slag on weight basis were prepared by modifying the control mixture prepared with 0% FCA. Na_2O dosage (4%) and $M_s = 0.75, 1, 1.25, 1.5$ and 1.75 were used to prepare alkaline solutions. Fresh mortars containing 0, 25 and 50% FCA replacing slag on mass basis were prepared by modifying the control mixture prepared with 0% FCA. Na_2O dosage (4, 5 and 6%) and $M_s = 1.25$ were used to prepare alkaline solutions. Potable water was used in all the experiments undertaken. Table 3.7 shows the different materials composition of FCA based AAS mortar mixtures used for the study in this work.

Table 3.7: Mixture composition of FCA based AAS mortar mixtures.

Sl. No	Composition of Binders	Influencing Factors used for Alkaline Solution Preparation
1	(100% GGBS + 0% FCA)	Na_2O : 4% by weight of binder (Constant) M_s : 0.75, 1, 1.25, 1.5 and 1.75 Remark: Discussed in Chapter 4
	(75% GGBS + 25% FCA)	
	(50% GGBS + 50% FCA)	
2	(100% GGBS + 0% FCA)	Na_2O : 4, 5 and 6% 4% by weight of binder M_s : 1.25 (Constant) Remark: Discussed in Chapter 5 and Chapter 6
	(75% GGBS + 25% FCA)	
	(50% GGBS + 50% FCA)	

3.5 SCANNING ELECTRON MICROSCOPY, X-RAY DIFFRACTION and FOURIER-TRANSFORM INFRARED SPECTROSCOPY

Attempts were made to ascertain the likely reasons for strength development using advanced characterizing instruments like the field emission SEM (FESEM-EDAX) and the XRD. The FESEM images of the AAS mortars were obtained using the Carl Zeiss scanning electron microscope. Elemental analysis was carried out using the EDAX. Mineralogical composition or the hydration products of the AAS mortar with different FCA replacement levels were studied using the XRD with Cu-K α radiation of wavelength (λ) = 1.5406 Å. The Fourier Transformed Infrared (FTIR) spectra were measured by the Bruker (Alpha) using the attenuated total reflection technique in the scan range of 600-4000cm⁻¹.

3.6 VOLUME OF PERMEABLE VOIDS ON ALKALI ACTIVATED SLAG BASED MORTAR MIXTURES

VPV is calculated based on ASTM C-642-13. Oven dry mass of FCA based AAS mortar mixtures were determined by placing mortars at 110 \pm 5 °C (Minimum 24 hours for oven drying). Saturated mass of FCA based AAS mortar mixtures after immersion and boiling were recorded as per the standards. Oven-dry mass, saturated mass were measured by immersion and boiling in water respectively to find out the VPV of FCA based AAS mortar mixture.

3.7 ACID RESISTANT TESTS ON ALKALI ACTIVATED SLAG BASED MORTAR MIXTURES

Acid resistant tests were conducted on FCA based AAS mortar specimen by immersing them under sulphuric acid (H₂SO₄) solution. 1% H₂SO₄ solution is prepared for pH value of \approx 1 is used (Conc H₂SO₄ having density of 1.83g/cm³ and 98% purity). Specimens

were placed in tub with minimum clearance to each other. Minimum 30 mm depth of solution was maintained from the top surface of specimen to ensure uniform exposure of H_2SO_4 . pH of the solution was checked periodically using portable pH meter. If any variation in pH is observed, then solution is made up with additional H_2SO_4 to maintain the required pH of 1. FCA based AAS mortar specimen were kept in newly prepared solution for 30 days each upto testing period of 90 days. Residual compressive strengths were measured for every 30 days for upto 90 days (Attigobe and Rizakalla, 1988; Palankar et al. 2016). Figure 3.6 shows acid solution exposed FCA based AAS mortar specimen.



Figure 3.6: FCA based AAS mortar mixtures exposed to acid solution.

3.8 SULPHATE RESISTANT TEST ON FERROCHROME ASH BASED ALKALI ACTIVATED SLAG MORTAR MIXTURES

Sulphate resistant test were conducted on FCA based AAS mortars specimen by immersing them in magnesium sulphate ($MgSO_4$) solution. 5% $MgSO_4$ solution media is chosen for the present study (Xie et al. 2019c, Gu et al. 2015, Yi et al. 2015, Yi et al. 2014, Rajamane et al. 2012, Bonen and Cohen, 1992).

After immersion of FCA based AAS mortar specimens in $MgSO_4$ solution, prepared $MgSO_4$ solution was maintained under constant pH in the range 6.5-7.5, by addition of concentrated nitric acid. FCA based AAS mortar specimens were kept in freshly prepared $MgSO_4$ solution for every month until the test period of 6 months. Residual compressive strength was measured for 30, 90 and 180 days. $MgSO_4$ solution immersed and air dried FCA based AAS mortar specimen. Figure 3.7 shows the $MgSO_4$ solution exposed FCA based AAS mortar mixtures.



Figure 3.7: FCA based AAS mortar mixtures exposed to $MgSO_4$ solution.

3. 9 ELEVATED TEMPERATURE STUDIES ON FERROCHROME ASH BASED MORTARS

After 90 days of water curing, test specimens were dried at room temperature for 1 hour. Afterwards, the specimens were subjected to elevated temperatures in a programmable electrical furnace. Figure 3.8 shows, programmable electric furnace used in the present study. The samples were set to maintain little gap from bottom of furnace chamber and were relatively at a large distance from heating coils to enable uniform dispersion of heat

to specimen and also avoid damage to the furnace coils in case of severe spalling (Yaragal et al. 2010, Kulkarni et al. 2017, Kulkarni et al. 2019). Specimen were heated at the rate of 5 °C/min to reach desired temperature level (upto 800°C), after reaching the desired test temperature, specimen were held for a retention period of half an hour. Then power supply to furnace was turned off and specimen were cooled to room temperature. Prior to conduct of compressive test, specimen were stored in laboratory condition for 20 hours (Hiremath and Yaragal, 2018).



Figure 3.8: Programmable electric furnace used for elevated temperature studies.

3.10 ECOLOGICAL STUDIES OF FERROCHROME ASH BASED MORTAR MIXTURES

Ecological analysis was carried out based on the guidelines of ISO 14040 and ISO 14044 (Ueda et al. 2019). The OpenLCA software by Greendelta with Ecoinvent 3.5 as the background database was used in the present study (Navarro et al. 2018). For ecological analysis, the processes which come under the “Cradle to Gate” stages were considered in the present study. Four major steps were considered in the ecological analysis: 1)

Definition of scope and system boundaries, i.e., functional unit and production of 1:3 mortar was considered as a functional unit in the present study. Further, AAS mortar mixtures emissions with the different levels of FCA replacement (i.e., 0, 25 and 50% of FCA) were compared with the OPC based mortar mixture emissions, 2) Collection of the inventory of raw materials used, i.e., lifecycle inventory was done based on Ecoinvent 3.5. Table 3.8 shows the quantity of the different materials and Ecoinvent modules used in the present study, 3) Lifecycle impact assessment was done based on two major impact categories, namely, embodied carbon dioxide (ECO_{2eq}) and embodied energy (EE_{eq}). Intergovernmental panel on climate change (IPCC) based impact assessment method was adopted for the calculation of ECO_{2eq} , i.e., IPCC 2013 GWP 100a. The EE_{eq} calculations were done based on cumulative energy demand (CED) method suggested by Ecoinvent. The calculations were carried out by the open sourced OpenLCA 1.9 Software with Ecoinvent 3.5 as the background data and 4). The interpretation or comparison of the impacts for different mixtures, i.e., 100% OPC-based mortar, 100% GGBS + 0% FCA, 75% GGBS + 25% FCA and 50% GGBS + 50% FCA, AAS based mixtures has been done. Further, the cost analysis was carried out for different mortar mixtures based on the market rates given in Table 3.8.

Table 3.8: Quantity, Ecoinvent modules and market rates of materials of FCA based mortar mixtures used in ecological analysis.

Raw Materials	Quantity	Ecoinvent Modules	Market Rate in USD/kg
Cement	1000 kg for OPC based mortar	Cement production, Portland cement, Portland Cutoff, S – RoW (Pradhan et al. 2019)	0.055
GGBS	1000, 750 and 500 kg of GGBS was used for 0, 25 and 50% for FCA replacement, respectively.	Ground granulated blast furnace slag production ground granulated blast furnace slag Cutoff, S – RoW (Marinković et al. 2018; Abdulkareem et al. 2019)	0.028
FCA	0, 250 and 500 kg of	Waste flow, Unspecified. (Gettu et al.	0

	FCA was used for 0, 25 and 50% for FCA replacement, respectively.	2019)	
Water	400 kg for OPC based mortar mixtures. 319.6 kg for AAS based mortar mixtures.	Water production, deionised, from tap water, at user water, deionised, from tap water, at user Cutoff, S – RoW (Pradhan et al. 2019)	0.00014
Sand	3000 kg for OPC and AAS based mixtures.	Gravel and sand quarry operation sand Cutoff, S – RoW (Pradhan et al. 2019)	0.014
Sodium silicate	152.2 kg for AAS based mortar mixtures.	Sodium silicate production, hydrothermal liquor, product in 48% solution state sodium silicate, without water, in 48% solution state Cutoff, S – RoW (Marinković et al. 2018; Abdulkareem et al. 2019)	0.19
Sodium hydroxide	22.6 kg for AAS based mortar mixtures.	Chlor-alkali electrolysis, mercury cell sodium hydroxide, without water, in 50% solution state Cutoff, S – RoW (Marinković et al. 2018; Abdulkareem et al. 2019)	0.31

Note: RoW = Rest of World

3.11 OPTIMIZATION METHODS USED FOR FERROCHROME ASH BASED ALKALI ACTIVATED SLAG MORTAR MIXTURES

Three different optimization techniques were employed in the present study, 1) Grey relational analysis (GRA), 2) Technique for order preference by similarity to ideal solution (TOPSIS) and 3) Desirability function approach (DFA). Optimization techniques were used to check the effectiveness of control factor (FCA and Na₂O dosage) influence on the responses of mortar by converting multi response optimization problem (In Chapter 5: VPV, sulphate resistance and acid resistance; In Chapter 6: Residual

compressive strength under elevated temperature, EE_{eq} and ECO_{2eq}) into single response optimization problem (Papathanasiou and Ploskas, 2018).

3.11.1 Grey relational analysis

GRA is firstly introduced and formulated by Deng Julong (Deng, 1989). GRA is suitable for solving complicated interrelationships between multi factors and variables. GRA has been carried out based on the literature given by Singh et al. 2016; Gopal and Prakash, 2018.

Step 1: Normalization of responses

First step of GRA is either to maximize or minimize the response. In the present study, maximization and minimization of responses were done using Equation (3.1) and (3.2) respectively.

$$y_{i(k)}^* = \frac{(x_i^0 - \min x_i^0)}{(\max x_i^0 - \min x_i^0)} \quad (3.1)$$

$$y_{i(k)}^* = \frac{(\max x_i^0 - x_i^0)}{(\max x_i^0 - \min x_i^0)} \quad (3.2)$$

Where, x_i^0 = Responses value

$\max x_i^0$ and $\min x_i^0$ = Maximum and minimum values of responses respectively

Step 2: Calculation of grey relational coefficient (GRC)

Equation (3.3) is employed to calculate the GRC of normalized values from step 1.

$$\xi_{i(k)} = \frac{\Delta_{\min} + \zeta \Delta_{\max}}{\Delta_{oi(k)} + \zeta \Delta_{\max}} \quad (3.3)$$

Where, $\Delta_{oi(k)}$ = Offset in the absolute values

Δ_{\max} and Δ_{\min} = Maximum and minimum values of $\Delta_{oi(k)}$

ζ = Characteristic coefficient

Step 3: Calculation of grey relational grade (GRG)

GRG can be computed using the Equation (3.4):

$$\gamma_i = \frac{1}{n} \sum_{k=1}^n \omega \xi_{i(k)} \quad (3.4)$$

Where, n = Number of experimental runs

ω = Weightage of each response (0.33)

γ_i = Grey relational grade

3.11.2 Technique for order of preference by similarity to ideal solution

TOPSIS is one of the multi-objective based optimization technique. TOPSIS was mainly based on the closeness coefficient values. Closeness coefficient values involve conversion of multi-objective responses into single dimensionless quantity. Closeness coefficients were calculated based on literature given by Simsek et al. 2013; Vijayaraghavan et al. 2017; Mousavi-Nasab and Sotoudeh-Anvari, 2017.

Step 1: Preliminary step is to arrange the responses into matrix form to normalize the response.

$$D_m = \begin{pmatrix} x_{11} & \dots & x_{1n} \\ \dots & \dots & \dots \\ x_{m1} & \dots & x_{mn} \end{pmatrix}$$

Where, x_{mn} = Response of i^{th} alternative about the j^{th} attribute.

Step 2: Normalization of responses

Normalization of responses were done using the Equation (3.5):

$$\gamma_{ij} = \frac{x_{ij}}{\sqrt{\sum_{i=1}^n x_{ij}^2}} \quad (3.5)$$

Where, x_{ij} = Actual values of responses

γ_{ij} = Normalized values of responses

Step 3: Calculation of weighted normalized responses

Weighted normalized responses were calculated using Equation (3.6):

$$V_{ij} = \gamma_{ij} \times w_{ij} \quad (3.6)$$

Where, w_{ij} = Weightage of response (0.33)

V_{ij} = Weighted normalized response

Step 4: Calculation of positive and negative ideal solution

Positive and negative ideal solutions were calculated, based on Equations (3.7a and b).

$$V^+ = \left\{ \left(\sum_i^{\max} U_{ij} \mid j \in J \right), \left(\sum_i^{\min} \mid j \in J \mid i = 1, 2, 3..m \right) \right\} \quad (3.7a)$$

$$= \{V_1^+, V_2^+, V_3^+, \dots, V_n^+\}$$

$$V^- = \left\{ \left(\sum_i^{\min} U_{ij} \mid j \in J \right), \left(\sum_i^{\max} \mid j \in J \mid i = 1, 2, 3..m \right) \right\} \quad (3.7b)$$

$$= \{V_1^-, V_2^-, V_3^-, \dots, V_n^-\}$$

Step 5: Calculation of Euclidean distance and closeness coefficient

Euclidean distance or separation was calculated using the positive and negative ideal solution using Equation (3.8a and b). Closeness coefficient is evaluated based on Equation (9).

$$D_i^+ = \sqrt{\sum_{j=1}^n (V_{ij} - V_j^+)^2}, i = 1, 2, \dots, i \quad (3.8a)$$

$$D_i^- = \sqrt{\sum_{j=1}^n (V_{ij} - V_j^-)^2}, i = 1, 2, \dots, i \quad (3.8b)$$

$$CC = \frac{D^-}{D^+ + D^-} \quad (3.9)$$

3.11.3 Desirability function approach

To maximize the responses like compressive strength and residual compressive strength of AASFC mixtures, desirability function approach was used. Steps involved in DFA have been based on the work of Sengul and Tasdemir, 2009.

Step 1: Conversion of responses into individual desirability (d_i)

Individual desirability is computed based on whether the responses are to be maximized or minimized. In the present case, compressive strength and residual compressive strength should be maximized. To maximize responses, each response is to be translated to individual desirability. Equation (3.10) is used to maximize the responses into individual desirability. Individual desirability values usually vary from 0-1.

$$d_i = \begin{cases} 0 & y_i \leq y_{i\min} \\ \left[\frac{y_i - y_{i\min}}{y_{i\max} - y_{i\min}} \right]^r & y_{i\min} < y_i < y_{i\max} \\ 1 & y_i \geq y_{i\max} \end{cases} \quad (3.10)$$

Where, y_i = Individual responses value

y_{imax} and y_{imin} = Maximum and minimum values of responses

d_i = Individual desirability value

r = Weightage of each response (0.33)

Step 2: Calculation of overall desirability (D)

Each individual desirability values were converted to overall desirability. Overall desirability can be computed using the Equation (3.11). The lower value of overall desirability indicates the worst case and the higher value of overall desirability is considered as optimized FCA based AAS mortar mixture.

$$D = (d_1 \times d_2 \times \dots \times d_n)^{\frac{1}{n}} \quad (3.11)$$

Where, D = Overall desirability of responses value

$d_1, d_2, d_3, \dots, d_n$ = Individual desirability (d_i) and n represents a number of experimental runs.

3.12 FLOW CHART OF PRESENT RESEARCH WORK

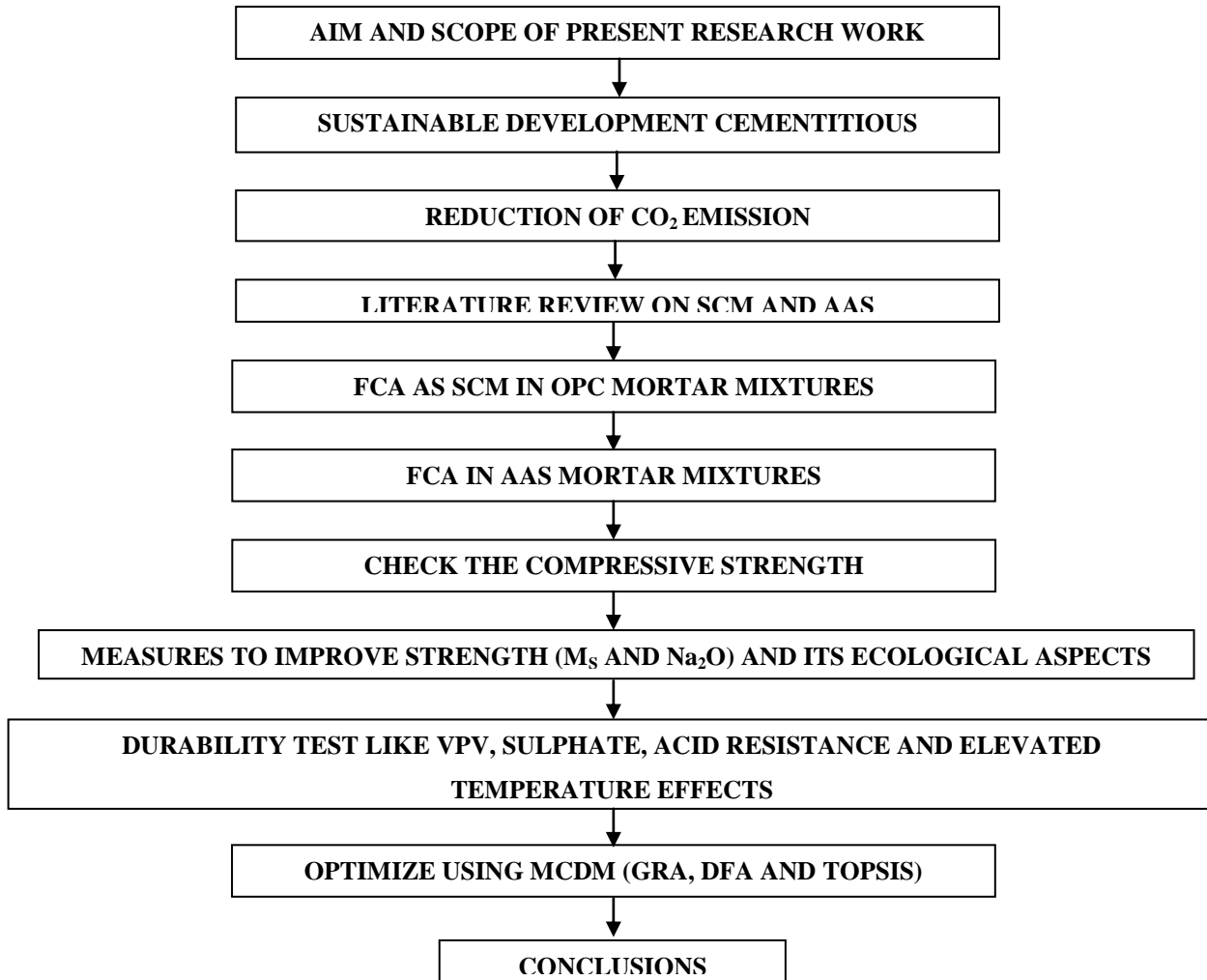


Figure 3.9: Flow chart of present research work.

3.13 CLOSURE

Physical and chemical properties of OPC, FCA, GGBS, lime, NFA, alkaline solution and water are used in the preparation of FCA based mortars is presented. Testing procedure for mechanical properties, microstructure studies, ecological studies and optimization methods used for FCA based mortars in the present thesis is also detailed comprehensively.

CHAPTER 4

FERROCHROME ASH– ITS USAGE POTENTIAL IN ORDINARY PORTLAND CEMENT AND ALKALI ACTIVATED SLAG MORTARS

4.1 GENERAL

In this chapter, an attempt is made to ascertain the usage of FCA. Study is carried out in two phases. First phase deals with utilization of FCA as SCM for OPC based mortar mixtures. Consistency, compressive strength, mineralogical studies, elevated temperature studies were carried out with various levels of FCA (0, 10 and 20%) replacement to OPC. Second phase deals with on AAS in combination with FCA as a replacement to OPC. The effect of the various levels of FCA (0, 25 and 50%) replacing GGBS in AAS mortars with 4% of Na₂O dosage is studied. Further, five levels of Ms = 0.75, 1.00, 1.25, 1.5 and 1.75 are chosen to achieve targeted compressive strength at 28 days under ambient temperature curing conditions. In addition, microstructure and mineralogical studies are undertaken to ascertain the formation of different hydration products with the aid of SEM and XRD.

4.2 FERROCHROME ASH AS SUPPLEMENTARY CEMENTITIOUS MATERIAL IN ORDINARY PORTLAND CEMENT BASED MORTAR MIXTURES

Studies related to the effect of FCA as SCM in OPC based mortars is carried out. Flow table test, compressive strength test, elevated temperature studies, SEM and XRD analysis were carried out to ascertain the effect of FCA on OPC based mortar mixtures.

4.2.1 Consistency of ferrochrome ash based ordinary Portland cement mortar mixtures

The consistency of fresh mortar mixtures was determined by flow table method as per IS 1727-1967. As FCA replacement increases from 0% to 20%, the spread value is found to be varied from 101 mm to 108 mm, This change in spread value can be attributed to spherical shape (Kong et al. 2007) of FCA (Figure 4.1). W/B ratio of 0.4 is sufficient to make consistent homogeneous mixture and also meets the requirement (IS 1727-1967) of 105 ± 5 mm spread.

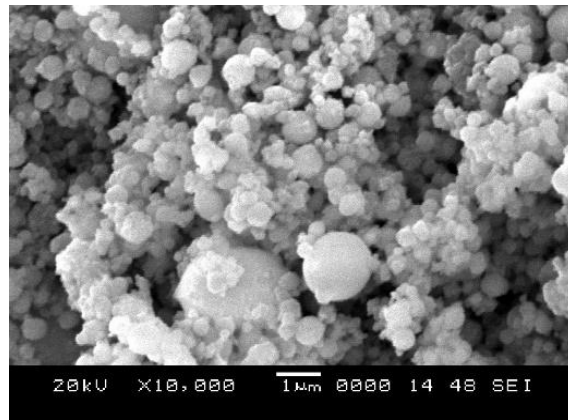


Figure 4.1: SEM image of FCA particles.

4.2.2 Compressive strength of ferrochrome ash based ordinary Portland cement mortar mixtures

Table 4.1 and Figure 4.2, present the observed values of compressive strengths, for FCA based OPC mortar mixtures at the age of 28, 56 and 84 days. From the compressive strength values, it is observed that, like other SCM, FCA did not show any strength development by secondary hydration. This may be due to the insufficient reactive silica from FCA to react with Ca(OH)_2 to form C-S-H in secondary hydration process. This effect is usually known as “dilution effect” (Ashraf et al. 2009). Nevertheless, FCA based

mortar mixtures showed comparable compressive strength as that of OPC based mortar mixtures.

Table 4.1: Compressive strength of FCA based mortar mixtures at various levels of water curing period

Mixture ID	Compressive Strength (MPa)		
	28 days	54 days	84 days
M1	47.7	47.7	48.4
M2	49.4	50.1	48.1
M3	44.4	45.7	45.7

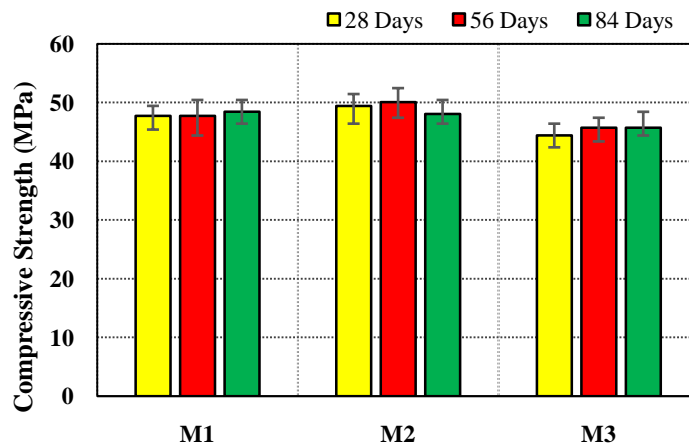


Figure 4.2: Compressive strength of FCA based OPC mortar mixtures at various levels of water curing periods.

4.2.3 Mineralogical studies on ferrochrome ash based ordinary Portland cement mortar mixtures

Figure 4.3 shows the mineralogical features of FCA based OPC mortar mixtures. C-S-H which is responsible for strength development is more intense in OPC based mortar mixture, compared to FCA based OPC mortar mixture. As FCA replacement increases, unreacted SiO₂ is also more pronounced. Decrease in C-S-H and increase in SiO₂ may be

the main reasons for the slight decrease in compressive strength of FCA based mortar mixtures. With increase in FCA content, secondary hydration products like calcium carbonate (CaCO_3 or CC), calcium oxide (CaO) and calcium aluminum chromium oxide hydrate [$\text{Ca}_4\text{Al}_2\text{O}_6(\text{CrO}_4)\cdot 9\text{H}_2\text{O}$] have been observed. This increase in secondary hydration products will hinder the formation of C-S-H (Sezer, 2012).

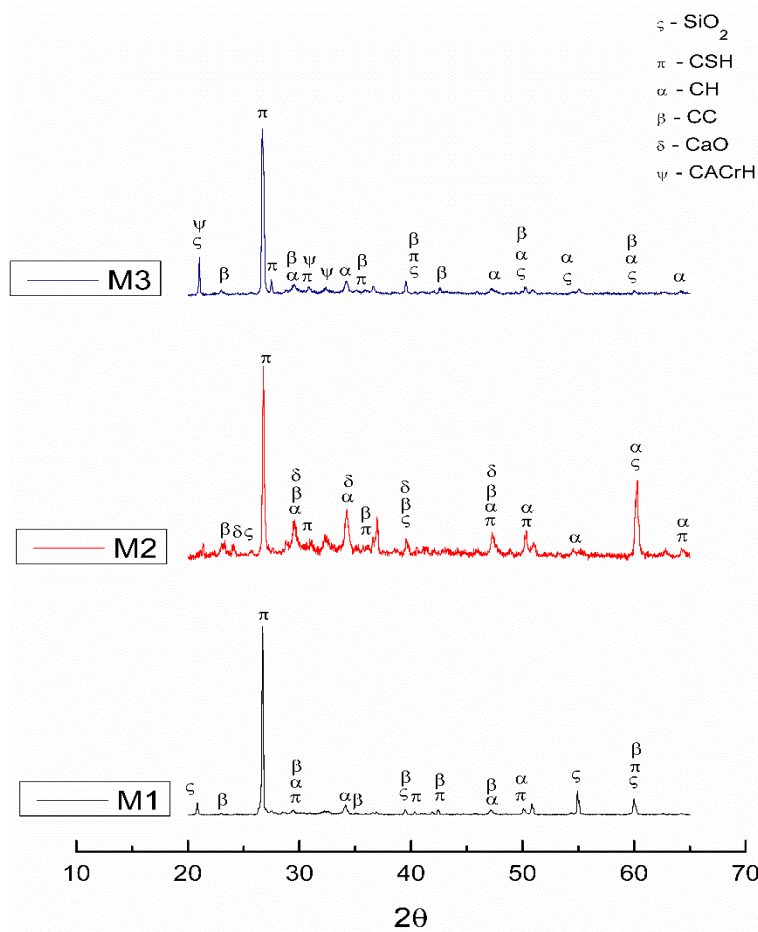


Figure 4.3: XRD analysis of control and FCA based OPC mortar mixtures.

4.2.4 Elevated temperature studies on ferrochrome ash based ordinary Portland cement mortar mixtures

Figure 4.4 and Table 4.2 shows, residual compressive strength of FCA based mortar mixtures subjected to elevated temperatures. With increase in temperature levels,

decrease in compressive strength was observed for all the mortar mixtures. Least residual compressive strength was observed in case of 20% FCA based mortar specimen. A close observation of Figure 4.4 reveals that, at temperature around 200⁰C, slight improvement in compressive strength was observed in all the mortar mixtures. Due to evaporation of chemically bound water, which is responsible for “internal autoclaving”, that enhances the mechanical strength slightly (Yaragal et al. 2010). At 400⁰C, mortar specimen did not show any significant change in compressive strength. However, least residual compressive strength is observed in case of 20% FCA based mortar with 75% residual compressive strength. Similar observations were also made at 600⁰C exposed specimen, which shows 53% residual compressive strength. This decrease in compressive strength is due to the decomposition of Ca(OH)₂ and CaCO₃. Severe strength loss was observed in case of 800⁰C exposed specimen, where 43% residual compressive strength was found in case of 20% FCA based mortar mixture.

Table 4.2: Residual compressive strength of FCA based OPC mortar mixtures

Mixture ID	Residual Compressive Strength (MPa)				
	Room temperature	200 °C	400 °C	600 °C	800 °C
M1	48.4	49.4	42.4	29.6	25.9
M2	48.1	49.1	42.4	26.9	22.2
M3	45.7	44.7	34.3	24.2	19.8

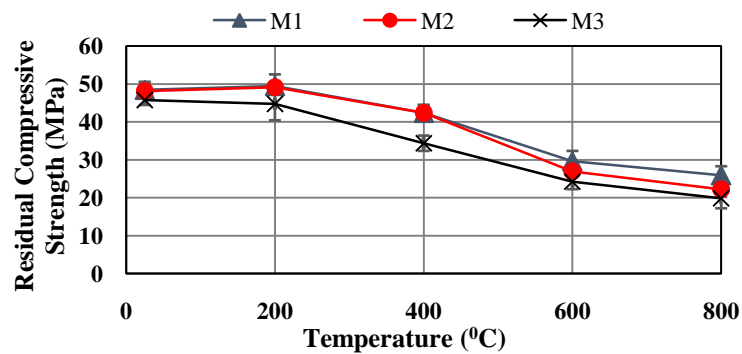


Figure 4.4: Residual compressive strength variation of FCA based OPC mortar with temperature.

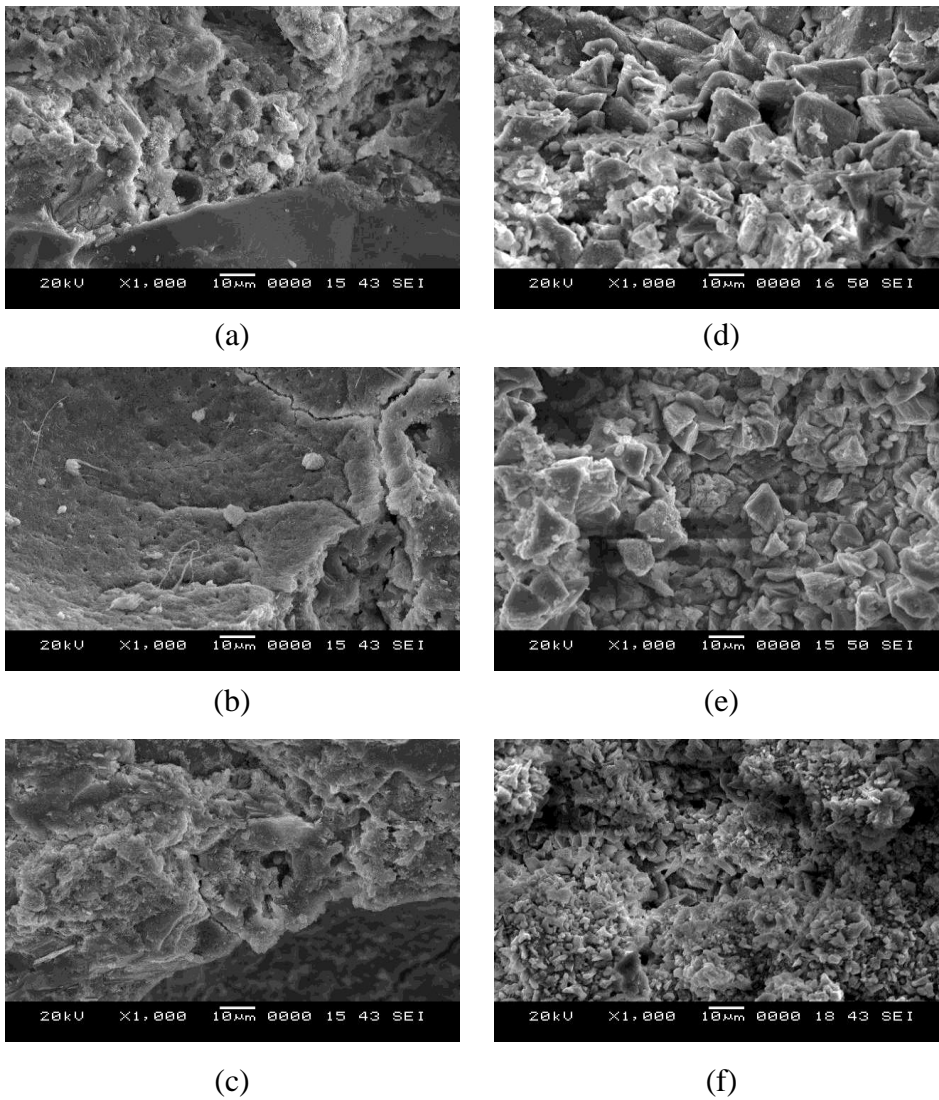


Figure 4.5: SEM image of M1, M2 and M3 mortar mixtures exposed to 400⁰C (a, b and c) and 800⁰C (d, e and f) respectively.

SEM analysis was conducted on M1, M2, M3 mortar specimen exposed to elevated temperatures of 400 and 800⁰C. Figure 4.5 (a, b and c) shows SEM images of specimen exposed to 400⁰C for M1, M2 and M3 mortar specimen respectively. Figure 4.5 (d, e and f) shows SEM images of specimen exposed to 800⁰C for M1, M2 and M3 mortar specimen respectively. SEM images were taken to compare the morphological changes

observed in the microstructure of OPC and FCA based mortar specimen exposed to elevated temperatures. Upto 400⁰C, all the mortar specimen showed dense and intact paste system. Whereas, specimen exposed to 800⁰C showed disintegrated paste system. Disintegrated paste system is the reason behind the severe strength loss in all the mixtures.

4.3 EFFECT OF FERROCHROME ASH IN ALKALI ACTIVATED SLAG MORTAR MIXTURES

In the present section, effect of FCA in AAS mortar mixtures was carried out by conducting compressive strength test, microstructural and mineralogical studies SEM and XRD analysis respectively. Further, FTIR studies were carried out to identify the functional group presence in FCA based AAS mortar mixtures. And also, ecological and economical studies were also carried out using OpenLCA software.

4.3.1 Effect of ferrochrome ash replacement on compressive strength of alkali activated slag mortar binder system

The compressive strength of the AAS mortar system with different FCA replacements (0, 25 and 50%) under ambient curing condition was investigated. The strength variation results with Ms (0.75, 1, 1.25, 1.5 and 1.75) and 4% Na₂O dosage is presented in Table 4.3 and Figure 4.6 for 3, 7 and 28 days, respectively. It was observed that compressive strength decreases with the increase in FCA replacement level. The highest compressive strength was achieved in the case of 1.25 Ms in all levels of FCA replacement in the AAS mortars. The strength development was mainly due to the soluble calcium present in the precursors used, which significantly enhanced the formation of the strength giving calcium aluminosilicate hydrate (C-A-S-H) gel. The decrease in compressive strength may be attributed to the decrease in the calcium ion concentration (Yip et al. 2008; Dombrowski et al. 2007). It was observed that except for 50% replacement of FCA in the

AAS mortar, the M_s ratio of 1.25 satisfied the minimum compressive strength requirement of OPC for all the durations under ambient curing condition.

Table 4.3: Compressive strength of different AAS binders with different curing period.

M_s	(100% GGBS + 0% FCA)			(75% GGBS + 25% FCA)			(50% GGBS + 50% FCA)		
	Curing Period (days)								
	3	7	28	3	7	28	3	7	28
0.75	29	36	54	26	36	49	18	27	38
1	30	46	54	27	42	52	18	29	39
1.25	32	48	57	30	43	54	19	35	41
1.5	29	40	55	28	40	51	17	24	39
1.75	28	38	53	25	38	48	18	25	40

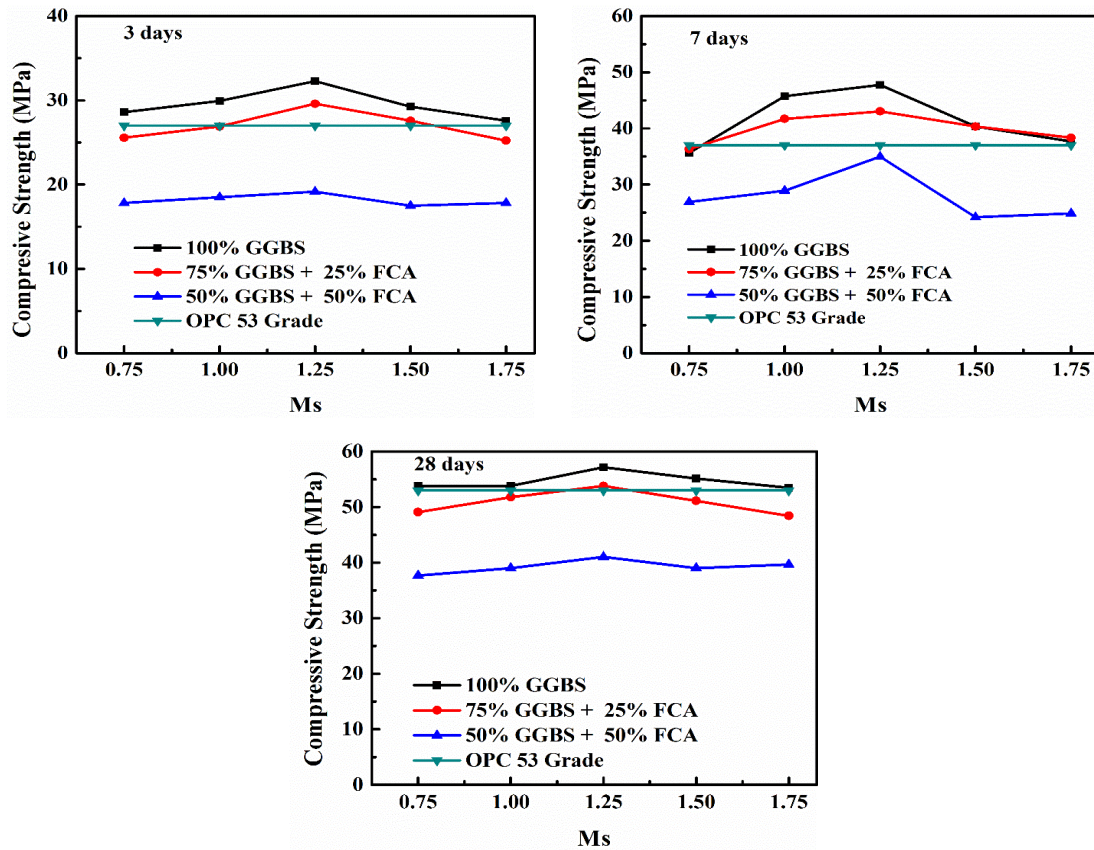


Figure 4.6: Compressive strength variation of different binders with respect to curing period.

4.3.2 X-ray diffraction analysis of ferrochrome based alkali activated slag binder system

FCA based AAS binders with $M_s = 1.25$ and $Na_2O = 4\%$ were studied using the XRD. The XRD patterns are presented in Figure 4.7(a, b and c) for 0, 25 and 50% replacement of FCA in the AAS system. The results show the presence of crystalline phases of calcium silicate hydrate (C-S-H, PDF#-00-033-0306), calcium aluminium silicate hydrate (C-A-S-H, PDF# -00-021-0132), calcite ($CaCO_3$, PDF#-00-024-0027) and gismondine ($CaAl_2Si_2O_8 \cdot 4H_2O$, PDF#-00-020-0452) in the AAS system with slag as the sole binder. The addition of 25% FCA in the AAS system introduces sodium aluminium silicate hydrate, (N-A-S-H, PDF# - 00-042-0120) and traces of un-reacted cristobalite (SiO_2 ,

PDF#-00-011-0695), whereas, 50% replacement of FCA in the AAS system introduces aluminium oxide (Al_2O_3 , PDF#-00-013-0373).

The strength development of the AAS binder may be mainly due to hydration products like, gismondine, C-S-H and C-A-S-H in the 0% FCA-based AAS system. Gismondine is usually found in low MgO (less than 5%) and high Al_2O_3 precursors. It is reported that gismondine belongs to the zeolite family and its presence signifies the strength of the mixture (Bernal et al. 2010). C-S-H gel with low Ca/Si ratio (OPC, Ca/Si = 1.5-2) is also the reason for strength development. C-A-S-H is found in NaOH activated slag matrix. Puertas et al. (2011) have shown that alkali silicate activated slag can form the C-A-S-H phase, which is likely to have tobermorite like structure.

In case of 25% and 50% replacement of FCA in the AAS system reduces, the zeolite, C-S-H gel and tobermorite like C-A-S-H with the formation of N-A-S-H geopolymeric gel. This may be the reason for strength reduction in FCA replaced AAS system. Chen and Brouwers (2007) stated that Ca^{2+} in C-A-S-H can be replaced by Na^+ leading to the formation of C-(N)-A-S-H. This type of phase was not found in the present study. Usually this type of phase can be seen in the interfacial transition zone between the aggregate and the binder (Bernal et al. 2014). C-A-S-H type gel, formed due to alkali hydroxide, tends to possess a low degree of cross-linking (Fernandez-Jimenez et al. 2003). Al substitution in C-A-S-H is limited due to chain length and degree of cross-linking that leads to the formation of secondary Al rich phase (Myers et al. 2013) and this may be the reason for the formation of Al_2O_3 .

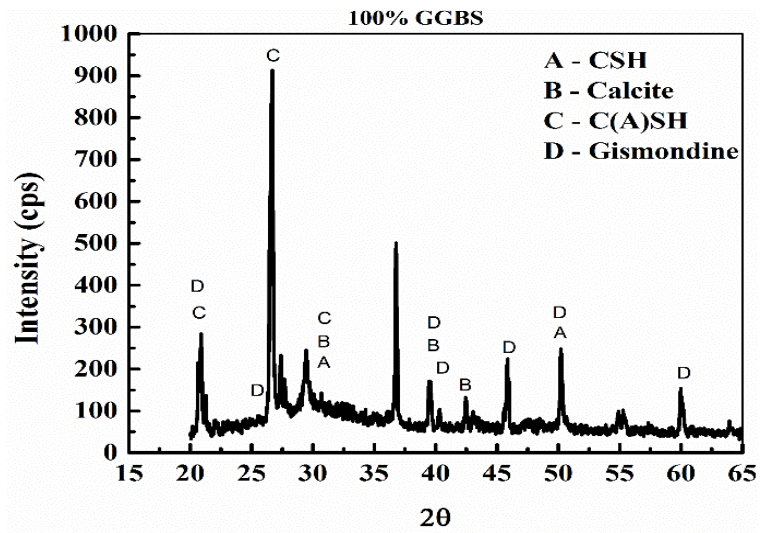


Figure 4.7 (a): XRD pattern of AAS mortar with 0% FCA and 100% GGBS.

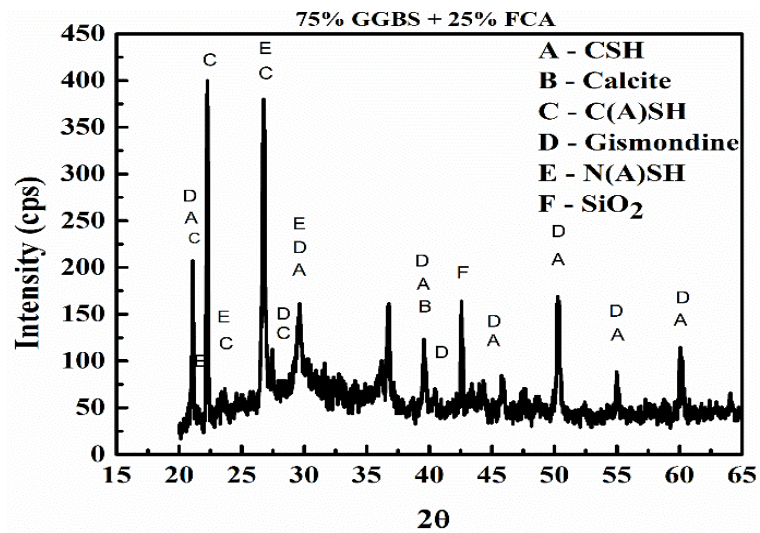


Figure 4.7 (b): XRD pattern of AAS mortar with 25% FCA and 75% GGBS.

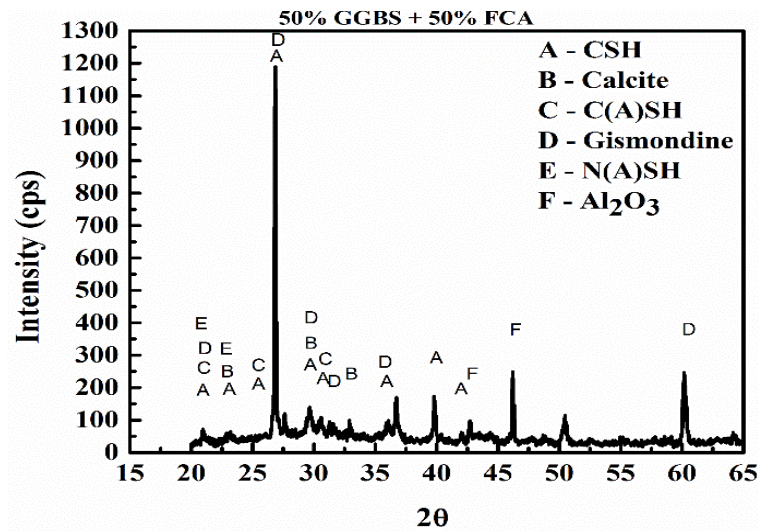


Figure 4.7 (c): XRD pattern of AAS mortar with 50% FCA and 50% GGBS.

4.3.3 Scanning electron microscopy-Energy dispersive spectroscopy analysis of ferrochrome ash based alkali activated slag binder system

In order to explain the variation in mechanical strength due to the replacement of FCA in the AAS system, SEM analysis was carried out to study the microstructure of the AAS system with FCA. For this purpose, samples were collected from the broken mortar specimen of $M_s = 1.25$ and 4% Na_2O dosage. Figure 4.8 (a, b, c and d), shows the microstructure of the AAS binder replaced with 0, 25 and 50% FCA. Figure 4.8 (a) show a dense microstructure. Also, a dark grey area representing the aggregate is surrounded by a light grey area of C-S-H, tobermorite like, C-A-S-H and zeolite like gismondine. These are the main hydration products as confirmed through XRD analysis and are responsible for strength development. In spite of a dense matrix, the mixture is composed of micro cracks. The micro crack initiation and propagation mechanism controls the strength development of the AAS binder matrix. These micro cracks can be easily recognized in Figure 4.8 (b). Brough and Atkinson (2002) reported that these micro cracks were due to the drying shrinkage of the AAS binders. Collins and Sanjayan (1999b) showed that drying shrinkage is 1.6-2.1 times more than that of the OPC based

cementitious materials. However, these micro cracks, at a later age of the hydration period, can be reduced due to full hydration.

Figure 4.8 (c). shows the details of the white spherical FCA particles that participated in the hydration process. Figure 4.8 (d). shows an exaggerated view of the FCA blended AAS binder matrix. FCA particles are usually spherical in shape and due to alkali activation, this spherical shape may get distorted. Since the size of FCA is less than 1 μ m, morphological changes are difficult to identify in the SEM due to alkali activation. However, the formation of N-A-S-H was confirmed with XRD analysis in Figure 4.8 (b and c).

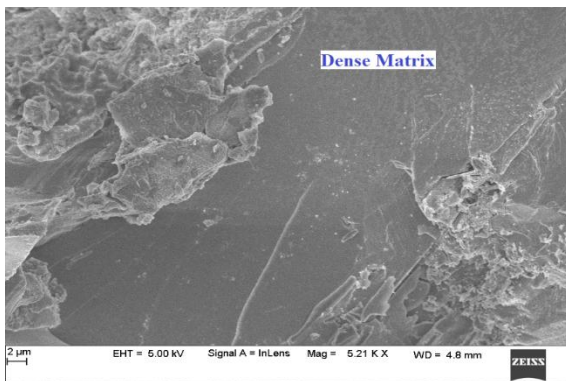


Figure 4.8 (a): SEM image of AAS binder.

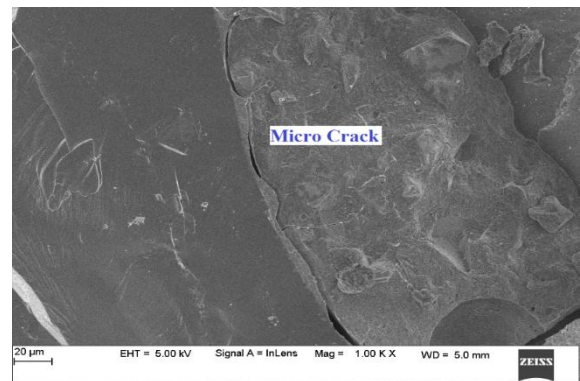


Figure 4.8 (b): SEM image of AAS binder showing micro crack.

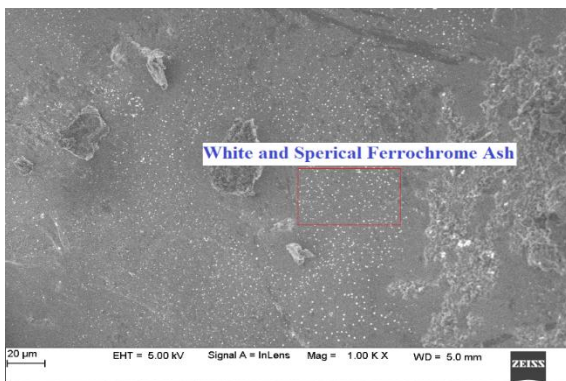


Figure 4.8 (c): SEM image of AAS binder with 25% FCA and 75% GGBS.

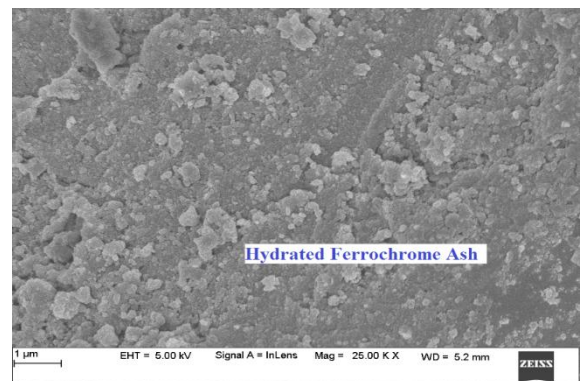


Figure 4.8 (d): SEM image of AAS binder with 50% FCA and 50% GGBS.

In order to assess strength loss due to the addition of FCA in the AAS binder, EDAX studies were carried out on 0, 25 and 50% replacement of FCA in AAS with $M_s = 1.25$. Figure 4.9 (a, b and c) shows the EDAX analysis of 0, 25 and 50% FCA replacement on AAS binders. In order to ascertain the reason for strength loss due to the addition of FCA in AAS system, major elements like Ca, Si, Al and Na were considered and the ratios of Ca/Si, Si/Al, Na/Al were analyzed and are tabulated in Table 4.4. As the FCA replacement increases, the Ca/Si ratio decreases from 1.38-1.01, Si/Al ratio decreases from 2.58-2.08 and Na/Al ratio increases from 0.67-1.08, for 0% FCA to 50% FCA, replacement in the AAS mixtures.

As the Ca/Si ratio decreases, the compressive strength also decreases. This is in agreement with Nath and Kumar (2013), they used iron making slag with FA to form a geopolymerization reaction and found that with increase in FA content in the iron making slag, the Ca/Si ratio decreases to 1.23-0.99. According to Davidovits (1991), as the Si/Al ratio increases, i.e, 1, 2 and 3, the basic silico aluminate structure changes to polysilicate, polysilicate-siloxo and polysilicate-disiloxo, respectively. The matrix gets reorganized into a 3D-crosslinked chain as the Si/Al ratio increases. In the present investigation, the Si/Al ratio decreased from 2.58-2.08 with 50% replacement of FCA in the AAS binder system. This may be the reason for decrease in the strength. But interestingly with 25% FCA replacement in the AAS binder system, the Si/Al ratio increased to 3.61. This is in good agreement with Chindaprasirt et al. (2009), where the hydrated Si/Al ratio was not the same as the input Si/Al ratio. In the present study, the Na/Al ratio increased to 0.67 - 1.08 as the FCA replacement increased in the AAS binder system. As the Na/Al ratio decreased, the compressive strength increased (Songpiriyakij et al. 2010). So, there may be chances of decrease in compressive strength as the FCA replacement increases.

Table 4.4: EDAX analysis of atomic weight percentage of the AAS binder system.

AAS Binder System	Ca	Si	Al	Na	Ca/Si	Si/Al	Na/Al
100% GGBS + 0% FCA	24.49	17.67	6.97	4.66	1.38	2.53	0.67
75% GGBS + 25% FCA	29.33	22.29	6.16	4.96	1.31	3.61	0.80
50% GGBS + 50% FCA	25.29	25.05	12.01	13.08	1.01	2.08	1.08

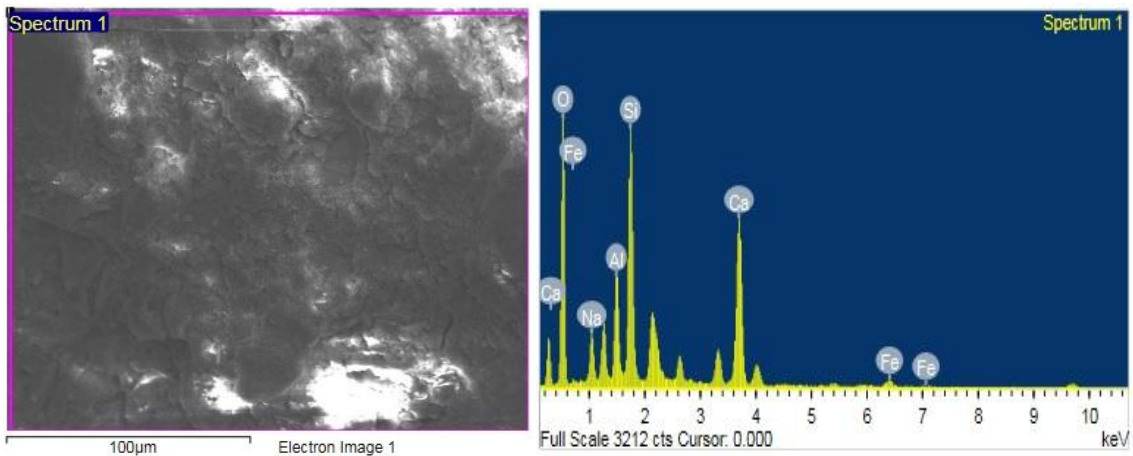


Figure 4.9 (a): EDAX analysis of 100% GGBS in the AAS binder system.

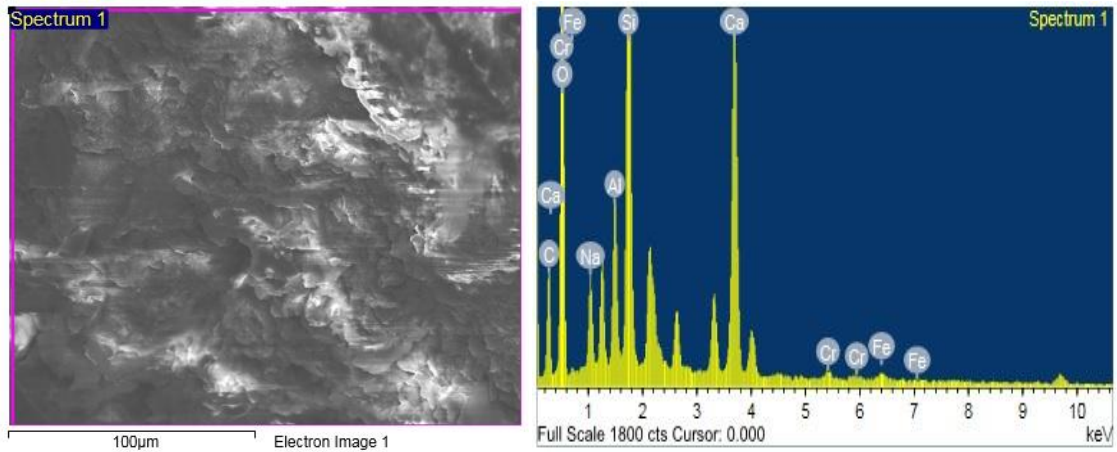


Figure 4.9 (b): EDAX analysis of 75% GGBS and 25% FCA in the AAS binder system.

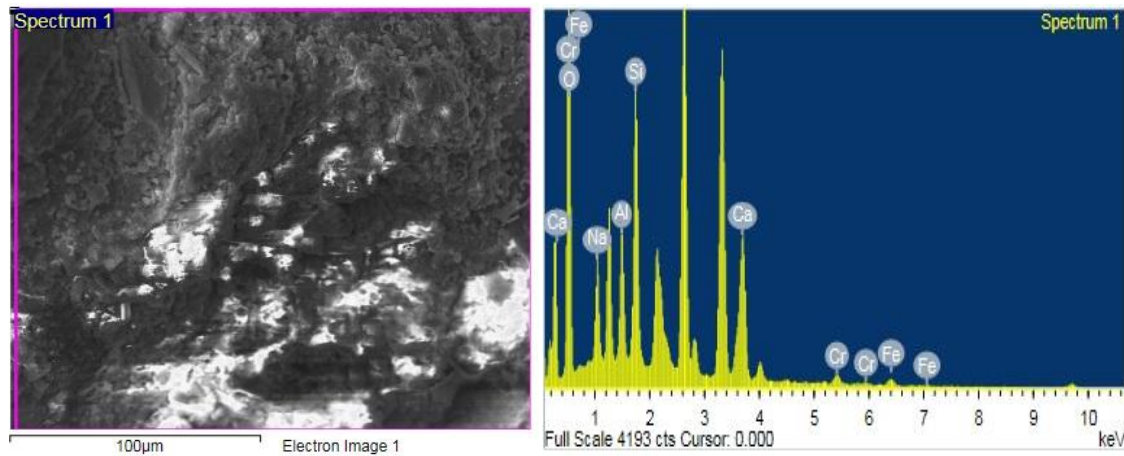


Figure 4.9 (c): EDAX analysis of 50% GGBS and 50% FCA in the AAS binder system.

4.3.4 Fourier-transform infrared spectroscopy of alkali activated slag mortar mixtures

Figure 4.10 presents the FTIR spectra of the raw materials and the AAS mortar mixtures for $M_s = 1.25$. The analysis result shows that minor bands in the range $600-720\text{ cm}^{-1}$ indicate the presence of siliceous and alumina-silicate material in the raw materials used. No significant peak shift is observed in all the AAS mortar spectra. Nevertheless, peaks in the region of $940-980\text{ cm}^{-1}$ indicates the presence of the functional group Si-O-T (often called as main band), where, T = Si or Al and due to vibration, these peaks are majorly attributed to the formation of the geopolymer gel structure (Puertasans and Torres-Carrasco, 2014). Further, minor peaks present at 1410 cm^{-1} indicate bonding of the CO_3^{2-} ions, which may be due to the formation of carbonated minerals caused due to the absorbance of CO_2 from the atmosphere (Pereira et al. 2015).

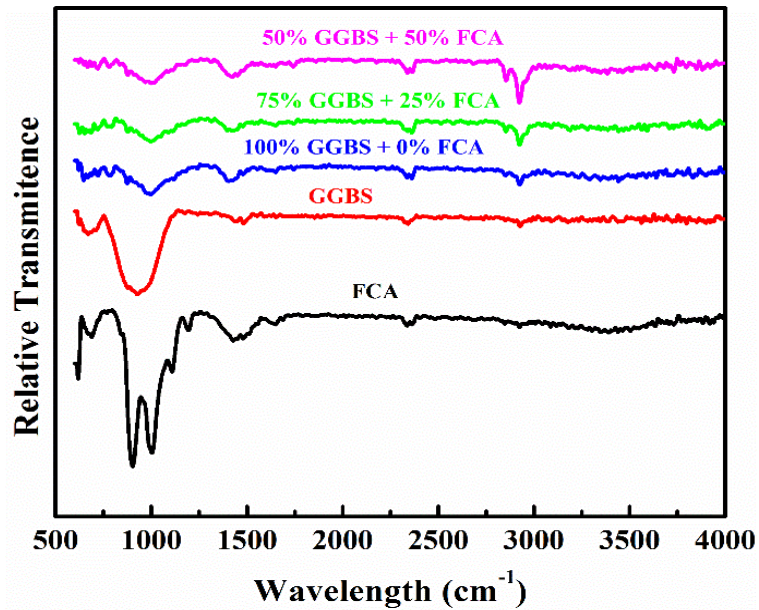


Figure 4.10: FTIR spectra of raw materials (GGBS and FCA) and AAS binder with 0, 25 and 50% FCA replacement.

4.3.5 Ecological studies and cost analysis of ferrochrome ash based mortar mixtures

Table 4.5 gives the ECO_{2eq} ($kgCO_2$), EE_{eq} (MJ) and cost (USD) values of the various mortar mixtures studied. The ECO_{2eq} of the OPC based mortar mixtures is higher compared with to all the AAS mortar mixtures considered. As the replacement of FCA level increases in the AAS mortar mixtures, the calculated ECO_{2eq} value decreases, due to the decrease in quantity of the GGBS. Since the production of GGBS involves the processing and grinding of the raw blast furnace slag, the EE_{eq} of OPC based mortar and the 100% GGBS + 0% FCA are comparable with each other. Nevertheless, EE_{eq} gets reduced with the addition of FCA in the AAS based mortar. The production of GGBS is an energy intensive process compared with FCA, as the production of FCA does not consume any energy. Cost analysis was done based on market rates and a decrease in cost was observed with the increase in the replacement level of the FCA in the AAS mortar mixtures.

Table 4.5: ECO_{2eq} , EE_{eq} and cost of different mortar mixtures.

Sl No	Mortar Mixtures	ECO_{2eq} (kgCO ₂)	EE_{eq} (MJ)	Cost (USD)
1	100% OPC	920	4053	152.62
2	100% GGBS + 0% FCA (for 1.25 M _s)	271	4162	133.58
3	75% GGBS + 25% FCA (for 1.25 M _s)	247	3768	119.71
4	50% GGBS + 50% FCA (for 1.25 M _s)	223	3374	105.84

4.4 CLOSURE

Study on effect of FCA in OPC mortar mixtures shows reduced compressive strength. Mineralogical study reveals that reduced compressive strength is due to the dilution effect. Whereas, 25% FCA in AAS mortar mixtures prepared with 4% Na₂O dosage showed satisfactory results in compressive strength, ecological and economical studies.

CHAPTER 5

DURABILITY AND OPTIMIZATION STUDIES OF ALKALI ACTIVATED SLAG/ FERROCHROME ASH BASED MORTARS

5.1 GENERAL

Durability is ability to retain desired engineering properties under weathering action, chemical ingress and other abrasion damage. Durability studies of any new construction material manufactured or prepared is essential since new construction materials needs to with-stand the aggressive environment in a long period of time. In the present chapter durability studies were carried out for alkali activated slag/ferrochrome ash based mortars. Further optimal mixtures were identified based on responses (VPV, residual compressive strength under sulphate and acid attack) using MCDM methods like, GRA, TOPSIS and DFA.

In order to evaluate the durability of AAS mortar mixtures, three different levels of FCA and three different levels of alkaline solution concentration were considered. Replacement levels of FCA with respect to GGBS are considered as 0, 25 and 50% by weight. Alkaline solution concentration is varied by means of Na₂O dosage. Na₂O concentration is considered as 4, 5 and 6% of binder content used for AAS mortar preparation. In order to access durability performance, VPV, sulphate resistance tests and acid resistance test were carried out. Based on two input parameters, (i.e., FCA replacement and Na₂O dosage) total nine different mixtures were used to evaluate the durability of AAS mortar mixtures.

5.2 VOLUME OF PERMEABLE VOIDS OF ALKALI ACTIVATED SLAG MORTAR MIXTURES

Durability directly depends on porosity of mortar mixtures. Increase in the porosity will increase the ingress of external agents. Increase in the amount of external agents

increases the deterioration mechanism in the mortar. So porosity of mortar is considered as an important parameter from the durability point of view.

In the present study, VPV is considered to evaluate the porosity of mortar mixtures. VPV is computed based on the standard specifications of ASTM C642-13. VPV gives, the value of total percentage of voids by integrating gel pores, capillary pores, air voids and micro cracks present in the mortars prepared. Table 5.1 and Figure 5.1 gives the value of VPV of different FCA based AAS mortars under different concentration levels of alkaline solution. The VPV value is observed to be lesser in case of 0% FCA and 6% Na₂O dosage based AAS mortar mixture. A higher value of VPV is observed in case of 50% FCA and 4% Na₂O dosage based AAS mortar mixture.

VPV values decrease, with the increase in amount of alkali solution concentration. Further, decrease in VPV value is observed with increase in Na₂O dosage (i.e., alkaline solution concentration) with different binder combination used in AAS mortar mixtures. Increase in amount of Na₂O dosage (i.e., from 4 to 6% by weight of binder content) results in decrease in VPV values of 2.4, 3.6 and 4.5% for 0, 25 and 50% FCA based AAS mortar mixtures respectively. Increase in Na₂O content results in decrease in pore size. Decrease in pore size results in decrease in VPV value (Zhang et al. 2020b; Ismail et al. 2013).

However, with increase in FCA content in AAS mortar mixture results in increase in VPV value. Increase in VPV value is observed for increase in FCA content (i.e., 0, 25 and 50% of GGBS) with different alkaline solution concentration in AAS mortar mixtures. Increase in amount of FCA content (i.e., from 0 to 50% replacement to GGBS) as binder results, in increase in VPV values of 8.5, 7.4 and 6.3% for 4, 5 and 6% Na₂O dosage based AAS mortar mixtures respectively.

Increase in the VPV values with increase in FCA content in AAS mortar mixtures is due to the final reaction products obtained. Higher value of VPV is observed for 50% FCA based AAS mortar mixture. Higher value of VPV is attributed to the gels formation in 50% FCA based AAS mortar mixture. 50% FCA based AAS mortar mixture reduces the C-A-S-H gel formation (as discussed in Chapter 4) which results in more VPV value, compared to 0% FCA based AAS mortar mixture. C-A-S-H dominates the microstructure AAS based mortar mixture. Higher amount of C-A-S-H

gels formation results in denser microstructure. Increase in FCA content results in reduction of C-A-S-H gels formation which directly results in reduction of dense microstructure. As a result of reduced closely compacted microstructure, VPV increases in FCA dominated AAS mortar mixtures (Zhang et al. 2020b; Yaragal et al. 2020; Ismail et al. 2013).

Table 5.1: VPV of FCA based AAS mortar mixtures with various levels of alkaline solution concentration.

Sl No	Mixture ID	Binders		Alkaline Solution Concentration	VPV
		GGBS	FCA	Na ₂ O	
		(%)			
1	AAS100F0N4	100	0	4	8.2
2	AAS100F0N5	100	0	5	8.1
3	AAS100F0N6	100	0	6	8.0
4	AAS75F25N4	75	25	4	8.3
5	AAS75F25N5	75	25	5	8.2
6	AAS75F25N6	75	25	6	8.0
7	AAS50F50N4	50	50	4	8.9
8	AAS50F50N5	50	50	5	8.7
9	AAS50F50N6	50	50	6	8.5

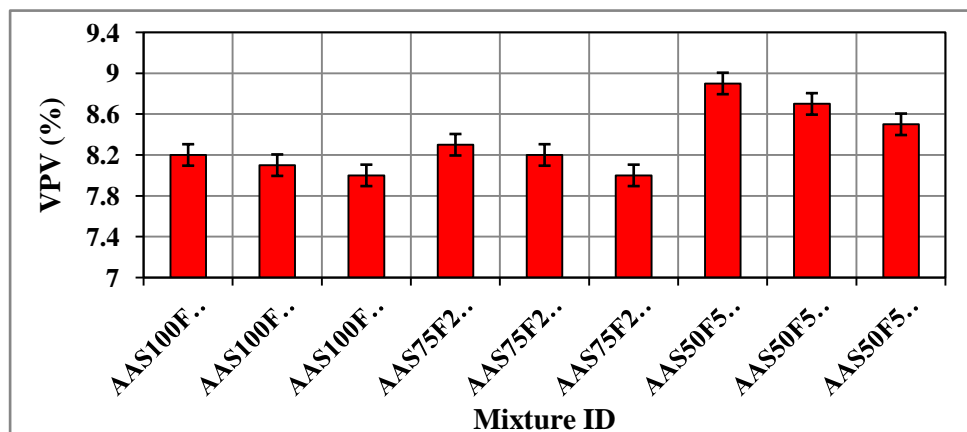


Figure 5.1: VPV of FCA based AAS mortar mixture with various levels of alkaline solution concentration.

5.3 SULPHATE ATTACK ON ALKALI ACTIVATED SLAG MORTAR MIXTURES

Sulphate attack is complex form of chemical deterioration observed in AAS binder system. Sulphate attack might be either external or internal. External ingress of sulphate ion might be caused due to AAS binder which is in contact with natural sources like soil, fertilizer, ground water etc.,. Internal sulphate attack might be caused due to the presence of sulphate ion within the binder composition used for the preparation of AAS mixtures. Ingress of sulphate ion into the AAS binder system results in expansion of AAS binder system. This expansion results in disintegration of denser microstructure. Which in turn results in reduction of mechanical strength of AAS binder matrix. So, in order to ensure the sulphate resistance of AAS mortar mixture for long term durability and therefore the present study involves the investigation of AAS mortar mixture under sulphate attack.

As detailed in the methodology section, sulphate attack tests were carried out on total nine AAS mortar mixtures. Sulphate attack is evaluated by immersion of AAS mortar mixture in 5% $MgSO_4$ solution. Sulphate attack on AAS mortar is studied for time period of 180 days as show in Figure 5.2 and Table 5.2. Compressive strength test is conducted and reported on sulphate exposed specimen of FCA based AAS mortar mixtures. Exposure period of 30, 90 and 180 days were considered to assess the residual compressive strengths. Figure 5.2 and Table 5.2 shows, residual compressive strength of different concentration of alkaline solutions (i.e., 4, 5 and 6% Na_2O dosage) and different FCA binder contents as a replacement to GGBS (i.e., 0, 25 and 50% of FCA). For all the AAS mixtures studied, as sulphate exposure period, decrease in compressive strength is observed due to the progress in deterioration mechanism.

Table 5.2: Compressive strength of sulphate exposed AAS mortar mixtures for the time period of 180 days.

Sl No	Mixture ID	Binders		Alkaline Solution Concentration	Compressive Strength (MPa)			
		GGBS	FCA	Na ₂ O	0 days	30 days	90 days	180 days
		(%)						
1	AAS100F0N4	100	0	4	58	54	44	38
2	AAS100F0N5	100	0	5	62	59	48	42
3	AAS100F0N6	100	0	6	63	60	50	43
4	AAS75F25N4	75	25	4	56	52	43	39
5	AAS75F25N5	75	25	5	58	55	46	41
6	AAS75F25N6	75	25	6	62	59	51	45
7	AAS50F50N4	50	50	4	43	40	34	31
8	AAS50F50N5	50	50	5	45	42	36	33
9	AAS50F50N6	50	50	6	48	45	40	36

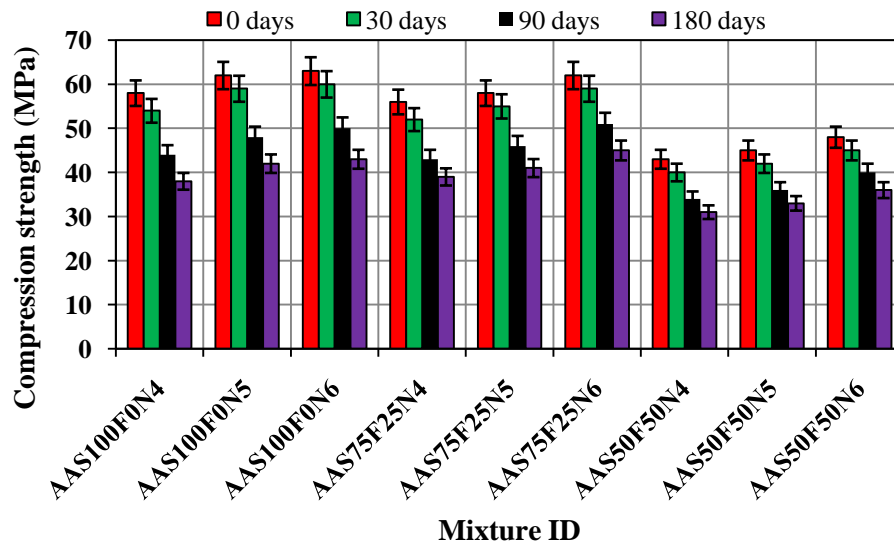


Figure 5.2: Compressive strength of sulphate exposed AAS mortar mixtures for a time period of 180 days.

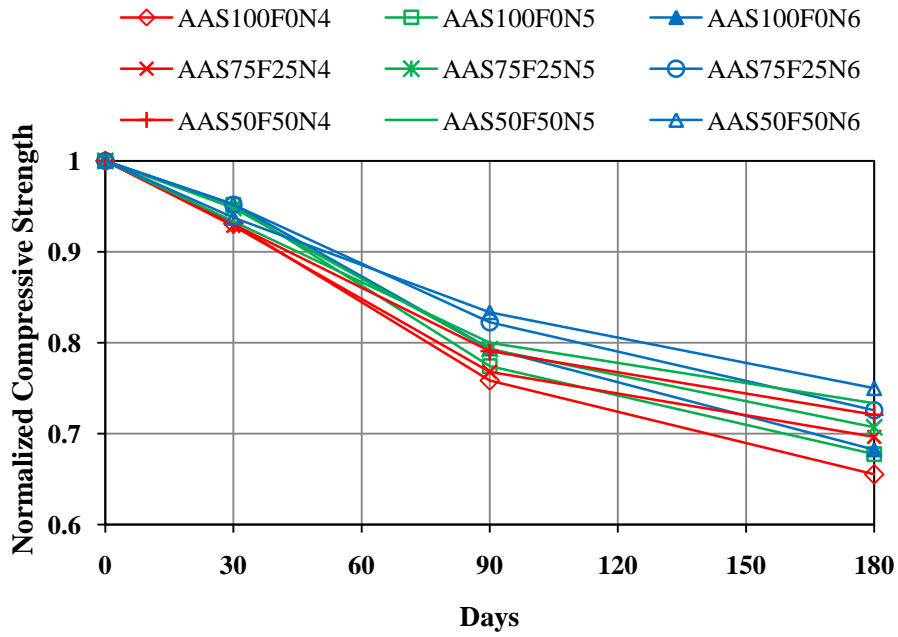


Figure 5.3: Normalized compressive strength value of sulphate exposed AAS mortar mixtures.

Table 5.3: Normalized compressive strength value of sulphate exposed AAS mortar mixtures.

Sl No	Mixture ID	Binders		Alkaline Solution Concentration	Normalized Compressive Strength			
		GGBS	FCA	Na ₂ O	0 days	30 days	90 days	180 days
		(%)						
1	AAS100F0N4	100	0	4	1	0.93	0.76	0.66
2	AAS100F0N5	100	0	5	1	0.95	0.77	0.68
3	AAS100F0N6	100	0	6	1	0.95	0.79	0.68
4	AAS75F25N4	75	25	4	1	0.93	0.77	0.70
5	AAS75F25N5	75	25	5	1	0.95	0.79	0.71
6	AAS75F25N6	75	25	6	1	0.95	0.82	0.73
7	AAS50F50N4	50	50	4	1	0.93	0.79	0.72
8	AAS50F50N5	50	50	5	1	0.93	0.80	0.73
9	AAS50F50N6	50	50	6	1	0.94	0.83	0.75

Table 5.3 and Figure 5.3 shows the normalized compressive strength values of all the AAS mortar mixtures studied. In case of 30 days exposed AAS mortar mixtures to sulphate environment, residual compressive strength values of all the nine AAS mortar mixtures were in similar range i.e., 93-95%. In case of 90 days exposed AAS mortar mixtures, residual compressive strength values of all the nine AAS mortar mixtures were in the range of 76-83%. Higher compressive strength loss is observed for 180 days exposed AAS mortar mixtures and is in the range of 66-75%.

Considering 180 days exposed AAS mortar mixtures, 50% FCA based AAS mixture shows 72% of residual compressive strength. Whereas, 0% FCA based AAS mixture shows 66% of residual compressive strength under 4% Na₂O dosage of alkaline solution concentration. Also, 50% FCA based AAS mixture shows 73% of residual compressive strength. Whereas, 0% FCA based AAS mixture shows 68% of residual compressive strength under 5% Na₂O dosage of alkaline solution concentration. Similarly, 50% FCA based AAS mixture shows 75% of residual compressive strength. Whereas, 0% FCA based AAS mixture shows 68% of residual compressive strength under 6% Na₂O dosage of alkaline solution concentration. From the results shown, increase in FCA content and alkaline solution concentration of AAS mortar mixtures improves the residual compressive strength under sulphate environment.

Improvement in residual compressive strength with FCA as a partial replacement to GGBS in AAS mortar mixtures is due to the final reaction products obtained. FCA as a replacement to GGBS in AAS mortar mixtures result in decrease in C-S-H formation. Lesser amount of C-S-H gel formation will be beneficial in sulphate resistance. Since, magnesium ions present in MgSO₄ solution (which is considered as sulphate exposure medium) will get to react with C-S-H gel, to form M-S-H by decalcification of calcium ion present in C-S-H gel. M-S-H is non-cementitious and expansive in nature and results in reduction of the compressive strength in GGBS rich AAS mortar mixtures. Compressive strength obtained by FCA rich AAS mortar is lesser compared to GGBS rich AAS mortar mixture under unexposed sulphate environment. However, resistance to sulphate environment of FCA rich AAS mortar is higher compared to GGBS rich AAS mortar mixture due to the lesser amount of M-S-H formation.

Similarly, improvement in residual compressive strength with increase in Na₂O dosage is observed for AAS mortar mixtures. Increased resistance to sulphate environment is due to the formation of denser microstructure with increase in Na₂O dosage (Liu et al. 2020). Formation of denser microstructure inhibits the ingress of sulphate and magnesium ions into the mortar and result in the improved compressive strength.

5.4 ACID ATTACK ON ALKALI ACTIVATED SLAG MORTAR MIXTURES

Acid attack results in disintegration and leaching of paste matrix in cementitious material. Disintegration and leaching of paste matrix, usually results in increase in porosity and decrease in the cohesiveness of cementitious material. Increase in porosity and decrease in cohesiveness will result in turn to loss of mechanical strength of the cementitious material.

Present study is intended to measure the amount of mechanical strength loss due to acid attack on FCA based AAS mortar mixtures under different levels of alkaline solution dosage. Table 5.4 and Figure 5.4 shows the results of compressive strength of FCA based AAS mortar mixtures under different alkaline solution concentration, for different levels of duration of acid solution exposure. Total nine mixtures composed with two input variables are studied. Two input variables are FCA as binder and percentage of Na₂O dosage for preparation of alkaline solution. Three different levels of FCA (i.e., 0, 25 and 50% FCA as a replacement to GGBS) and Na₂O dosage (i.e., 4, 5 and 6% Na₂O dosage for alkaline solution preparation) are considered in the present study. Compressive strengths of nine different mixtures exposed to acid solution for the duration of 90 days, is evaluated.

Table 5.4 and Figure 5.4 shows that, decrease in the compressive strengths with increase in duration of exposure in all the AAS mixtures studied. Table 5.5 and Figure 5.5 shows normalized compressive strength of FCA based AAS mortar mixtures. Compressive strength loss at 30 days of exposure were found to be 55, 58, 65, 61, 60, 66, 70, 69 and 77% for AAS100F0N4, AAS100F0N5, AAS100F0N6, AAS75F25N4, AAS75F25N5, AAS75F25N6, AAS50F50N4, AAS50F50N5 and

AAS50F50N6 mixtures respectively. Compressive strength loss at 90 days of exposure was found to be 34, 40, 43, 41, 36, 45, 49, 51 and 56% for above mixtures respectively. Decrease in compressive strength with increase in duration of exposure is due to the continuous disintegration of the AAS mortar mixtures.

At 90 days of external acid media, 4% Na_2O dosage based AAS mixtures, show compressive strength loss of 34, 41 and 49% with increase in FCA content from 0, 25 and 50% respectively. In case of 5% Na_2O dosage based AAS mixtures show compressive strength loss of 40, 36 and 51% with increase in FCA content from 0, 25 and 50% respectively. Similarly, 6% Na_2O dosage based AAS mixtures show compressive strength loss of 43, 45 and 56% with increase in FCA content from 0, 25 and 50% respectively. As the amount FCA content increases resistance to compressive strength loss were observed to be increased with all the Na_2O dosage levels. Improved acid resistance in FCA based AAS mortar mixtures compared to GGBS based AAS mortar mixtures is mainly due to the change in the chemical composition of binder gels formed. Increase in FCA content decreases the C-S-H gels content. Decalcification of the C-S-H gel gets reduced with incorporation of FCA in AAS mortar mixtures. GGBS based AAS mortar suffers predominant decalcification and eventually result in more strength loss compared to FCA based AAS mortar mixture (Yaragal et al. 2020).

At 90 days of external acid media, 100% GGBS based AAS mortar shows compressive strength loss of 34, 40 and 43% with increase in Na_2O dosage from 4, 5 and 6% respectively. Similar trend of compressive strength loss is observed in case of 75% GGBS + 25% FCA and 50% GGBS + 50% FCA based AAS mortars with increase in Na_2O dosage of alkaline solution used. Increase in Na_2O dosage reduces the compressive strength loss. Improved acid resistance is due to the microstructure improvement. Increase in the Na_2O dosage will result in the decrease in the porosity of the mortar matrix. Decrease in the porosity will mitigate/inhibit the ingress of the acid media to cause decalcification of C-S-H gel formed. Formation of denser microstructure was the prime reason behind the improvement in acid resistance of AAS mortar mixtures studied (Liu et al. 2020).

Table 5.4: Compressive strength of acid exposed AAS mortar mixtures for a time period of 90 days.

Sl No	Mixture ID	Binders		Alkaline Solution Concentration	Compressive Strength (MPa)			
		GGBS	FCA	Na ₂ O	0 days	30 days	60 days	90 days
		(%)						
1	AAS100F0N4	100	0	4	58	32	26	20
2	AAS100F0N5	100	0	5	62	36	30	25
3	AAS100F0N6	100	0	6	63	41	35	27
4	AAS75F25N4	75	25	4	56	34	28	23
5	AAS75F25N5	75	25	5	58	35	27	21
6	AAS75F25N6	75	25	6	62	41	34	28
7	AAS50F50N4	50	50	4	43	30	26	21
8	AAS50F50N5	50	50	5	45	31	27	23
9	AAS50F50N6	50	50	6	48	37	29	27

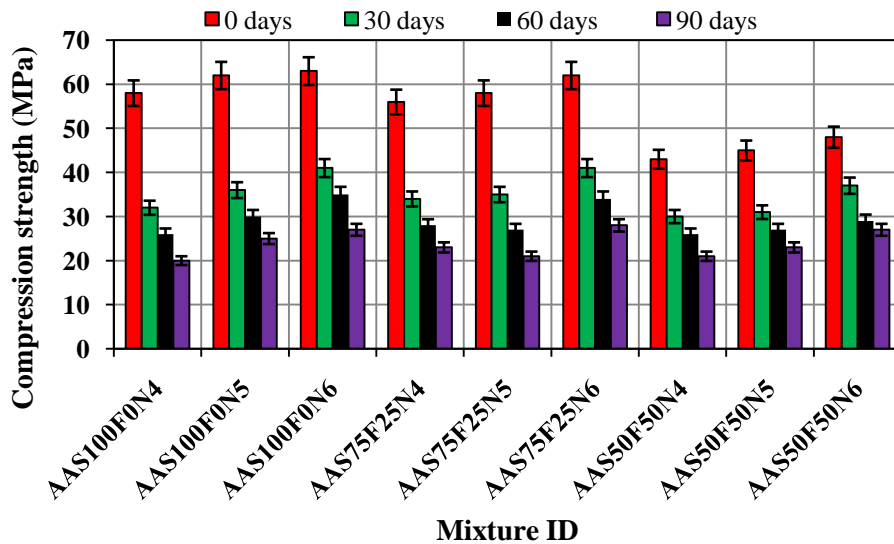


Figure 5.4: Compressive strength of acid exposed AAS mortar mixtures for a time period of 90 days.

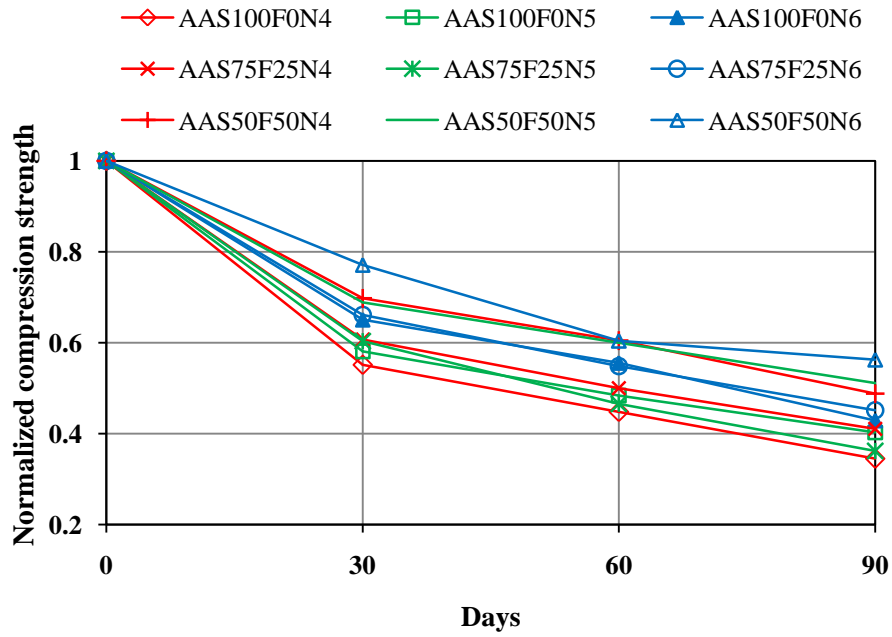


Figure 5.5: Normalized compressive strength value of acid exposed AAS mortar mixtures.

Table 5.5: Normalized compressive strength value of acid exposed AAS mortar mixtures.

Sl No	Mixture ID	Binder		Alkaline Solution Concentration	Normalized Compressive Strength			
		GGBS	FCA	Na ₂ O	0 days	30 days	60 days	90 days
		(%)						
1	AAS100F0N4	100	0	4	1	0.55	0.45	0.34
2	AAS100F0N5	100	0	5	1	0.58	0.48	0.40
3	AAS100F0N6	100	0	6	1	0.65	0.56	0.43
4	AAS75F25N4	75	25	4	1	0.61	0.50	0.41
5	AAS75F25N5	75	25	5	1	0.60	0.47	0.36
6	AAS75F25N6	75	25	6	1	0.66	0.55	0.45
7	AAS50F50N4	50	50	4	1	0.70	0.60	0.49
8	AAS50F50N5	50	50	5	1	0.69	0.60	0.51
9	AAS50F50N6	50	50	6	1	0.77	0.60	0.56

5.5 OPTIMIZATION OF FERROCHROME ASH BASED ALKALI ACTIVATED SLAG MORTAR MIXTURES BY GREY RELATIONAL ANALYSIS

GRA is used to FCA based AAS mortar mixtures to rank the different mixtures studied. Grey relational generation of responses is initial step in the GRA. Grey relational generation is calculated based on Equation 3.1 and 3.2. Three responses were considered for Grey relational generation i.e., VPV, normalized compressive strength under sulphate and acid environment of FCA based AAS mortar mixtures. Minimization equation is used for the VPV values shown in Table 5.1. Maximization equation is used for the 180 days normalized compressive strength values shown in Table 5.3 in case of sulphate resistance. Similar to sulphate resistance, maximization equation is used for the 90 days normalized compressive strength values shown in Table 5.5 in case of acid resistance. Table 5.6 shows the grey relational generation values of the nine AAS mortar mixtures. Deviation values were computed using grey relational generation values shown in Table 5.6. Deviation values were computed by subtracting previously obtained grey relational generation value with unit value.

Further, ranking of different FCA based AAS mortar mixtures were computed based on GRC and GRG value. Higher GRG value will eventually gives first rank to the FCA based AAS mortar mixture. GRC and GRG values were computed based on the Equation 3.3 and 3.4 respectively by using previously obtained deviation values of different FCA based AAS mortar mixtures. Table 5.7 shows computed values of GRC and GRG values of FCA based AAS mortar mixtures. Equal weightage (0.33) is used for the calculation of GRG value.

Ranking order of the different FCA based AAS mortar mixtures can be given as below:

AAS50F50N6 > AAS75F25N6 > AAS100F0N6 > AAS50F50N5 > AAS100F0N5 > AAS75F25N5 > AAS50F50N4 > AAS75F25N4 > AAS100F0N4.

50% FCA based AAS mortar mixture prepared with 6% Na₂O dosage obtained first rank and 0% FCA based AAS mortar mixture prepared with 4% Na₂O dosage obtained last rank considering durability aspect like VPV, residual compressive strength under sulphate and acid attack.

Table 5.6: Grey relational generation and deviation of FCA based AAS mortar mixtures.

S l N o	VPV (%)	Sulphate Attack (Normal ized Compre ssive Strength)	Acid Attack (Normaliz ed Compress ive Strength)	Grey Relational Generation			Deviation		
				VPV	Sulpha te Attack	Acid Attack	VPV	Sulphate Attack	Acid Attack
1	8.2	0.66	0.34	0.778	0.000	0.000	0.222	1.000	1.000
2	8.1	0.68	0.40	0.889	0.235	0.268	0.111	0.765	0.732
3	8.0	0.68	0.43	1.000	0.289	0.385	0.000	0.711	0.615
4	8.3	0.70	0.41	0.667	0.435	0.303	0.333	0.565	0.697
5	8.2	0.71	0.36	0.778	0.545	0.079	0.222	0.455	0.921
6	8.0	0.73	0.45	1.000	0.745	0.491	0.000	0.255	0.509
7	8.9	0.72	0.49	0.000	0.693	0.659	1.000	0.307	0.341
8	8.7	0.73	0.51	0.222	0.824	0.764	0.778	0.176	0.236
9	8.5	0.75	0.56	0.444	1.000	1.000	0.556	0.000	0.000

Table 5.7: GRC, GRG and ranking of FCA based AAS mortar mixtures.

Sl No.	Mixture ID	GRC			GRG	Rank
		VPV	Sulphate Attack	Acid Attack		
1	AAS100F0N4	0.692	0.333	0.333	0.149	9
2	AAS100F0N5	0.818	0.395	0.406	0.178	5
3	AAS100F0N6	1.000	0.413	0.448	0.205	3
4	AAS75F25N4	0.600	0.470	0.418	0.164	8
5	AAS75F25N5	0.692	0.524	0.352	0.172	6
6	AAS75F25N6	1.000	0.662	0.495	0.237	2
7	AAS50F50N4	0.333	0.620	0.595	0.170	7
8	AAS50F50N5	0.391	0.740	0.679	0.199	4
9	AAS50F50N6	0.474	1.000	1.000	0.272	1

Table 5.8 provides responses of GRG values of FCA based AAS mortar mixtures prepared with different Na₂O % values. Table 5.8 shows the ranking of two input variables i.e., FCA content and Na₂O dosage concentration. Level 1, Level 2 and Level 3 represents the average value of GRG in case of input variable FCA. Level 1 corresponds to 0% FCA based AAS mixture, Level 2 corresponds to 25% FCA based AAS mortar mixture and Level 3 corresponds to 50% FCA based AAS mortar mixture. Since delta value of Na₂O dosage is higher compared to FCA content, overall durability performance (considering durability factors, VPV, sulphate attack and acid attack) of FCA based AAS mortar mixtures can be effectively increased with increasing Na₂O dosage of alkaline solution. Compared to Na₂O dosage, increase in durability performance is less with increase in FCA content of AAS mortar mixtures.

Table 5.8: Response table for GRG by considering durability aspects.

Input Variables	Level 1	Level 2	Level 3	Max	Min	Delta (Max - Min)	Rank
FCA	0.177	0.191	0.214	0.214	0.177	0.036	2
Na ₂ O	0.161	0.183	0.238	0.238	0.161	0.077	1

5.6 OPTIMIZATION OF FERROCHROME ASH BASED ALKALI ACTIVATED SLAG MORTAR MIXTURES BY TECHNIQUE FOR ORDER OF PREFERENCE BY SIMILARITY TO IDEAL SOLUTION

TOPSIS method is used to find optimal mixture in FCA based AAS mortar mixtures under different alkaline solution concentration. First step in TOPSIS is normalization of responses by means of forming decision matrix. Equation 3.5 was used to compute the normalized decision matrix. Weighted normalized decision matrix is calculated by considering Equation 3.6 with weightage of 0.33. Computed values of normalized decision matrix and weighted normalized decision matrix are shown in Table 5.9. Further, positive and negative ideal solution is computed by considering previously computed weighted normalized decision matrix and Equation 3.7(a and b). Table 5.10 shows the values of positive and negative ideal solution values of responses considered in the study. Closeness coefficient is the key parameter to identify the ranking of different FCA based mortar mixtures. Closeness coefficient is calculated based on the Equation 3.8 and Equation 3.9. Computed values of closeness coefficient are given in Table 5.10. Higher value of closeness coefficient decides the first rank in FCA based AAS mortar mixtures.

Table 5.9: Normalized decision matrix and weighted normalized decision matrix of FCA based AAS mortar mixtures.

Sl No	Normalized Decision Matrix			Weighted Normalized Decision Matrix		
	VPV	Sulphate Attack (Normalized Compressive Strength)	Acid Attack (Normalized Compressive Strength)	VPV	Sulphate Attack (Normalized Compressive Strength)	Acid Attack (Normalized Compressive Strength)
1	0.328	0.309	0.258	0.108	0.102	0.085
2	0.324	0.320	0.302	0.107	0.106	0.100
3	0.320	0.322	0.321	0.106	0.106	0.106
4	0.332	0.329	0.307	0.110	0.109	0.101
5	0.328	0.334	0.271	0.108	0.110	0.089
6	0.320	0.343	0.338	0.106	0.113	0.112

7	0.356	0.340	0.366	0.118	0.112	0.121
8	0.348	0.346	0.383	0.115	0.114	0.126
9	0.340	0.354	0.421	0.112	0.117	0.139

Ranking order of the different FCA based AAS mortar mixtures can be given as below:

AAS50F50N6 > AAS50F50N5 > AAS50F50N4 > AAS75F25N6 > AAS100F0N6 > AAS75F25N4 > AAS100F0N5 > AAS75F25N5 > AAS100F0N4.

50% FCA based AAS mortar mixture prepared with 6% Na₂O dosage obtained first rank and 0% FCA based AAS mortar mixture prepared with 4% Na₂O dosage obtained last rank considering durability aspect like, VPV, residual compressive strength under sulphate and acid attack in TOPSIS method.

Table 5.10: Positive and negative ideal solution, closeness coefficient and ranking of FCA based AAS mortar mixtures.

Sl No	Mixture ID	Positive Ideal Solution	Negative Ideal Solution	Closeness Coefficient	Rank
1	AAS100F0N4	0.056	0.009	0.142	9
2	AAS100F0N5	0.041	0.018	0.308	7
3	AAS100F0N6	0.035	0.024	0.411	5
4	AAS75F25N4	0.039	0.019	0.332	6
5	AAS75F25N5	0.050	0.013	0.206	8
6	AAS75F25N6	0.028	0.031	0.528	4
7	AAS50F50N4	0.022	0.037	0.623	3
8	AAS50F50N5	0.016	0.043	0.729	2
9	AAS50F50N6	0.01	0.06	0.895	1

Table 5.11 provides responses of closeness coefficient values of and ranking of two input variables i.e., FCA content and Na₂O dosage concentration. Level 1, Level 2

and Level 3 represents the average value of closeness coefficient value in case of input variable FCA and Na₂O dosage. Level 1 corresponds to 0% FCA based AAS mixture, Level 2 corresponds to 25% FCA based AAS mortar mixture and Level 3 corresponds to 50% FCA based AAS mortar mixture. Since delta value of FCA content is high compared to Na₂O dosage, overall durability performance (considering durability factors like, VPV, residual compressive strength under sulphate attack and acid attack) of FCA based AAS mortar mixtures can be effectively increased with increase in FCA content. Compared to FCA content, increase in durability performance is less with increase in Na₂O dosage in AAS mortar mixture.

Table 5.11: Response table for closeness coefficient by considering durability aspects.

Input variables	Level 1	level 2	Level 3	Max	Min	Delta (Max - Min)	Rank
FCA	0.287	0.355	0.749	0.749	0.287	0.462	1
Na ₂ O	0.366	0.414	0.611	0.611	0.366	0.245	2

5.7 OPTIMIZATION OF FERROCHROME ASH BASED ALKALI ACTIVATED SLAG MORTAR MIXTURES BY DESIRABILITY FUNCTION APPROACH

DFA method was the third MCDM method used in the present study. Compared to GRA and TOPSIS methods, DFA method is simple and less time consuming to arrive at final rankings of the FCA based AAS mortar mixtures. Initial step in DFA method is computation of individual desirability values of each response. Equation 3.10 and Equation 3.11 are used to compute individual desirability value and overall desirability value respectively for each of the responses. Weightage of 0.33 is used to compute the overall desirability values of responses studied. Table 5.12 gives the overall desirability value of the FCA based AAS mortar mixtures. Similar to GRG and closeness coefficient values in GRA and TOPSIS method respectively, overall desirability value plays a vital role in deciding ranking of different FCA based AAS mortar mixture.

Ranking order of the different FCA based AAS mortar mixtures can be given as below:

AAS50F50N6 > AAS75F25N6 > AAS50F50N5 > AAS100F0N6 > AAS75F25N4 > AAS100F0N5 > AAS75F25N5 > AAS100F0N4 = AAS50F50N4.

50% FCA based AAS mortar mixture prepared with 6% Na₂O dosage obtained first rank. 0% FCA based AAS mortar mixture prepared with 4% Na₂O dosage and 50% FCA based AAS mortar mixture prepared with 4% Na₂O dosage obtained last rank (Since overall desirability value of two mixtures are zero) considering durability aspect like VPV, residual compressive strength under sulphate and acid attack in DFA method.

Table 5.12: Individual desirability, overall desirability values and ranking of FCA based AAS mortar mixtures.

Sl No	Mixture ID	Individual desirability			Overall Desirability	Rank
		Sulphate Attack (Normalized Compressive Strength)	Acid Attack (Normalized Compressive Strength)	VPV		
1	AAS100F0N4	0.000	0.000	0.778	0.000	8
2	AAS100F0N5	0.235	0.268	0.889	0.618	6
3	AAS100F0N6	0.289	0.385	1.000	0.693	4
4	AAS75F25N4	0.435	0.303	0.667	0.666	5
5	AAS75F25N5	0.545	0.079	0.778	0.567	7
6	AAS75F25N6	0.745	0.491	1.000	0.845	2
7	AAS50F50N4	0.693	0.659	0.000	0.000	8
8	AAS50F50N5	0.824	0.764	0.222	0.720	3
9	AAS50F50N6	1.000	1.000	0.444	0.873	1

Table 5.13: Response table for overall desirability by considering durability aspects.

Input Variables	Level 1	Level 2	Level 3	Max	Min	Delta (Max - Min)	Rank
FCA	0.437	0.693	0.531	0.693	0.437	0.256	2
Na ₂ O	0.222	0.635	0.804	0.804	0.222	0.582	1

Table 5.13 provides responses of overall desirability values of all the FCA based AAS mortar mixtures prepared with different Na₂O dosage concentration. Table 5.13 shows the ranking of two input variables i.e., FCA content and Na₂O dosage concentration. Level 1, Level 2 and Level 3 represents the average value of overall desirability value in case of input variable FCA and Na₂O dosage. Level 1 corresponds to 0% FCA based AAS mixture, Level 2 corresponds to 25% FCA based AAS mortar mixture and Level 3 corresponds to 50% FCA based AAS mortar mixture. Similarly, Level 1, Level 2 and Level 3 correspond to 4, 5 and 6% Na₂O dosage respectively. As like GRA and TOPSIS method discussed previously, delta value of FCA content is high compared to Na₂O dosage. Overall durability performance (considering VPV, residual compressive strength of sulphate and acid attack) of FCA based AAS mortar mixtures can be effectively increased by increasing in FCA content. Compared to FCA content, increase in durability performance is less with increase in Na₂O dosage in AAS mortar mixtures.

5.8 SPEARMAN'S CORRELATION COEFFICIENT OF GREY RELATIONAL ANALYSIS, TECHNIQUE OF ORDER PREFERENCE SIMILARITY TO THE IDEAL SOLUTION and DESIRABILITY FUNCTION APPROACH METHOD RANKING

Interestingly first (AAS50F50N6) and last (AAS100F0N4) rank obtained in GRA, TOPSIS and DFA methods are same. However, the ranking orders obtained in all the three methods are different. In order to obtain suitable order of ranking in FCA based AAS mortar mixtures; Spearman's correlation coefficient is used for arriving final ranking of FCA based AAS mortar mixtures (Sadhukhan et al. 2014). Correlation coefficient between GRA and TOPSIS is 0.667, between TOPSIS and DFA is 0.669

and DFA and GRA is 0.870. Correlation coefficient value suggests that, DFA method strongly correlates with GRA and TOPSIS methods. Finally, ranking order obtained by DFA method is preferred for different FCA based AAS mortar mixtures.

5.9 CLOSURE

From the chapter discussed, durability study gives an insight to the acceptability of FCA based AAS mortar mixture as construction material considering VPV, residual compressive strength under sulphate and acid attack are considered as durability parameters. In order to choose material under durability condition GRA, TOPSIS and DFA methods were employed for the intended purpose of obtaining ranking of FCA based AAS mortar mixtures.

CHAPTER 6

ELEVATED TEMPERATURE AND ECOLOGICAL STUDIES OF ALKALI ACTIVATED SLAG/ FERROCHROME ASH BASED MORTARS

6.1 GENERAL

Elevated temperatures and ecological studies on FCA based AAS mortar mixtures were carried out on the FCA based AAS mortar mixtures in the present chapter. Mortars are likely to get exposed to elevated temperature under the event of accidental fire or when it is near to furnaces or reactors (Arioz, 2007). Elevated temperature exposure on mortar will lead to the reduction of the mechanical properties. Reduction of mechanical strength will further lead to the considerable damage to the structure. Present chapter discusses the residual compressive strength of FCA based AAS mortar mixtures under elevated temperatures ranging between 200 - 800 °C.

Ecological studies on any newly developed material is essential to promote or to encourage its use in market for its intended purpose. Ecological studies were carried out by means of evaluating ECO_{2eq} and EE_{eq} of FCA based AAS mortar mixtures using “Ecoinvent” database. In the present chapter, two input factors (% of FCA as binder and alkaline solution concentration) and three output responses (Residual compressive strength under elevated temperature, ECO_{2eq} and EE_{eq}) were considered to optimize the FCA based AAS mortar mixtures. In order to optimize the FCA based AAS mortar mixture GRA, TOPSIS and DFA methods were implemented along with spearman’s correlation coefficient.

6.2 ELEVATED TEMPERATURES STUDIES ON FERROCHROME ASH BASED ALKALI ACTIVATED SLAG MORTAR MIXTURES

Elevated temperatures study is carried out on FCA based AAS mortar mixture for the temperature range between 200-800 °C using programmable electrical muffle furnace. Total nine FCA based AAS mortar mixtures were considered for the elevated temperatures study. Detailed methodology on conducting elevated temperature studies can be obtained in the methodology chapter. Residual compressive strength of different FCA based AAS mortar mixtures can be observed in Table 6.1 and Figure 6.1. Increase in residual compressive strength is observed at 200 °C for all the FCA based AAS mortar mixtures. Increase in compressive strength is due to the autoclave effect. Decrease in compressive strength is observed with elevated temperatures ranging between 400-800 °C. Higher compressive strength loss is observed in case of 800 °C exposure. Decrease in compressive strength is due to the chemical composition changes in FCA based AAS mixtures.

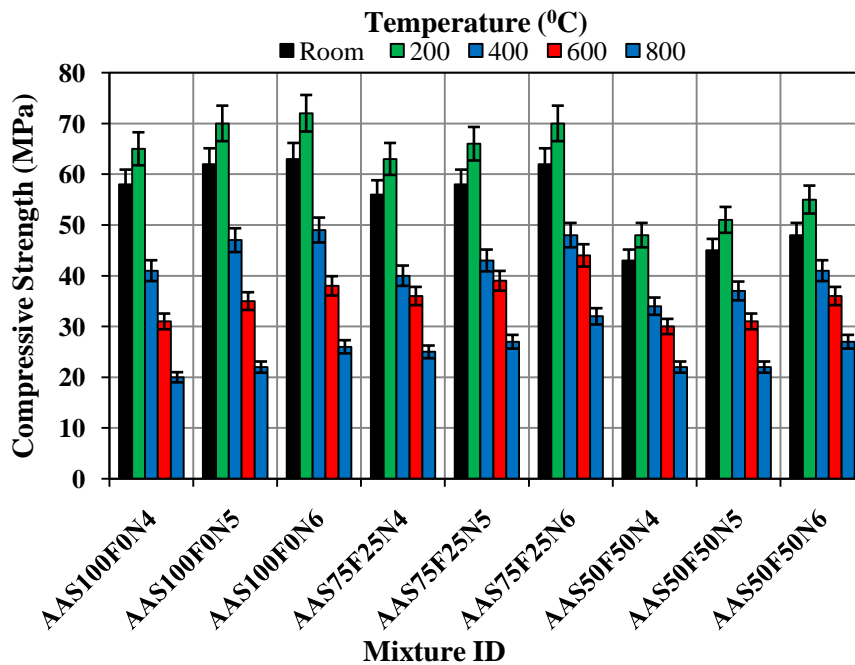


Figure 6.1: Compressive strength and residual compressive strength of FCA based AAS mortar mixtures under ambient and elevated temperatures condition.

Increase in compressive strength at 200 °C exposure is ranging between 12 – 15% for all the FCA based AAS mortar mixture. Decrease in compressive strength for 400, 600 and 800 °C exposure is ranging between 15-29, 25-47 and 44-66 respectively for all the FCA based AAS mortar mixture. At 800 °C, 66, 65, 59, 55, 53, 48, 49, 51 and 44% compressive strength loss is observed in case of AAS100F0N4, AAS100F0N5, AAS100F0N6, AAS75F25N4, AAS75F25N5, AAS75F25N6, AAS50F50N4, AAS50F50N5 and AAS50F50N6 mixtures respectively. Higher compressive strength loss is observed for 0% FCA based AAS mortar mixture prepared with 4% Na₂O dosage alkaline solution. Minimal compressive strength loss is observed with 50% FCA based AAS mortar mixture prepared with 6% Na₂O dosage alkaline solution. As the amount of FCA increases, resistance to compressive strength loss also increases. Increase in resistance with incorporation of FCA in AAS mortar mixtures, is due to the decrease in C-S-H gel formation reduction. Whereas, in case of FCA incorporation results in decrease of C-S-H gels with formation N-A-S-H gel and decomposition of C-S-H gels also gets reduced (Guerrieri and Sanjayan, 2010, Yaragal et al. 2020). Similarly, increase in resistance to compressive strength loss is observed with increase in Na₂O dosage. Increase in Na₂O dosage improves the microstructure of AAS mortar system by formation of denser microstructure (Rashad et al. 2012; Nasr et al. 2018).

Table 6.1: Compressive strength and residual compressive strength of FCA based AAS mortar mixtures under ambient and elevated temperatures condition.

Sl. No	Mixture ID	GGBS (%)	FCA (%)	Na ₂ O (%)	Compressive Strength and Residual Compressive Strength under Elevated Temperatures (MPa)				
					Room Temperature	200 °C	400 °C	600 °C	800 °C
1	AAS100F0N4	100	0	4	58	65	41	31	20
2	AAS100F0N5	100	0	5	62	70	47	35	22
3	AAS100F0N6	100	0	6	63	72	49	38	26
4	AAS75F25N4	75	25	4	56	63	40	36	25
5	AAS75F25N5	75	25	5	58	66	43	39	27
6	AAS75F25N6	75	25	6	62	70	48	44	32
7	AAS50F50N4	50	50	4	43	48	34	30	22
8	AAS50F50N5	50	50	5	45	51	37	31	22
9	AAS50F50N6	50	50	6	48	55	41	36	27

6.3 COMPARISON BETWEEN OPENLCA AND ECOINVENT BASED ANALYSIS RESULTS OF EMBODIED CARBON DI-OXIDE EMISSION AND EMBODIED ENERGY

ECO_{2eq} and EE_{eq} are important parameters needed to ascertain before using any new material. In Chapter 4, OpenLCA software was used to analyze the FCA based AAS mortar mixtures for ECO_{2eq} calculation. OpenLCA software uses ZOLCA file as a input database source. Uploading of ZOLCA file to OpenLCA software requires lot of space in hard disk, random-access memory and yearly license renewal. Further, analyzing the FCA based AAS mortar mixtures with OpenLCA software requires lot of time too. In order to address this issue, Ecoinvent database .pdf files were considered to evaluate the ECO_{2eq} and EE_{eq}.

Comparison between OpenLCA and Ecoinvent based analysis results are presented in Table 6.2 and Table 6.3 for ECO_{2eq} and EE_{eq} respectively. Three mixtures studied (AAS100F0N4, AAS75F25N4 and AAS50F50N4) in the Chapter 4 were considered for comparing OpenLCA and Ecoinvent based analysis. Results show that, percentage difference of OpenLCA and Ecoinvent based ECO_{2eq} and EE_{eq} calculations were less than one. So, Ecoinvent based methodology can be accepted for the calculation of ECO_{2eq} and EE_{eq} . Moreover, Ecoinvent based methodology reduces computing time and space utilization of system.

Table 6.2: Comparison between OpenLCA and Ecoinvent based analysis results of ECO_{2eq} .

ECO _{2eq} (kgCO ₂)			
Mixture ID / Software	AAS100F0N4	AAS75F25N4	AAS50F50N4
OpenLCA	271	247	223
Ecoinvent alone	273	249	224
% Difference of ECO_{2eq}	0.80	0.71	0.59

Table 6.3: Comparison between OpenLCA and Ecoinvent based analysis results of EE_{eq} .

EE _{eq} (MJ)			
Mixture ID /Software	AAS100F0N4	AAS75F25N4	AAS50F50N4
OpenLCA	4162	3768	3374
Ecoinvent 3.5	4191	3795	3398
% Difference of EE_{eq}	0.69	0.70	0.72

6.4 EMBODIED CARBON DI-OXIDE EMISSION STUDIES ON FERROCHROME ASH BASED ALKALI ACTIVATED SLAG MORTAR MIXTURES

Detailed calculation of ECO_{2eq} using Ecoinvent database is shown in Table 6.4. Calculation includes all the nine FCA based AAS mortar mixtures. Figure 6.1 show the variation of ECO_{2eq} with respect to different FCA based AAS mortar mixtures. As the amount of FCA increases, in ECO_{2eq} values decreases. Decrease in ECO_{2eq} is observed with addition of FCA in AAS mortar mixtures, since FCA is a byproduct generated during ferrochrome production and does not release CO_2 during its production. Further, increase in Na_2O dosage from 4-6% increases the ECO_{2eq} value of FCA based AAS mortar mixtures. Increase in ECO_{2eq} value is due to the increase in the $NaOH$ and Na_2SiO_3 solution quantity for the preparation of alkaline solution. $NaOH$ and Na_2SiO_3 solution releases lot of CO_2 during its production process. 50% FCA based AAS mortar mixture prepared with 4% Na_2O dosage shows lesser ECO_{2eq} compared to all other FCA based AAS mortar mixtures. 0% FCA based AAS mortar mixture prepared with 6% Na_2O dosage shows highest ECO_{2eq} value compared to all other FCA based AAS mortar mixtures.

Compared to ECO_{2eq} value of 4% Na_2O dosage with 0% FCA based AAS mortar mixture, 9 and 18% decrease in ECO_{2eq} value is observed with 25% and 50% FCA based AAS mortar mixtures respectively. Similar observations were made for 5 and 6% Na_2O dosage for FCA based AAS mortar mixtures with increase in FCA content.

Compared to ECO_{2eq} value of 0% FCA based AAS mortar mixture prepared with 4% Na_2O dosage, ECO_{2eq} values increases to 15 and 30% for 0% FCA based AAS mortar mixtures prepared with 5 and 6% Na_2O dosage alkaline solution concentration respectively. Similar observations were made for 25 and 50% FCA based AAS mortar mixtures with increase in Na_2O dosage.

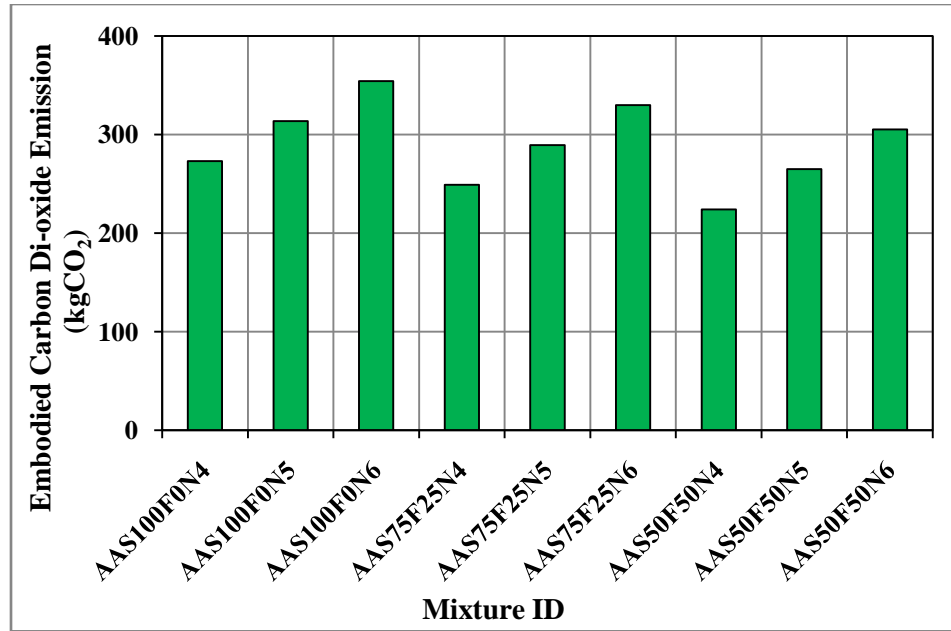


Figure 6.2: ECO_{2eq} value of FCA based AAS mortar mixtures for varies levels alkaline solution of concentration (i.e., 4 - 6% Na_2O dosage).

Table 6.4: Calculation of ECO_{2eq} of FCA based AAS mortar mixtures using Ecoinvent database.

Mixture ID	GGBS	FCA	Fine Aggregate	Water	Na ₂ SiO ₃	NaOH	GGBS	FCA	Fine Aggregate	Water	Na ₂ SiO ₃	NaOH	ECO _{2eq}
	kg						CO ₂ eq/kg						kgCO ₂
AAS100F0N4	1000	0	3000	320	152.4	22.7	0.098	0	0.004	0.002	0.835	1.531	273
AAS100F0N5	1000	0	3000	300	190.5	28.4	0.098	0	0.004	0.002	0.835	1.531	314
AAS100F0N6	1000	0	3000	280	228.7	34.0	0.098	0	0.004	0.002	0.835	1.531	354
AAS75F25N4	750	250	3000	320	152.4	22.7	0.098	0	0.004	0.002	0.835	1.531	249
AAS75F25N5	750	250	3000	300	190.5	28.4	0.098	0	0.004	0.002	0.835	1.531	289
AAS75F25N6	750	250	3000	280	228.7	34.0	0.098	0	0.004	0.002	0.835	1.531	330
AAS50F50N4	500	500	3000	320	152.4	22.7	0.098	0	0.004	0.002	0.835	1.531	224
AAS50F50N5	500	500	3000	300	190.5	28.4	0.098	0	0.004	0.002	0.835	1.531	265
AAS50F50N6	500	500	3000	280	228.7	34.0	0.098	0	0.004	0.002	0.835	1.531	305

Table 6.5: Calculation of EE_{eq} of FCA based AAS mortar mixtures using Ecoinvent database.

Mixture ID	GGBS	FCA	Fine Aggregate	Water	Na ₂ SiO ₃	NaOH	GGBS	FCA	Fine Aggregate	Water	Na ₂ SiO ₃	NaOH	EE _{eq}
	kg						MJ/kg						MJ
AAS100F0N4	1000	0	3000	320	152.4	22.7	1.585	0	0.062	0.022	12.577	21.896	4191
AAS100F0N5	1000	0	3000	300	190.5	28.4	1.585	0	0.062	0.022	12.577	21.896	4794
AAS100F0N6	1000	0	3000	280	228.7	34.0	1.585	0	0.062	0.022	12.577	21.896	5397
AAS75F25N4	750	250	3000	320	152.4	22.7	1.585	0	0.062	0.022	12.577	21.896	3795
AAS75F25N5	750	250	3000	300	190.5	28.4	1.585	0	0.062	0.022	12.577	21.896	4398
AAS75F25N6	750	250	3000	280	228.7	34.0	1.585	0	0.062	0.022	12.577	21.896	5001
AAS50F50N4	500	500	3000	320	152.4	22.7	1.585	0	0.062	0.022	12.577	21.896	3398
AAS50F50N5	500	500	3000	300	190.5	28.4	1.585	0	0.062	0.022	12.577	21.896	4001
AAS50F50N6	500	500	3000	280	228.7	34.0	1.585	0	0.062	0.022	12.577	21.896	4605

6.5 EMBODIED ENERGY STUDIES ON FERROCHROME ASH BASED ALKALI ACTIVATED SLAG MORTAR MIXTURES

Detailed calculation of EE_{eq} using Ecoinvent database is shown in Table 6.5. Calculation includes all the nine FCA based AAS mortar mixtures. Figure 6.3 show the variation of EE_{eq} with respect to different FCA based AAS mortar mixtures. As the amount of FCA increases in EE_{eq} values decreases. Decrease in EE_{eq} is observed with addition of FCA in AAS mortar mixture, since FCA is a byproduct generated in ferrochrome production and does not consume energy during its production. Further, increase in Na_2O dosage from 4% to 6% increases the EE_{eq} value of FCA based AAS mortar mixtures. Increase in EE_{eq} value is due to the increase in $NaOH$ and Na_2SiO_3 solution quantity for the preparation of alkaline solution. $NaOH$ and Na_2SiO_3 solution consumes lot of energy during their production process. 50% FCA based AAS mortar mixture prepared with 4% Na_2O dosage shows lesser EE_{eq} compared to all other FCA based AAS mortar mixtures. 0% FCA based AAS mortar mixture prepared with 6% Na_2O dosage shows highest EE_{eq} value compared to all other FCA based AAS mortar mixtures.

Compared to EE_{eq} value of 4% Na_2O dosage with 0% FCA based AAS mortar mixture, 9 and 19% decrease in EE_{eq} value is observed with 25% and 50% FCA based AAS mortar mixtures respectively. Similar observations were made for 5 and 6% Na_2O dosage based FCA based AAS mortar mixtures with increase in FCA content.

Compared to EE_{eq} value of 0% FCA based AAS mortar mixture prepared with 4% Na_2O dosage, EE_{eq} values increases to 14 and 29% for 0% FCA based AAS mortar mixtures prepared with 5 and 6% Na_2O dosage alkaline solution concentration respectively. Similar observations were made for 25 and 50% FCA based AAS mortar mixtures with increase in Na_2O dosage.



Figure 6.3: EE_{eq} values of FCA based AAS mortar mixtures for varies levels alkaline solution of concentration (i.e., 4 - 6% Na_2O dosage).

6.6 GREY RELATIONAL ANALYSIS ON ELEVATED TEMPERATURE AND ECOLOGICAL PARAMETERS OF FERROCHORME ASH BASED ALKALI ACTIVATED SLAG MORTAR MIXTURES

Table 6.6 shows the input responses used in the GRA method. Residual compressive strength (at 800 °C) is converted to normalized residual compressive strength. Normalized residual compressive strength was maximized. Whereas, ECO_{2eq} and EE_{eq} were minimized for optimizing the different FCA based AAS mortar mixtures.

Grey relational generation is first step in the optimization of FCA based AAS mortar mixtures in the process of optimizing FCA based AAS mortar mixtures considering residual compressive strength under elevated temperature condition, ECO_{2eq} and EE_{eq} . Using Equation 3.1 and 3.2, grey relational generation is computed. Computed values of grey relational generation are shown in Table 6.7. Equation 3.1 is used to maximization of normalized residual compressive strength under elevated temperature. Equation 3.2 is used to minimize the ECO_{2eq} and

EE_{eq} in GRA method. Using grey relational generation, deviation values are computed. Deviation values of FCA based AAS mixtures were obtained by using the formula: one minus grey relational grey relational generation value of each response. Computed deviation values are shown in Table 6.7.

Table 6.6: Responses used in GRA, TOPSIS and DFA method.

Sl No	Mixture ID	Binder		Alkaline Solution Concentration	Normalized Residual Compressive Strength	ECO ₂ (kgCO ₂)	EE _{eq} (MJ)
		GGBS	FCA	Na ₂ O			
		%					
1	AAS100F0N4	100	0	4	0.34	273	4191
2	AAS100F0N5	100	0	5	0.35	314	4794
3	AAS100F0N6	100	0	6	0.41	354	5397
4	AAS75F25N4	75	25	4	0.45	249	3794
5	AAS75F25N5	75	25	5	0.47	289	4398
6	AAS75F25N6	75	25	6	0.52	330	5001
7	AAS50F50N4	50	50	4	0.51	224	3398
8	AAS50F50N5	50	50	5	0.49	265	4001
9	AAS50F50N6	50	50	6	0.56	305	4605

Table 6.7: Grey relational generation and deviation values of GRA method.

SI No	Grey Relational Generation			Deviation		
	Normalized Residual Compressive Strength	ECO _{2eq}	EE _{eq}	Normalized Residual Compressive Strength	ECO _{2eq}	EE _{eq}
1	0.000	0.623	0.603	1.000	0.377	0.397
2	0.046	0.311	0.302	0.954	0.689	0.698
3	0.312	0.000	0.000	0.688	1.000	1.000
4	0.467	0.808	0.802	0.533	0.192	0.198
5	0.554	0.499	0.500	0.446	0.501	0.500
6	0.787	0.188	0.198	0.213	0.812	0.802
7	0.766	1.000	1.000	0.234	0.000	0.000
8	0.662	0.686	0.698	0.338	0.314	0.302
9	1.000	0.375	0.396	0.000	0.625	0.604

Table 6.8: GRC, GRG value and rank of different FCA based AAS mortar mixtures.

SI No	Mixture ID	GRC			GRG	Rank
		Normalized Residual Compressive Strength	ECO _{2eq}	EE _{eq}		
1	AAS100F0N4	0.333	0.570	0.558	0.161	7
2	AAS100F0N5	0.344	0.421	0.417	0.130	8
3	AAS100F0N6	0.421	0.333	0.333	0.120	9
4	AAS75F25N4	0.484	0.722	0.716	0.211	2
5	AAS75F25N5	0.529	0.499	0.500	0.168	5
6	AAS75F25N6	0.701	0.381	0.384	0.161	6
7	AAS50F50N4	0.681	1.000	1.000	0.295	1
8	AAS50F50N5	0.597	0.615	0.624	0.202	4
9	AAS50F50N6	1.000	0.445	0.453	0.209	3

GRC is calculated using Equation 3.3. GRC value is tabulated in Table 6.8. GRG value is calculated using previously calculated GRC and Equation 3.4 by considering equal weightage of each response (i.e., 0.33) for each responses. GRG value decides the ranking order of FCA based AAS mortar mixtures under elevated temperature and ecological aspects. Higher value of GRG will attain first rank and lowest value will attain the last rank. GRG and Ranking order of different FCA based AAS mortar mixtures are shown in Table 6.9.

Ranking order of the different FCA based AAS mortar mixtures based on GRA method can be given as below:

AAS50F50N4 > AAS75F25N4 > AAS50F50N6 > AAS50F50N5 > AAS75F25N5 > AAS75F25N6 > AAS100F0N4 > AAS100F0N5 > AAS100F0N6

50% FCA based AAS mortar mixture prepared with 4% Na₂O dosage obtained first rank. 0% FCA based AAS mortar mixture prepared with 6% Na₂O dosage obtained last rank considering elevated temperature and ecological aspects.

Table 6.9 shows the responses of GRG values obtained from the GRA method. These responses will be useful in identifying which input factor is more influencing on the output parameters considered for the study in GRA method. FCA has higher delta value compared to Na₂O dosage. So, FCA is more influencing factor when compared to Na₂O dosage considering elevated temperature and ecological aspects.

Table 6.9: Responses of GRG values of FCA based AAS mortar mixtures in GRA method.

Input Variables	Level 1	Level 2	Level 3	Max	Min	Delta (Max - Min)	Rank
FCA	0.137	0.180	0.235	0.235	0.137	0.098	1
Na ₂ O	0.222	0.167	0.163	0.222	0.163	0.059	2

6.7 TECHNIQUE OF ORDER PREFERENCE SIMILARITY TO THE IDEAL SOLUTION ON ELEVATED TEMPERATURE AND ECOLOGICAL PARAMETERS OF FCA BASED ALKALI ACTIVATED SLAG MORTAR MIXTURES

Similar to GRA and TOPSIS method is used as one of the optimizing method. Initial step in TOPSIS is framing normalized decision matrix of responses relating to residual compressive strength under elevated temperatures, ECO_{2eq} and EE_{eq} of different FCA based AAS mortar mixtures. Responses are tabulated in Table 6.6 and Equation 3.5 was used for calculation of normalized decision matrix. Equation 3.6 is used to calculation of weighted normalized decision matrix with calculated value of normalized decision matrix. Further, equal weightage is considered for weighted normalized decision matrix calculation (i.e., weightage value of 0.33 for each response). Computed value of normalized decision matrix and weighted normalized decision matrix are tabulated in Table 6.10.

Table 6.11 shows positive and negative ideal solution of different FCA based AAS mortar mixtures. Calculation of positive and negative ideal solution is based on the weighted matrix decision matrix using Equation 3.7(a and b). Important factor in TOPSIS method is finding of closeness coefficient. Closeness coefficient is calculated based on positive and negative ideal solution and separation distance [Separation distance can be calculated by Equation 3.8 (a and b)]. Calculated values of closeness value are shown in Table 6.11. Higher closeness coefficient value is observed for 50% FCA based AAS mortar mixture prepared with 4% Na_2O dosage. Lowest value of closeness coefficient is observed for 0% FCA based AAS mortar mixture prepared with 6% Na_2O dosage.

Table 6.10: Normalized decision matrix and weighted decision matrix of different FCA based AAS mortar mixtures used in TOPSIS method.

SI No	Normalized Decision Matrix			Weighted Normalized Decision Matrix		
	Normalized Residual Compressive Strength	ECO _{2eq}	EE _{eq}	Normalized Residual Compressive Strength	ECO _{2eq}	EE _{eq}
1	0.249	0.312	0.315	0.082	0.103	0.104
2	0.256	0.358	0.360	0.085	0.118	0.119
3	0.298	0.405	0.405	0.098	0.134	0.134
4	0.323	0.284	0.285	0.106	0.094	0.094
5	0.336	0.330	0.330	0.111	0.109	0.109
6	0.373	0.377	0.376	0.123	0.124	0.124
7	0.370	0.256	0.255	0.122	0.084	0.084
8	0.353	0.303	0.301	0.117	0.100	0.099
9	0.407	0.349	0.346	0.134	0.115	0.114

Table 6.11: Positive and negative ideal solution, closeness coefficient and ranking order of FCA based AAS mortar mixtures.

SI No	Mixture ID	Positive Ideal Solution	Negative Ideal Solution	Closeness Coefficient	Rank
1	AAS100F0N4	0.059	0.043	0.422	7
2	AAS100F0N5	0.069	0.021	0.237	8
3	AAS100F0N6	0.078	0.016	0.171	9
4	AAS75F25N4	0.031	0.061	0.665	3
5	AAS75F25N5	0.042	0.045	0.519	5
6	AAS75F25N6	0.057	0.043	0.429	6
7	AAS50F50N4	0.012	0.080	0.869	1
8	AAS50F50N5	0.028	0.059	0.681	2
9	AAS50F50N6	0.043	0.058	0.577	4

50% FCA based AAS mortar mixture prepared with 4% Na₂O dosage (AAS50F50N4) occupies first rank, since closeness coefficient value of AAS50F50N4 is higher compared to all other FCA based AAS mortar mixtures. 0% FCA based AAS mortar mixture prepared with 6% Na₂O dosage (AAS100F0N6) attains last rank, since closeness coefficient value of AAS100F0N6 is lowest compared to all other FCA based AAS mortar mixtures.

Ranking order of the different FCA based AAS mortar mixtures based on TOPSIS method can be given as below:

AAS50F50N4 > AAS50F50N5 > AAS75F25N4 > AAS50F50N6 > AAS75F25N5 > AAS75F25N6 > AAS100F0N4 > AAS100F0N5 > AAS100F0N6

Table 6.12 gives the response of closeness coefficient value of different FCA based AAS mortar mixture using TOPSIS method. Responses of closeness coefficient values are used to evaluate and to identify the most influencing input parameter which affects the output parameters. In the present case, FCA as a replacement to GGBS and Na₂O concentration in alkaline solution preparation are the two input parameters. Delta value of FCA is higher compared to Na₂O dosage. So, FCA as a replacement to GGBS is found to be most influencing on output responses like, residual compressive strength under elevated temperatures, ECO_{2eq} and EE_{eq} . Even, response table of GRG in GRA methodology shows FCA is most influencing factor compared to Na₂O dosage.

Table 6.12: Response of closeness coefficient values of FCA based AAS mortar mixtures.

Input Variables	Level 1	Level 2	Level 3	Max	Min	Delta (Max - Min)	Rank
FCA	0.277	0.537	0.709	0.709	0.277	0.432	1
Na ₂ O	0.652	0.479	0.392	0.652	0.392	0.260	2

6.8 DESIRABILITY FUNCTION APPROACH ON ELEVATED TEMPERATURE AND ECOLOGICAL PARAMETERS OF FERROCHROME ASH BASED ALKALI ACTIVATED SLAG MORTAR MIXTURES

DFA method is simplest method in computation compared to GRA and TOPSIS method. Since calculation will be done with two steps to identify the ranking of each mixture. Two steps involved in DFA methods are, 1) Computation of individual desirability value and 2) Computation of overall desirability value. Individual desirability was obtained using Table 6.6 responses, Equation 3.10 and Equation 3.11 for optimizing FCA based AAS mortar mixtures under elevated temperature and ecological conditions. Equation 3.10 is used to maximize the residual compressive strength of FCA based AAS mortar mixtures. Equation 3.11 is used to minimize the ECO_{2eq} and EE_{eq} response of FCA based AAS mortar mixtures. Further, computed individual desirability values of FCA based AAS mortar mixtures are tabulated in Table 6.13. Finally, overall desirability values of FCA based AAS mortar mixtures were computed and tabulated in Table 6.13 using previously computed individual desirability value and Equation 3.13. Overall desirability value optimizes the different FCA based AAS mortar mixtures. Higher overall desirability value was observed in 50% FCA based AAS mortar mixture prepared with 4% Na_2O dosage (AAS50F50N4). Lowest overall desirability is observed in two FCA based AAS mortar mixtures [i.e., 0% FCA based AAS mortar prepared with 4 and 6% Na_2O dosage (AAS100F0N4 and AAS100F0N6)].

Ranking order of the different FCA based AAS mortar mixtures based on DFA method can be given as below:

AAS50F50N4 > AAS50F50N5 > AAS75F25N4 > AAS50F50N6 > AAS75F25N5 > AAS75F25N6 > AAS100F0N5 > AAS100F0N4 = AAS100F0N6

50% FCA based AAS mortar mixture prepared with 4% Na₂O dosage attains first rank. 100% FCA based AAS mortar mixtures prepared with 4 and 6% Na₂O dosage attains last rank considering residual compressive strength under elevated temperatures, ECO_{2eq} and EE_{eq} as output factors.

Table 6.13: Individual desirability, overall desirability and ranking order of different FCA based AAS mortar mixtures.

Sl No	Mixture ID	Individual Desirability			Overall Desirability	Rank
		Normalized Residual Compressive Strength	ECO _{2eq}	EE _{eq}		
1	AAS100F0N4	0.000	0.623	0.603	0.000	8
2	AAS100F0N5	0.046	0.311	0.302	0.403	7
3	AAS100F0N6	0.312	0.000	0.000	0.000	8
4	AAS75F25N4	0.467	0.808	0.802	0.819	3
5	AAS75F25N5	0.554	0.499	0.500	0.719	5
6	AAS75F25N6	0.787	0.188	0.198	0.555	6
7	AAS50F50N4	0.766	1.000	1.000	0.957	1
8	AAS50F50N5	0.662	0.686	0.698	0.825	2
9	AAS50F50N6	1.000	0.375	0.396	0.727	4

Table 6.14 shows responses of overall desirability value of FCA based AAS mortar mixtures used in DFA method. Delta value shown in Table 6.14 is useful in identifying the most influencing input factor versus output considered in the present study. Delta value of FCA is higher compared to Na₂O dosage. So, FCA content variation will be more influencing factor on output responses compared to Na₂O dosage.

Table 6.14: Response of overall desirability values of FCA based AAS mortar mixtures.

Input variables	Level 1	Level 2	Level 3	Max	Min	Delta (Max - Min)	Rank
FCA	0.134	0.697	0.837	0.837	0.134	0.702	1
Na ₂ O	0.592	0.649	0.427	0.649	0.427	0.222	2

6.9 SPEARMAN'S CORRELATION COEFFICIENT OF GREY RELATIONAL ANALYSIS, TECHNIQUE OF ORDER PREFERENCE SIMILARITY TO THE IDEAL SOLUTION and DESIRABILITY FUNCTION APPROACH METHOD RANKING

Though first rank obtained by 50% FCA based AAS mortar mixture prepared with 4% Na₂O dosage is same in GRA, TOPSIS and DFA methods but ranking order obtained by GRA, TOPSIS and DFA methods are different. In order to ascertain this issue, Spearman's correlation coefficient is used to identify one best method to follow ranking order (Sadhukhan et al. 2014). Spearman's correlation coefficient value between GRA and TOPSIS method is 0.950. Spearman's correlation coefficient value in case of GRA and DFA method is 0.921. Lastly, Spearman's correlation coefficient value between TOPSIS and DFA is 0.971. Based on Spearman's correlation, TOPSIS method strongly correlates with GRA and DFA method. So, TOPSIS method can be used for final ranking order.

6.10 CLOSURE

This chapter has presented a clear overview regarding the use of FCA as binder material in AAS mortar system. Elevated temperatures and ecological studies to substantiate the use of value added materials like, FCA are studied. Use of FCA in AAS mortar system is a means to address and reduce the overburden of vast volume of waste disposal. Apart from that, FCA incorporation in AAS mortar mixtures improves the mechanical property under elevated temperature resistance of AAS mortar system. Further, FCA can also be used as construction material under elevated temperature situations without increasing the ECO_{2eq} and EE_{eq} .

CHAPTER 7

CONCLUSIONS

7.1 GENERAL

FCA was obtained from the gas cleaning plant of ferrochrome industries during the production of chromium. The utilization of FCA in the AAS system, addresses issues of global warming, waste utilization and waste management for sustainable development. Important findings from the present study i.e., compressive strength, microstructure, mineralogical tests, cost and ecological aspects are presented.

7.2 CONCLUSIONS

Following are the important conclusions;

1. Addition of Ferrochrome Ash (FCA) influences the flow property of mortar mixtures. As FCA replacement increases, spread value of mortar increases which can be attributed to the spherical nature of FCA particles.
2. Compressive strength of FCA based mortar mixtures is comparable with OPC based mortar mixtures.
3. Mineralogical studies reveals that, FCA based mortar mixtures did not show any progressive increase of C-S-H gel during secondary hydration process.
4. Residual compressive strength of mortar mixtures was found to be lower in case of higher replacement level of FCA. At 800⁰C, SEM image morphological studies reveal the disintegrated paste system of OPC and FCA based mortar mixtures.
5. Replacing 100% GGBS based AAS mortars with FCA as binder in AAS mortars resulted in reduced compressive strength. From the micro structural and mineralogical studies, it can be observed that C-S-H, C-A-S-H and gismondine are the main reaction

products in 100% GGBS based AAS mortars.

6. As the replacement of FCA increases in the AAS mortar, N-A-S-H is observed to be predominant with the co-existence of C-S-H, C-A-S-H and gismondine. The increase of N-A-S-H reduces the C-S-H, C-A-S-H and gismondine in the final composition of the FCA based AAS mortars when compared with 100% GGBS based AAS mortars.
7. The reduction of C-S-H, C-A-S-H and gismondine is the main reason for the reduction in compressive strength in FCA-based AAS mortars compared with 100% GGBS based AAS mortars.
8. The present study recommends optimum usage of 25% FCA replacement to GGBS in AAS mortars to achieve the desired compressive strength. Ecological and cost analysis studies showed that FCA based AAS mortars are found to be suitable with the benefit of having lower carbon footprint, lower embodied energy and reduced cost compared with 100% GGBS based AAS mortars.
9. As the amount of Na_2O dosage increases the compressive strength of FCA based AAS mortar mixture increases.
10. VPV of FCA based AAS mortar mixture decreases with increase in Na_2O dosage. Further, sulphate and acid resistance of FCA based AAS mortar mixture increases with increase in Na_2O dosage.
11. VPV of FCA based AAS mortar mixture increases with increase in FCA content. Further, sulphate and acid resistance of FCA based AAS mortar mixture decreases with increase in FCA content.
12. Ranking order obtained from DFA method was found to be best alternative for optimal mixture identification in term of VPV, sulphate resistance and acid resistance of FCA based AAS mortar mixtures.
13. Elevated temperature resistance of FCA based mortar mixture increases with increase in FCA content and Na_2O dosage. $\text{ECO}_{2\text{eq}}$ and EE_{eq} of FCA based AAS mortar mixture increases with increase in Na_2O dosage. However, $\text{ECO}_{2\text{eq}}$ and EE_{eq} of FCA based AAS mortar mixture decreases with increase in FCA content.
14. Ranking order obtained from TOPSIS method was found to be best alternative for

optimal mixture identification in term of elevated temperature resistance, ECO_{2eq} and EE_{eq} of FCA based AAS mortar mixtures.

7.3 SCOPE FOR FUTURE RESEARCH

As there is no data available for the use of FCA in AAS, the present study provides a scientific background for the suitability of FCA in AAS production. A few of the possible research initiatives in this area in future that need consideration for refinement are as follows.

Different curing processes like, heat curing, steam curing etc., on FCA based AAS mixtures can be undertaken. Tests on FCA based AAS mixtures on structural elements needs to be carried out. Its long-term performance needs to be studied for wider potential use. Laboratory based work can be extended to field conditions.

REFERENCES

1. Abdulkareem, M., Havukainen, J. and Horttanainen, M. (2019). "How environmentally sustainable are fibre reinforced alkali-activated concretes?." *J. Clean. Prod.*, 236, 117601.
2. Acharya, P.K. (2014). "Properties of concrete made with industrial waste blended cement and lime." PhD Thesis, KIIT University, Odissa, India.
3. Acharya, P.K. and Patro, S.K. (2015). "Effect of lime and ferrochrome ash (FA) as partial replacement of cement on strength, ultrasonic pulse velocity and permeability of concrete." *Constr. Build. Mater.*, 94, 448-457.
4. Acharya, P.K. and Patro, S.K. (2016a). "Acid resistance, sulphate resistance and strength properties of concrete containing ferrochrome ash (FA) and lime." *Constr. Build. Mater.*, 120, 241-250.
5. Acharya, P.K. and Patro, S.K. (2016b). "Use of ferrochrome ash (FCA) and lime dust in concrete preparation." *J. Clean. Prod.*, 131, 237-246.
6. Acharya, P.K. and Patro, S.K., (2016c). "Utilization of ferrochrome wastes such as ferrochrome ash and ferrochrome slag in concrete manufacturing." *Waste Manage. Res.* 34(8), 764-774.
7. Adesina, A. and Das, S. (2020). "Drying shrinkage and permeability properties of fibre reinforced alkali-activated composites." *Constr. Build. Mater.*, 251, 119076.
8. Arıcı, E. and Keleştemur, O. (2019). "Optimization of mortars containing steel scale using Taguchi based grey relational analysis method." *Constr. Build. Mater.*, 214, 232-241.
9. Arioz, O. (2007). "Effects of elevated temperatures on properties of concrete." *Fire Safe. J.*, 42(8), 516-522.
10. Ashraf, M., Khan, A.N., Ali, Q., Mirza, J., Goyal, A. and Anwar, A.M. (2009). "Physico-chemical, morphological and thermal analysis for the combined pozzolanic activities of minerals additives." *Constr. Build. Mater.*, 23(6), 2207-2213.

11. ASTM C642: 2013. “*Standard test method for density, absorption, and voids in hardened concrete.*” ASTM International, West Conshohocken, Pennsylvania, 2013.
12. Atabey, İ.İ., Karahan, O., Bilim, C., and Atiş, C.D. (2020). “The influence of activator type and quantity on the transport properties of class F fly ash geopolymer.” *Constr. Build. Mater.*, 264, 120268.
13. Attiogbe, E.K. and Rizkalla, S.H. (1988). “Response of concrete to sulfuric acid attack.” *ACI Mater. J.*, 85(6), 481-488.
14. Aydın, S., Yazıcı, H., Yiğiter, H. and Baradan, B. (2007). “Sulfuric acid resistance of high-volume fly ash concrete.” *Build. Env.*, 42(2), 717-721.
15. Benhelal, E., Zahedi, G., Shamsaei, E. and Bahadori, A. (2013). “Global strategies and potentials to curb CO₂ emissions in cement industry.” *J. Clean. Prod.*, 51, 142-161.
16. Bernal, S.A., De-Gutierrez, R.M., Provis, J.L. and Rose, V. (2010). “Effect of silicate modulus and metakaolin incorporation on the carbonation of alkali silicate activated slags.” *Cem. Concr. Res.*, 40(6), 898-907.
17. Bernal, S.A., San-Nicolas, R., Provis, J.L., De-Gutierrez, R.M. and Van-Deventer, J.S.J. (2014). “Natural carbonation of aged alkali activated slag concretes.” *Mater. Struct.*, 47(4), 693-707.
18. Bonen, D. and Cohen, M.D. (1992). “Magnesium sulfate attack on Portland cement paste-I. Microstructural analysis.” *Cem. Concr. Res.*, 22(1), 169-180.
19. Brough, A.R. and Atkinson, A. (2002). “Sodium silicate based, alkali activated slag mortars - Part I. Strength, hydration and microstructure.” *Cem. Concr. Res.*, 32(6), 865-879.
20. Cao, H.T., Bucea, L., Ray, A. and Yozghatlian, S. (1997). “The effect of cement composition and pH of environment on sulfate resistance of Portland cements and blended cements.” *Cem. Concr. Compo.*, 19(2), 161-171.
21. Chen, W. and Brouwers, H.J.H. (2007). “The hydration of slag, Part 1: Reaction models for alkali activated slag.” *J. Mater. Sci.*, 42(2), 428-443.
22. Chi, M. and Huang, R. (2013). “Binding mechanism and properties of alkali activated fly ash/slag mortars.” *Constr. Build. Mater.*, 40, 291-298.

23. Chindaprasirt, P., Jaturapitakkul, C., Chalee, W. and Rattanasak, U. (2009). "Comparative study on the characteristics of fly ash and bottom ash geopolymers." *Waste Manage.* 29(2), 539-543.
24. Chougan, M., Marotta, E., Lamastra, F.R., Vivio, F., Montesperelli, G., Ianniruberto, U. and Bianco, A. (2020). "High performance cementitious nanocomposites: The effectiveness of nano-Graphite (nG)." *Constr. Build. Mater.*, 259, 119687.
25. Collins, F. and Sanjayan, J. (1999a). "Effects of ultra-fine materials on workability and strength of concrete containing alkali activated slag as the binder." *Cem. Concr. Res.*, 29(3), 459-462.
26. Collins, F. and Sanjayan, J.G. (1999b). "Workability and mechanical properties of alkali activated slag concrete." *Cem. Concr. Res.*, 29(3), 455-458.
27. Cülfik, M.S. and Özturan, T. (2002). "Effect of elevated temperatures on the residual mechanical properties of high-performance mortar." *Cem. Concr. Res.*, 32(5), 809-816.
28. Das, B.B. and Pandey, S.P. (2011). "Influence of fineness of fly ash on the carbonation and electrical conductivity of concrete." *J. Mat. Civ. Eng.*, 23(9), 1365-1368.
29. Dash, M.K. and Patro, S.K. (2018a). "Performance assessment of ferrochrome slag as partial replacement of fine aggregate in concrete." *European J. Env. Civil Eng.*, 1-20.
30. Dash, M.K. and Patro, S.K. (2018b). "Effects of water cooled ferrochrome slag as fine aggregate on the properties of concrete." *Constr. Build. Mater.*, 177, 457-466.
31. Dave, N., Misra, A.K., Srivastava, A. and Kaushik, S.K. (2017). "Setting time and standard consistency of quaternary binders: The influence of cementitious material addition and mixing." *Int. J. Sust. Built Env.*, 6(1), 30-36.
32. Davidovits, J. (1991). "Geopolymers: Inorganic polymeric new materials." *J. Therm. Anal. Calorim.*, 37(8), 1633-1656.
33. Deng, J. (1989), "Introduction to grey system theory", *J. Grey Sys.*, 1(1), 1-24.
34. Derringer, G. and Suich, R. (1980). "Simultaneous optimization of several response variables." *J. Qual. Tech.*, 12(4), 214-219.

35. Dombrowski, K., Buchwald, A. and Weil, M. (2007). "The influence of calcium content on the structure and thermal performance of fly ash based geopolymers." *J. Mater. Sci.*, 42(9), 3033-3043.
36. Douglas, E., Bilodeau, A., Brandstetr, J. and Malhotra, V.M. (1991). "Alkali activated ground granulated blast furnace slag concrete: Preliminary investigation." *Cem. Concr. Res.*, 21(1), 101-108.
37. Fernández- Jiménez, A., Puertas, F., Sobrados, I. and Sanz, J. (2003). "Structure of calcium silicate hydrates formed in alkaline- activated slag: Influence of the type of alkaline activator." *J. Am. Ceram. Soc.*, 86(8), 1389-1394.
38. Fu, Y., Ding, J. and Beaudoin, J.J. (1997). "Expansion of Portland cement mortar due to internal sulfate attack." *Cem. Concr. Res.*, 27(9), 1299-1306.
39. Gencil, O., Koksall, F., Ozel, C. and Brostow, W. (2012). "Combined effects of fly ash and waste ferrochromium on properties of concrete." *Constr. Build. Mater.*, 29, 633-640.
40. Gettu, R., Patel, A., Rathi, V., Prakasan, S., Basavaraj, A.S., Palaniappan, S. and Maity, S. (2019). "Influence of supplementary cementitious materials on the sustainability parameters of cements and concretes in the Indian context." *Mater. Struct.*, 52(1), 10.
41. Gopal, P.M. and Prakash, K.S. (2018). "Minimization of cutting force, temperature and surface roughness through GRA, TOPSIS and Taguchi techniques in end milling of Mg hybrid MMC." *Measure.*, 116, 178-192.
42. Gu, K., Jin, F., Al-Tabbaa, A., Shi, B. and Tang, C. (2015). "Evaluation of sulfate resistance of calcined dolomite activated ground granulated blast furnace slag." *J. Mat. Civ. Eng.*, 28(2), 04015135.
43. Guerrieri, M. and Sanjayan, J.G. (2010). "Behavior of combined fly ash/slag- based geopolymers when exposed to high temperatures." *Fire Mat.*, 34(4), 163-175.
44. Hiremath, P.N. and Yaragal, S.C. (2018). "Performance evaluation of reactive powder concrete with polypropylene fibers at elevated temperatures." *Constr. Build. Mater.*, 169, 499-512.

45. Hot, J., Cyr, M., Augéard, E. and Eekhout, M. (2015). "An investigation of CaSi silica fume characteristics and its possible utilization in cement based and alkali activated materials." *Constr. Build. Mater.*, 101, 456-465.
46. Indian Minerals Yearbook (2018). "Part- III: Mineral Reviews – Chromite." 57th Edition.
47. IS 10086:1982. "*Specification for moulds for use in tests of cement and concrete.*" Bureau of Indian Standards, New Delhi, India.
48. IS 12269:2013. "*Ordinary Portland cement, 53 Grade-Specification.*" Bureau of Indian Standards, New Delhi, India.
49. IS 1727: 1967. "*Methods of test for pozzolanic material.*" Bureau of Indian Standards, India. Bureau of Indian Standards, New Delhi, India.
50. IS 383:2016. "*Coarse and fine aggregate for concrete- Specification.*" Bureau of Indian Standards, New Delhi, India.
51. IS 4031(Part 6):1988. "*Methods of physical tests for hydraulic cement.*" Bureau of Indian Standards, New Delhi, India.
52. IS 455: 1989. "*Portland slag cement- Specification.*" Bureau of Indian Standards, New Delhi, India.
53. Ismail, I., Bernal, S.A., Provis, J.L., San-Nicolas, R., Brice, D.G., Kilcullen, A.R., Hamdan, S. and Van-Deventer, J.S.J. (2013). "Influence of fly ash on the water and chloride permeability of alkali activated slag mortars and concretes." *Constr. Build. Mater.*, 48 1187-1201.
54. Karahan, O. (2011). "Residual compressive strength of fire- damaged mortar after post- fire- air- curing." *Fire Mat.*, 35(8), 561-567.
55. Karahan, O. and Yakupoğlu, A. (2011). "Resistance of alkali-activated slag mortar to abrasion and fire." *Adv. Cem. Res.*, 23(6), 289-297.
56. Khater, H.M. (2013). "Effect of silica fume on the characterization of the geopolymer materials." *Int. J. Adv. Struct. Eng.*, 5(1), 1-10.
57. Kong, D.L., Sanjayan, J.G. and Sagoe-Crentsil, K. (2007). "Comparative performance of geopolymers made with metakaolin and fly ash after exposure to elevated temperatures." *Cem. Concr. Res.*, 37(12), 1583-1589.

58. Kuenzel, C., Grover, L.M., Vandeperre, L., Boccaccini, A.R. and Cheeseman, C. R. (2013). "Production of nepheline/quartz ceramics from geopolymer mortars." *J. Euro. Cer. Soc.*, 33(2), 251-258.
59. Kulkarni, K.S., Yaragal, S.C. and Narayan, K.S.B. (2019). "Core recovery: A damage diagnosis tool for thermally deteriorated concrete." *J. Struct. Fire Eng.*, 10(2), 126-137.
60. Kulkarni, K.S., Yaragal, S.C., Narayan, K.S.B. and Vardhan, H. (2017). "Assessment of thermally deteriorated concrete by drilling resistance test and sound level." *Russian J. Nondest. Testi.*, 53(11), 805-815.
61. Kumar, G.S. (2019). "Influence of fluidity on mechanical and permeation performances of recycled aggregate mortar." *Constr. Build. Mater.*, 213, 404-412.
62. Lee, N.K. and Lee, H.K. (2013). "Setting and mechanical properties of alkali activated fly ash/slag concrete manufactured at room temperature." *Constr. Build. Mater.*, 47, 1201-1209.
63. Lee, N.K., Jang, J.G. and Lee, H.K. (2014). "Shrinkage characteristics of alkali activated fly ash/slag paste and mortar at early ages." *Cem. Concr. Compos.*, 53, 239-248.
64. Lind, B.B., Fällman, A.M. and Larsson, L.B. (2001). "Environmental impact of ferrochrome slag in road construction." *Waste Manage.*, 21(3), 255-264.
65. Liu, L., Xie, M., He, Y., Li, Y., Wei, A. and Shi, C. (2020). "Expansion behavior and microstructure change of alkali-activated slag grouting material in carbonate environment." *Constr. Build. Mater.*, 262, 120593.
66. Maiti, M., Sarkar, M., Maiti, S., Malik, M.A. and Xu, S. (2020). "Modification of geopolymer with size controlled TiO₂ nanoparticle for enhanced durability and catalytic dye degradation under UV light." *J. Clean. Prod.*, 255, 120183.
67. Marinković, S., Dragaš, J., Ignjatović, I. and Tošić, N. (2017). "Environmental assessment of green concretes for structural use." *J. Clean. Prod.*, 154, 633-649.
68. McLellan, B.C., Williams, R.P., Lay, J., Van Riessen, A. and Corder, G.D. (2011). "Costs and carbon emissions for geopolymer pastes in comparison to ordinary portland cement." *J. Clean. Prod.*, 19(9-10), 1080-1090.
69. Mehta, P.K. (1983). "Mechanism of sulfate attack on Portland cement concrete- Another look." *Cem. Concr. Res.*, 13(3), 401-406.

70. Mousavi-Nasab, S.H. and Sotoudeh-Anvari, A. (2017). "A comprehensive MCDM-based approach using TOPSIS, COPRAS and DEA as an auxiliary tool for material selection problems." *Mat. Des.*, 121, 237-253.
71. Mundra, S., Sindhi, P. R., Chandwani, V., Nagar, R. and Agrawal, V. (2016). "Crushed rock sand—An economical and ecological alternative to natural sand to optimize concrete mix." *Perspectives in Science*, 8, 345-347.
72. Myers, R.J., Bernal, S.A., San-Nicolas, R. and Provis, J.L. (2013). "Generalized structural description of calcium sodium alumino silicate hydrate gels: The cross-linked substituted tobermorite model." *Langmuir*. 29(17), 5294-5306.
73. Nadeem, A., Memon, S.A. and Lo, T.Y. (2013). "Mechanical performance, durability, qualitative and quantitative analysis of microstructure of fly ash and Metakaolin mortar at elevated temperatures." *Constr. Build. Mater.*, 38, 338-347.
74. Nasr, D., Pakshir, A.H. and Ghayour, H. (2018). "The influence of curing conditions and alkaline activator concentration on elevated temperature behavior of alkali activated slag (AAS) mortars." *Constr. Build. Mater.*, 190, 108-119.
75. Nath, S.K. (2018). "Geopolymerization behavior of ferrochrome slag and fly ash blends." *Constr. Build. Mater.*, 181, 487-494.
76. Nath, S.K. and Kumar, S. (2013). "Influence of iron making slags on strength and microstructure of fly ash geopolymer." *Constr. Build. Mater.*, 38, 924-930.
77. Navarro, I.J., Yepes, V., Martí, J.V. and González-Vidosa, F. (2018). "Life cycle impact assessment of corrosion preventive designs applied to prestressed concrete bridge decks." *J. Clean. Prod.*, 196, 698-713.
78. Palankar, N., Shankar, A.U.R., and Mithun, B.M. (2016). "Durability studies on eco-friendly concrete mixes incorporating steel slag as coarse aggregates." *J. Clean. Prod.*, 129, 437-448.
79. Papathanasiou, J. and Ploskas, N. (2018). "Multiple criteria decision aid. In Methods, Examples and Python Implementations." *Springer*, 136.
80. Paris, J.M., Roessler, J.G., Ferraro, C.C., DeFord, H.D. and Townsend, T.G. (2016). "A review of waste products utilized as supplements to Portland cement in concrete." *J. Clean. Prod.*, 121, 1-18.
81. Pelisser, F., Vieira, A. and Bernardin, A.M. (2018). "Efficient self-compacting concrete with low cement consumption." *J. Clean. Prod.*, 175, 324-332.

82. Pereira, A., Akasaki, J.L., Melges, J.L.P., Tashima, M.M., Soriano, L., Borrachero, M.V., Monzó, J. and Payá, J. (2015). "Mechanical and durability properties of alkali activated mortar based on sugarcane bagasse ash and blast furnace slag." *Ceram. Int.*, 41(10), 13012-13024.
83. Pradhan, S., Tiwari, B.R., Kumar, S. and Barai, S.V. (2019). "Comparative LCA of recycled and natural aggregate concrete using Particle Packing Method and conventional method of design mix." *J. Clean. Prod.*, 228, 679-691.
84. Provis, J. L., and Van Deventer, J. S. (2013). "Alkali activated materials: State-of-the-art report." *RILEM TC 224-AAM, Springer*, 13.
85. Prusty, J.K. and Pradhan, B. (2020). "Multi-response optimization using Taguchi-Grey relational analysis for composition of fly ash-ground granulated blast furnace slag based geopolymer concrete." *Constr. Build. Mater.*, 241, 118049.
86. Puertas, F. and Torres-Carrasco, M. (2014). "Use of glass waste as an activator in the preparation of alkali activated slag: Mechanical strength and paste characterization." *Cem. Concr. Res.*, 57, 95-104.
87. Puertas, F., Palacios, M., Manzano, H., Dolado, J.S., Rico, A. and Rodríguez, J. (2011). "A model for the CASH gel formed in alkali activated slag cements." *J. Eur. Ceram. Soc.*, 31(12), 2043-2056.
88. Qu, F., Li, W., Tao, Z., Castel, A. and Wang, K. (2020). "High temperature resistance of fly ash/GGBFS-based geopolymer mortar with load-induced damage." *Mater. Struct.*, 53(4), 1-21.
89. Rajamane, N.P., Nataraja, M.C., Dattatreya, J.K., Lakshmanan, N. and Sabitha, D. (2012). "Sulphate resistance and ecofriendliness of geopolymer concretes." *Indian Concr. J.* 86(1), 13-22.
90. Rajan, H. S. and Kathirvel, P. (2020). "Sustainable development of geopolymer binder using sodium silicate synthesized from agricultural waste." *J. Clean. Prod.*, 124959.
91. Ramyar, K. and Inan, G. (2007). "Sodium sulfate attack on plain and blended cements." *Build. Env.*, 42(3), 1368-1372.
92. Rashad, A.M. (2015a). "A brief on high-volume Class F fly ash as cement replacement: A guide for civil engineer." *Int. J. Sust. Built Env.*, 4(2), 278-306.

93. Rashad, A.M. (2015b). "An investigation of high-volume fly ash concrete blended with slag subjected to elevated temperatures." *J. Clean. Pro.*, 93, 47-55.
94. Rashad, A.M. and Sadek, D.M. (2016). "An investigation on Portland cement replaced by high-volume GGBS pastes modified with micro-sized metakaolin subjected to elevated temperatures." *Int. J. Sust. Built Env.*, 6(1), 91-101.
95. Rashad, A.M., Bai, Y., Basheer, P.A.M., Collier, N.C. and Milestone, N.B. (2012). "Chemical and mechanical stability of sodium sulfate activated slag after exposure to elevated temperature." *Cem. Concr. Res.*, 42(2), 333-343.
96. Rashad, A.M., Sadek, D.M. and Hassan, H.A. (2016). "An investigation on blast-furnace slag as fine aggregate in alkali-activated slag mortars subjected to elevated temperatures." *J. Clean. Prod.*, 112, 1086-1096.
97. Rashid, K., Rehman, M. U., de Brito, J. and Ghafoor, H. (2020). "Multi-criteria optimization of recycled aggregate concrete mixes." *J. Clean. Prod.*, 276, 124316.
98. Sadhukhan, S. Banerjee, U.K. and Maitra, B. (2014). "Commuters' perception towards transfer facility attributes in and around metro stations: Experience in Kolkata", *J. Urb. Plan. Develop.*, 141(4), 04014038.
99. Saha, A.K., Sarker, P.K. and Golovanevskiy, V. (2019). "Thermal properties and residual strength after high temperature exposure of cement mortar using ferronickel slag aggregate." *Constr. Build. Mater.*, 199, 601-612.
100. Sahoo, S., Das, B.B. and Mustakim, S. (2016). "Acid, alkali, and chloride resistance of concrete composed of low carbonated fly ash." *J. Mat. Civ. Eng.*, 29(3), 04016242.
101. Samad, S. and Shah, A. (2017). "Role of binary cement including supplementary cementitious material (SCM), in production of environmentally sustainable concrete: A critical review." *Int. J. Sust. Built Env.*, 6(2), 663-674.
102. Santhanam, M., Cohen, M.D. and Olek, J. (2002). "Mechanism of sulfate attack: A fresh look - Part 1: Summary of experimental results." *Cem. Concr. Res.*, 32(6), 915-921.
103. Sengul, O. and Tasdemir, M.A. (2009). "Compressive strength and rapid chloride permeability of concretes with ground fly ash and slag." *J. Mat. Civ. Eng.*, 21(9), 494-501.

104. Sezer, G.İ. (2012). "Compressive strength and sulfate resistance of limestone and/or silica fume mortars." *Const. Build. Mater.*, 26(1), 613-618. .
105. Shah, S.F.A., Chen, B., Ahmad, M.R. and Haque, M.A. (2021). "Development of cleaner one-part geopolymer from lithium slag." *J. Clean. Prod.*, 125241.
106. Siddique, R. and Cachim, P. (2018). "Waste and Supplementary Cementitious Materials in Concrete: Characterisation, Properties and Applications." *Woodhead Publishing*.
107. Şimşek, B., İç, Y.T. and Şimşek, E.H. (2013). "A TOPSIS-based Taguchi optimization to determine optimal mixture proportions of the high strength self-compacting concrete." *Chemo Intel. Lab. Sys.*, 125, 18-32.
108. Singh, T. Patnaik, A. and Chauhan, R. (2016). "Optimization of tribological properties of cement kiln dust-filled brake pad using grey relation analysis." *Mat. Des.*, 89, 1335-1342.
109. Sonebi, M. (2010). "Optimization of cement grouts containing silica fume and viscosity modifying admixture." *J. Mat. Civ. Eng.*, 22(4), 332-342.
110. Songpiriyakij, S., Kubprasit, T., Jaturapitakkul, C., and Chindaprasirt, P. (2010). "Compressive strength and degree of reaction of biomass and fly ash based geopolymer." *Constr. Build. Mater.*, 24(3), 236-240.
111. Tasnim, S., Du, Y., Rahman, M. E., Ahmadi, R.B. and Doh, S.I. (2020). "Effect of using palm oil fuel ash on the durability of cement paste in ammonium nitrate solution." *Constr. Build. Mater.*, 257, 119597.
112. Türkmen, İ. and Fındık, S.B. (2013). "Several properties of mineral admixed lightweight mortars at elevated temperatures." *Fire Mat.*, 37(5), 337-349.
113. Ueda, T., Roberts, E.S., Norton, A., Styles, D., Williams, A.P., Ramos, H.M. and Gallagher, J. (2019). "A life cycle assessment of the construction phase of eleven micro-hydropower installations in the UK." *J. Clean. Prod.*, 218, 1-9.
114. Vasanthi, P. and Selvan, S.S. (2020). "Optimization of mixing parameters in nanosilica toughened cement mortar using Taguchi-Grey relational analysis." *Silicon*, 1-7.
115. Vedalakshmi, R. Rajagopal, K. and Palaniswamy, N. (2008). "Longterm corrosion performance of rebar embedded in blended cement concrete under macro cell corrosion condition", *Constr. Build. Mater.*, 22(3), 186-199.

116. Vijayaraghavan, J., Jude, A.B. and Thivya, J. (2017). "Effect of copper slag, iron slag and recycled concrete aggregate on the mechanical properties of concrete." *Res. Pol.*, 53, 219-225.
117. Wang, A., Zhang, C. and Sun, W. (2003). "Fly ash effects: I. The morphological effect of fly ash." *Cem. Concr. Res.*, 33(12), 2023-2029.
118. Wang, S.D., Pu, X.C., Scrivener, K.L. and Pratt, P.L. (1995). "Alkali activated slag cement and concrete: A review of properties and problems." *Adv. Cem. Res.*, 7(27), 93-102.
119. Wardhono, A., Law, D.W. and Strano, A. (2015). "The strength of alkali activated slag/fly ash mortar blends at ambient temperature." *Procedia Eng.*, 125, 650-656.
120. Wongkeo, W., Thongsanitgarn, P. and Chaipanich, A. (2012). "Compressive strength and drying shrinkage of fly ash-bottom ash-silica fume multi-blended cement mortars." *Mat. Des.*, 36, 655-662.
121. Xiao, R., Ma, Y., Jiang, X., Zhang, M., Zhang, Y., Wang, Y. and He, Q. (2020). "Strength, microstructure, efflorescence behavior and environmental impacts of waste glass geopolymers cured at ambient temperature." *J. Clean. Prod.*, 252, 119610.
122. Xie, J., Zhao, J., Wang, J., Wang, C., Huang, P. and Fang, C. (2019). "Sulfate resistance of recycled aggregate concrete with GGBS and fly ash-based geopolymer." *Mater.*, 12 (8), 1247.
123. Yan, S., Sagoe-Crentsil, K. and Shapiro, G. (2012). "Properties of cement mortar incorporating de-inking waste-water from waste paper recycling." *Constr. Build. Mater.*, 29, 51-55.
124. Yaragal, S., Kumar, C. and Abhinav, M.U. (2020). Numerical and experimental studies on sustainable alkali activated concretes at elevated temperatures. *J. Struct. Fire Eng.*,
125. Yaragal, S.C., Kumar, B.C. and Jitin, C. (2020). "Durability studies on ferrochrome slag as coarse aggregate in sustainable alkali activated slag/fly ash based concretes." *Sust. Mat. Tech.*, 23, e00137.

126. Yaragal, S.C., Kumar, B.C. and Mate, K. (2019). "Optimization of ferrochrome slag as coarse aggregate in concretes." *Comp. Concr.*, 23(6), 421-431.
127. Yaragal, S.C., Narayan, K.S.B., Venkataramana, K., Kulkarni, K., Gowda, H.C., Reddy, G.R. and Sharma, A. (2010). "Studies on normal strength concrete cubes subjected to elevated temperatures." *J. Struct. Fire Eng.*, 1(4), 249-262.
128. Yaragal, S.C., Teja, D.C. and Shaffi, M. (2016). "Performance studies on concrete with recycled coarse aggregates." *J. Adv. Concr. Constr.*, 4(4), 263-281.
129. Yazıcı, Ş., Sezer, G.İ. and Şengül, H. (2012). "The effect of high temperature on the compressive strength of mortars." *Constr. Build. Mater.*, 35, 97-100.
130. Ye, H. and Radlińska, A. (2016). "Quantitative analysis of phase assemblage and chemical shrinkage of alkali activated slag." *J. Adv. Concr. Technol.*, 14(5), 245-260.
131. Yi, Y., Li, C., Liu, S. and Al-Tabbaa, A. (2014). "Resistance of MgO-GGBS and CS-GGBS stabilised marine soft clays to sodium sulfate attack." *Géotechnique*, 64(8), 673-679.
132. Yi, Y., Li, C., Liu, S. and Jin, F. (2015). "Magnesium sulfate attack on clays stabilised by carbide slag-and magnesia-ground granulated blast furnace slag." *Geotech. Lett.*, 5(4), 306-312.
133. Yip, C.K., Lukey, G.C., Provis, J.L. and Van-Deventer, J.S.J. (2008). "Effect of calcium silicate sources on geopolymerisation." *Cem. Concr. Res.*, 38(4), 554-564.
134. Zannerni, G.M., Fattah, K.P. and Al-Tamimi, A.K. (2020). "Ambient-cured geopolymer concrete with single alkali activator." *Sust. Mat. Tech.*, 23, e00131.
135. Zelić, J. (2005). "Properties of concrete pavements prepared with ferrochromium slag as concrete aggregate." *Cem. Concr. Res.*, 35(12), 2340-2349.
136. Zhang, B., He, P. and Poon, C.S. (2020a). "Optimizing the use of recycled glass materials in alkali activated cement (AAC) based mortars." *J. Clean. Prod.*, 255, 120228.
137. Zhang, J., Ma, Y., Zheng, J., Hu, J., Fu, J., Zhang, Z. and Wang, H. (2020b). "Chloride diffusion in alkali-activated fly ash/slag concretes: Role of slag

content, water/binder ratio, alkali content and sand-aggregate ratio.” *Constr. Build. Mater.*, 261, 119940.

PUBLICATIONS

1. Chethan Kumar B., Subhash C. Yaragal., and Das, B.B. (2020). “Ferrochrome ash–Its usage potential in alkali activated slag mortars.” **Journal of Cleaner Production, 257**, 120577. **IF: 7.24**
2. Chethan Kumar B., Subhash C. Yaragal., and Das, B.B. (2019). “Effect of elevated temperatures on ferrochrome ash based mortars.” *Indian Concrete Journal*, **93(10)**, 14-20.

BIO-DATA

NAME : Chethan Kumar B
DATE OF BIRTH : 19-November-1989
PERMANENT ADDRESS : S/o Bomme Gowda C,
#2518, Mangala Nilaya, 6th Cross,
Thaveregere, Mandya Taluk,
Mandya District-571401.
CONTACT NUMBER : +91-7829812469
EMAIL : chethan.1911@gmail.com

ACADEMIC QUALIFICATION

Educational Qualification	University	Institution	Year of Passing
Ph.D (Civil Engineering)	National Institute of Technology Karnataka, Surathkal.	National Institute of Technology Karnataka, Surathkal.	2021
M.Tech (Structural Engineering)	Visvesvaraya Technological University, Belgaum	Dr. Ambedkar Institute of Technology, Bengaluru.	2013
B.E (Civil Engineering)	Visvesvaraya Technological University, Belgaum	M.S. Ramaiah Institute of Technology, Bengaluru.	2011

PUBLICATIONS

Peer Reviewed Journals (SCI and Scopus)	Conference Papers	Peer Reviewed Journals (Non SCI and Scopus)
10	9	5